

1
2
3
4 **Contemporary medicinal chemistry strategies for the discovery and**
5
6 **development of novel HIV-1 nonnucleoside reverse transcriptase**
7
8 **inhibitors**
9
10

11
12
13
14 Zhao Wang^a, Srinivasulu Cherukupalli^a, Minghui Xie^a, Wenbo Wang^a, Xiangyi Jiang^a,
15
16 Ruifang Jia^a, Christophe Pannecouque^b, Erik De Clercq^{b,*}, Dongwei Kang^{a,c,*}, Peng
17
18 Zhan^{a,c,*}, Xinyong Liu^{a,c,*}
19
20
21

22
23 *^aDepartment of Medicinal Chemistry, Key Laboratory of Chemical Biology (Ministry of Education),*
24
25 *School of Pharmaceutical Sciences, Cheeloo College of Medicine, Shandong University, 44 West*
26
27 *Culture Road, 250012 Jinan, Shandong, PR China.*
28

29 *^bRega Institute for Medical Research, Laboratory of Virology and Chemotherapy, K.U. Leuven,*
30
31 *Herestraat 49 Postbus 1043 (09.A097), B-3000, Leuven, Belgium.*
32

33 *^cChina-Belgium Collaborative Research Center for Innovative Antiviral Drugs of Shandong*
34
35 *Province, 44 West Culture Road, 250012 Jinan, Shandong, PR China.*
36
37
38
39
40
41
42
43
44
45
46
47
48
49
50
51
52
53
54
55
56
57
58
59
60

ABSTRACT

Currently, HIV-1 nonnucleoside reverse transcriptase inhibitors (NNRTIs) are a major component of the highly active antiretroviral therapy (HAART) regimen. However, the occurrence of drug-resistant strains and adverse reactions after long-term usage have inevitably compromised the clinical application of NNRTIs. Therefore, the development of novel inhibitors with distinct anti-resistance profiles and better pharmacological properties is still an enormous challenge. Herein, we summarize state-of-the-art medicinal chemistry strategies for the discovery of potent NNRTIs, such as structure-based design strategies, contemporary computer-aided drug design, covalent-binding strategies, and the application of multitarget-directed ligands. The strategies described here will facilitate the identification of promising HIV-1 NNRTIs.

1. INTRODUCTION

Acquired immune deficiency syndrome (AIDS) caused by human immunodeficiency virus-1 (HIV-1) still remains a serious epidemic disease that threatens human health worldwide.¹ According to the latest statistical data from the Joint United Nations Programme on HIV/AIDS (UNAIDS), there were 37.7 million HIV-infected patients globally and 0.68 million deaths from HIV-related illnesses in 2020.² In the fight against AIDS, a combination of multiple antiviral agents, namely, the highly active antiretroviral therapy (HAART) regimen, as the standard therapy for HIV, has successfully controlled the spread of AIDS and reduced the high-mortality disease into a chronic disease.³ The HAART regimen, which typically involves well-known reverse transcriptase (RT) inhibitors, has proven to be the most effective and safe treatment to suppress viral replication and reduce viral spread.⁴

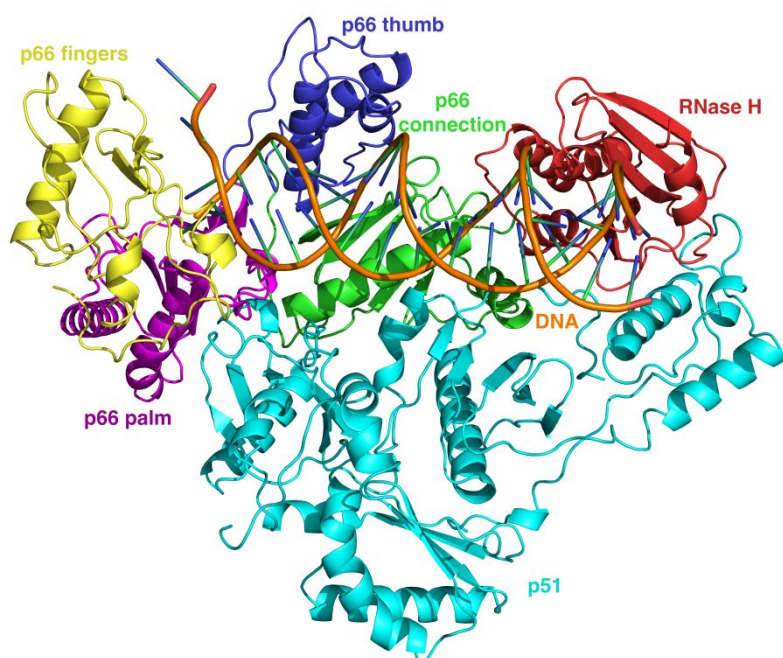
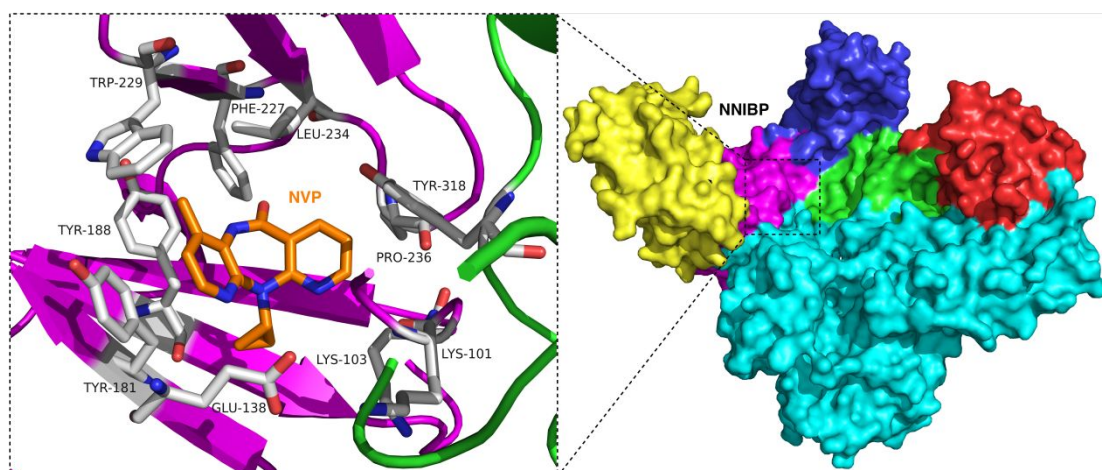


Figure 1. The X-ray crystal structure of HIV-1 RT (PDB code: 1RTD). The image was generated by PyMOL software.

1
2
3
4 Among all the therapeutic targets related to the HIV-1 infectious disease, RT is an
5
6 attractive target because of its well-solved X-ray crystallographic structure and high
7
8 tolerance to diverse chemical molecules.^{5, 6} In the heterodimeric protein RT, the p51
9
10 subunit does not have a catalytic function, but only participates in conformational
11
12 regulation for the p66 subunit.⁷ The p66 subunit, which responsible for performing all
13
14 catalytic activities, consists of the polymerase domain and the RNase H domain. The
15
16 shape of the polymerase domain is similar to that of the right hand, so the four
17
18 constituent subdomains are referred to as fingers, palm, thumb, and connection. The
19
20 RNase H domain is associated with the polymerase domain through the connection
21
22 subdomain (**Figure 1**).⁸ The RT enzyme plays a critical role during viral replication
23
24 and is responsible for the reverse transcription process.^{9, 10} To replicate inside the host
25
26 cell, RT first exhibits RNA-dependent DNA polymerase activity and uses viral RNA
27
28 as the template to synthesize RNA:DNA double strands. Subsequently, the RNase H
29
30 domain can degrade the RNA strand of hybrid intermediates. Finally, RT serves as a
31
32 DNA-dependent DNA polymerase to transform the remaining single-stranded DNA
33
34 into the double-stranded DNA product.¹¹

35
36
37
38
39
40
41
42
43
44
45 RT inhibitors are generally classified into nucleoside reverse transcriptase
46
47 inhibitors (NRTIs) and nonnucleoside reverse transcriptase inhibitors (NNRTIs) owing
48
49 to different binding sites and chemical classes of compounds.¹² The competitive
50
51 inhibitor NRTIs are converted intracellularly into their corresponding triphosphate
52
53 forms, with a structure similar to natural nucleotides, through three different
54
55 phosphorylation cascades and are then connected into growing DNA strands by
56
57
58
59
60 HIV-1

1
2
3
4 RT. These nucleotide analogs compete with their natural counterparts and prevent
5
6 insertion of the next endogenous nucleotide. NNRTIs can disrupt the normal function
7
8 of RT by occupying the NNRTI-binding pocket (NNIBP), thereby affecting the
9
10 conformation of the active catalytic site.^{13, 14} Unlike NRTIs, NNRTIs do not compete
11
12 for natural substrates and therefore will not directly interfere with DNA polymerization
13
14 but instead block the reverse transcription process by inducing conformational changes
15
16 of RT upon binding to NNIBP as allosteric inhibitors.¹⁵
17
18
19
20
21



22
23
24
25
26
27
28
29
30
31
32
33
34
35
36
37
38 **Figure 2.** The binding modes of NVP (orange) within the NNRTI-binding pocket (PDB code:
39
40 1VRT). The image was generated by PyMOL software.
41
42

43 Because of the rapid development of resistance to a single drug, NNRTIs have
44
45 been recognized as essential ingredients in the HAART regimen.¹⁶ The single-tablet
46
47 combination regimen shows obvious advantages, including lower doses and higher
48
49 genetic barriers to resistance due to synergistic inhibition between multiple drugs, as
50
51 well as improved patient compliance.¹⁷ The integrase inhibitor dolutegravir in
52
53 combination with NNRTI rilpivirine (Juluca[®]) represents the first approved two-drug
54
55 single-tablet regimen for maintenance therapy.¹⁸ According to the data of two phase
56
57
58
59
60

1
2
3
4 non-inferiority trials, the dolutegravir+rilpivirine coformulation was shown to be non-
5
6 inferior to the current therapy for the maintenance of HIV-1 suppression in treatment-
7
8 experienced individuals. Moreover, this well-tolerated single-tablet regimen was
9
10 characterized by safe cardiovascular, renal, bone, and lipid toxicity profiles.^{19, 20} In the
11
12 current landscape of antiretroviral options, there remains an urgent need for novel
13
14 classes of NNRTIs with favorable tolerance and convenience to make potential NNRTI-
15
16 based regimens more attractive.
17
18
19
20
21

22 To date, six NNRTI drugs have been approved by the U.S. FDA: including three
23
24 first-generation inhibitors nevirapine (**1**, NVP), delavirdine (**2**, DLV), and efavirenz (**3**,
25
26 EFV); two second-generation inhibitors etravirine (**4**, ETV) and rilpivirine (**5**, RPV);
27
28 and the newly approved drug doravirine (**6**, DOR) (**Figure 3**).^{21, 22} However, the
29
30 occurrence of resistance has compromised the clinical use of first-generation drugs,
31
32 especially the two most prevalent single mutants, K103N and Y181C, selected by
33
34 nevirapine and efavirenz. Although the second-generation NNRTIs belonging to the
35
36 diarylpyrimidine (DAPY) family exhibit prominent antiviral activity toward most of
37
38 the clinically common mutations, they suffer from poor aqueous solubility and
39
40 unfavorable pharmacokinetic properties. Compared to both DAPY-type drugs ETV and
41
42 RPV, the pyridone derivative DOR displayed more potent antiviral activity against the
43
44 two most prevalent mutations K103N and Y181C, while inferior potency was observed
45
46 in terms of mutations V106A, F227L, and L234I in clinical trials.²³ Therefore, the
47
48 discovery of novel NNRTIs with distinct resistance profiles and better pharmacological
49
50 properties remains an imminent and challenging toned in the research community.
51
52
53
54
55
56
57
58
59
60

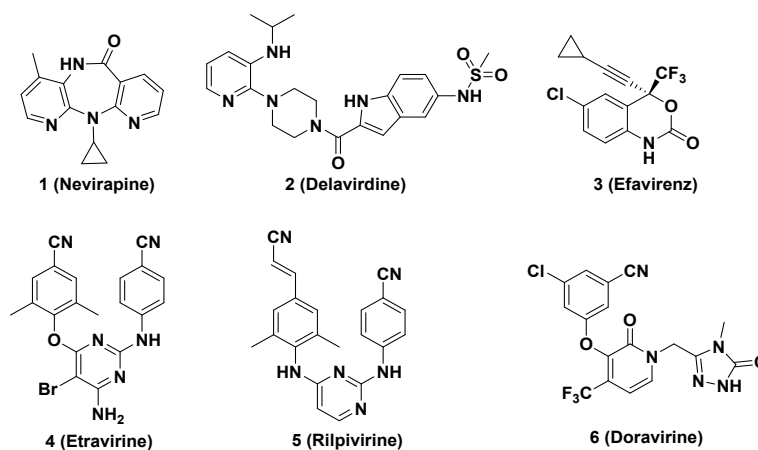


Figure 3. Six NNRTI drugs approved by the U.S. FDA.

The RT allosteric binding site is not directly related to the function of the catalytic active site of the polymerase domain, so NNIBP does not need to be highly conserved and can adapt to mutations without significantly impairing normal enzyme function or affecting viral fitness.²⁴ Almost all residues in NNIBP can be relatively easily mutated, and most of the resulting mutations can confer resistance to NNRTIs.^{25, 26} Therefore, resistance-associated mutations reduce susceptibility by altering the interaction between inhibitors and NNIBP *via* multiple mechanisms, such as steric hindrance (L100I and G190A/S), the prevention of effective entry into the pocket (K101E/P, K103N, and E138K), alteration of the hydrophobic interactions (V106A, V179D, and F227C/L), and loss of π - π stacking interactions with aromatic residues (Y181C and Y188L). Specifically, L100I and G190A/S mutate to a bulky amino acid, so the increase in the volume of the amino acid causes steric hindrance between the ligand and the protein by altering the shape of NNIBP.²⁷ Amino acid mutations at the K101, K103, and E138 positions in the entrance channel can interfere with the entry of NNRTI by extending the side chain out of the pocket.²⁸ Mutations occurring in hydrophobic residues V106, V179, and F227 confer high levels of resistance by weakening the

1
2
3
4 hydrophobic interaction with NNRTIs.²⁹ Similarly, the disappearance of crucial π - π
5
6 stacking interactions with the aromatic amino acids Tyr181 and Tyr188 causes
7
8 significantly reduced susceptibility to Y181C and Y188L.^{30, 31}
9
10

11 Herein, we will elaborate on the discovery and optimization of NNRTIs over the
12
13 last two decades. The following contents comprise not only traditional medicinal
14
15 chemistry principles but also, in certain chapters, the elucidation of nonclassical
16
17 antiviral strategies to block viral infection, including modern computer-aided drug
18
19 design and targeted covalent inhibitors. In addition, the inspiration and guidance of
20
21 these previous research efforts are discussed in detail. Most importantly, our current
22
23 viewpoints of the challenges and prospects of future drug development work are also
24
25 addressed. We hope that this review will contribute to highlighting the significant role
26
27 and potential of diverse medicinal chemistry strategies in the evolution of the ongoing
28
29 search for new and efficient NNRTIs.
30
31
32
33
34
35
36
37
38
39

40 **2. DISCOVERY OF HIV-1 NNRTIS LEADS**

41
42
43 The discovery of lead compounds represents one of the most significant research
44
45 areas in medicinal chemistry and usually relies on screening existing compounds to find
46
47 drug-like molecules that act on a specific target.³² Although traditional in-house
48
49 chemical library screening to identify leads through biochemical assays is conceptually
50
51 more sophisticated, the approach suffers from a heavy workload and false positives. In
52
53 contrast, current technologies, including virtual screening and diversity-oriented
54
55 synthesis combined with rapid screening as complementary strategies, have fully
56
57
58
59
60

1
2
3
4 ensured the efficient progress of novel NNRTI discovery.^{33, 34}
5

6 7 **2.1. Virtual Screening and Structure-Based Design Strategy** 8

9 The cost-intensive characteristics of the traditional drug development process,
10 coupled with the drug resistance challenge conferred by the easy mutation of viral genes,
11 highlight the importance and urgency of the rapid discovery of hit compounds. In the
12 past few decades, the application of computational technologies such as virtual
13 screening has accelerated lead identification and rationalized further structural
14 optimization, thereby making the drug design process more goal-oriented and
15 economical.³⁵⁻³⁷
16
17
18
19
20
21
22
23
24
25

26
27 By virtually screening the commercially available *ZINC* compound library based
28 on three different conformations of RT structures, compound **7**, with an EC₅₀ value of
29 4.8 μM toward the wild-type (WT) strain, was identified as a promising hit for further
30 optimization.³⁸ Subsequently, optimization of **7** was carried out based on free energy
31 perturbation (FEP) calculations of NNRTI/RT complexes, which was applied to
32 determine the optimal substitution patterns of the benzene moiety and evaluate the
33 feasibility of replacing the methylene linker with oxygen. Catechol diether **8**, featuring
34 terminal uracil and cyanovinylphenyl moieties, exhibited extraordinarily robust
35 potency against the WT strain (EC₅₀ = 55 pM).³⁹ Cocrystal structures of RT and **8**
36 suggested that the cyanovinyl group contacts Trp229 closely and accommodates it in
37 the pocket extremely well (**Figure 4**). In addition, more significant contacts with
38 Lys103 *via* hydrogen bonds were observed in the binding mode. In particular, the
39 chlorine atom forms a halogen bond with Pro95 to greatly improve the potency.⁴⁰
40
41
42
43
44
45
46
47
48
49
50
51
52
53
54
55
56
57
58
59
60

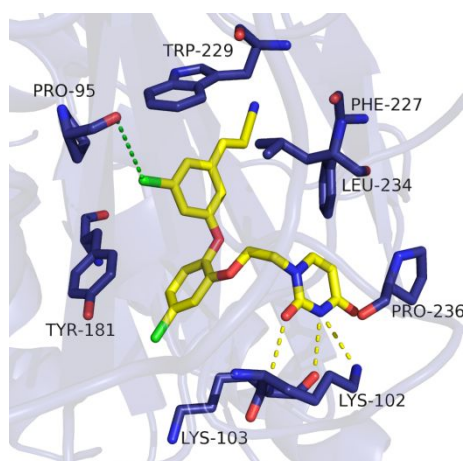


Figure 4. Cocystal structures of compound **8** (yellow) and WT RT (PDB code: 4H4M). Hydrogen bonds are shown as yellow dotted lines, and the halogen bond is indicated with a green dashed line.

Although **8** exhibited picomolar inhibitory activity toward the WT strain, significantly decreased activities were observed for the Y181C and K103N/Y181C mutants. Therefore, based on the predictions of the computational method, eliminating the chlorine atom of the central scaffold afforded analog **9** with improved resistance profiles and solubility. Analysis of cocystal structures indicated that the reduced steric hindrance caused by the absence of 5-Cl allows compound **9** to adopt favorable binding modes in all three complexes and maintain key hydrogen-bonding interactions with surrounding residues (**Figure 5**).⁴¹

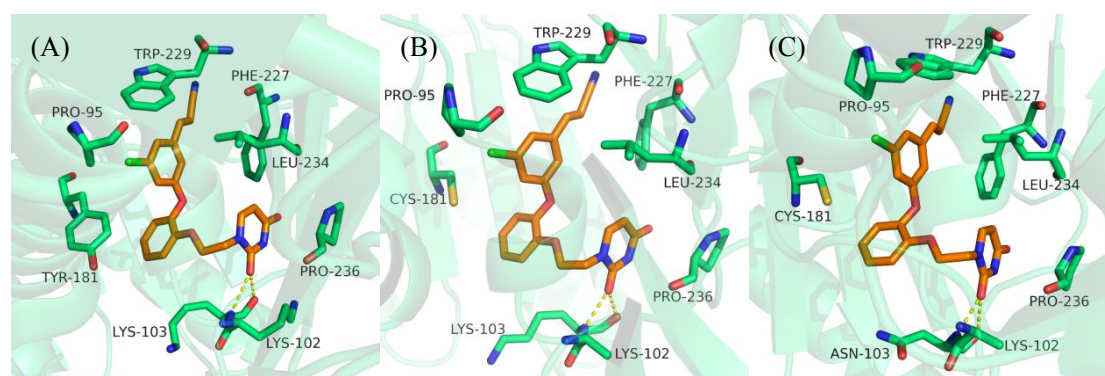
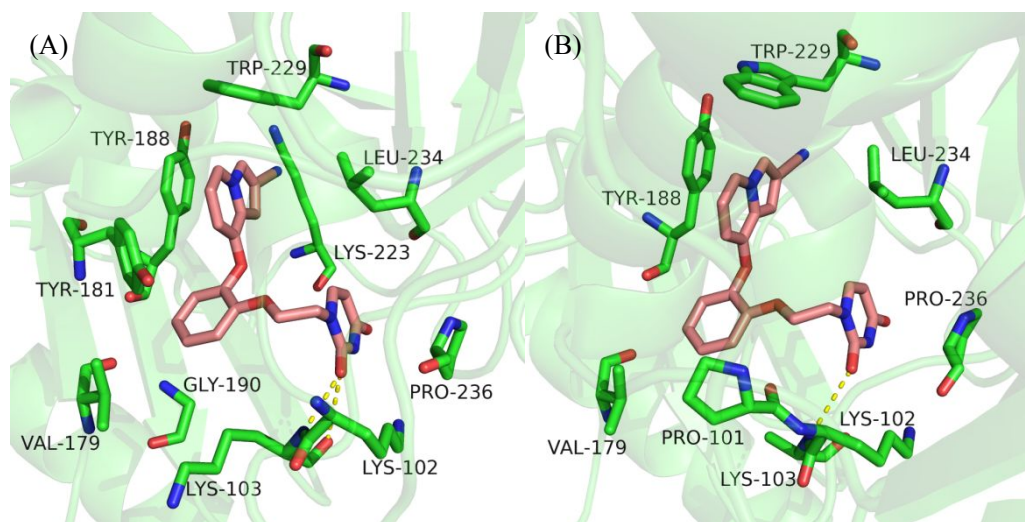


Figure 5. (A) Cocystal structures of compound **9** (orange) and WT RT (PDB code: 4RW8); (B) Cocystal structures of compound **9** (orange) and Y181C RT (PDB code: 4RW9); (C) Cocystal

1
2
3
4 structures of compound **9** (orange) and K103N/Y181C RT (PDB code: 4RW7). Hydrogen bonds
5
6 are shown as yellow dotted lines.
7
8

9
10 However, the electrophilic cyanovinyl group in **8** and **9** might act as a Michael
11
12 acceptor; further modification work was focused on the replacement of the
13
14 cyanovinylphenyl group, especially considering the possibilities of 6/5 heterobicyclic
15
16 groups. In accordance with the Monte Carlo/free energy perturbation prediction results,
17
18 the most potent 2-cyanoindolizinyll derivative, **10**, with suitable aqueous solubility was
19
20 proven to effectively inhibit the WT and K103N/Y181C strains. Cocrystal structures
21
22 showed that **10** forms intensive π - π stacking interactions and is involved in ion-dipole
23
24 interactions or hydrogen bonds (**Figure 6A**).⁴² In addition, **10** showed robust potency
25
26 against the K101P mutant strain (a low-frequency mutation with markedly reduced the
27
28 susceptibility to both EFV and RPV) with an EC₅₀ value of 1 nM. Crystallographic
29
30 studies revealed that **10** does not rely on salt bridge stabilization or direct backbone
31
32 hydrogen bonding with Lys101, so the K101P mutation will not damage the binding
33
34 affinity relative to that of WT RT (**Figure 6B**).⁴³
35
36
37
38
39
40
41
42



43
44
45
46
47
48
49
50
51
52
53
54
55
56
57
58
59
60
Figure 6. (A) Cocrystal structures of compound **10** (pink) and WT RT (PDB code: 4MFB); (B)

Cocrystal structures of compound **10** (pink) and K101P RT (PDB code: 5C42). Hydrogen bonds are shown as yellow dotted lines.

In general, the antiviral activities of NNRTIs almost always decrease significantly for a double variant compared to a single variant. However, the potency of **10** against the Y181C mutant was approximately 30-fold less than that of the K103N/Y181C mutant. To improve the activity of catechol diethers toward the Y181C mutant, the introduction of a bulky naphthalene ring under the guidance of the BOMB program was expected to establish additional π - π interactions. The resulting compounds, 2-naphthyl analog **11** and 1-naphthyl analog **12**, possessed markedly improved anti-resistance profiles compared to **10** in the case of the Y181C mutation (**Figure 7**).^{44, 45}

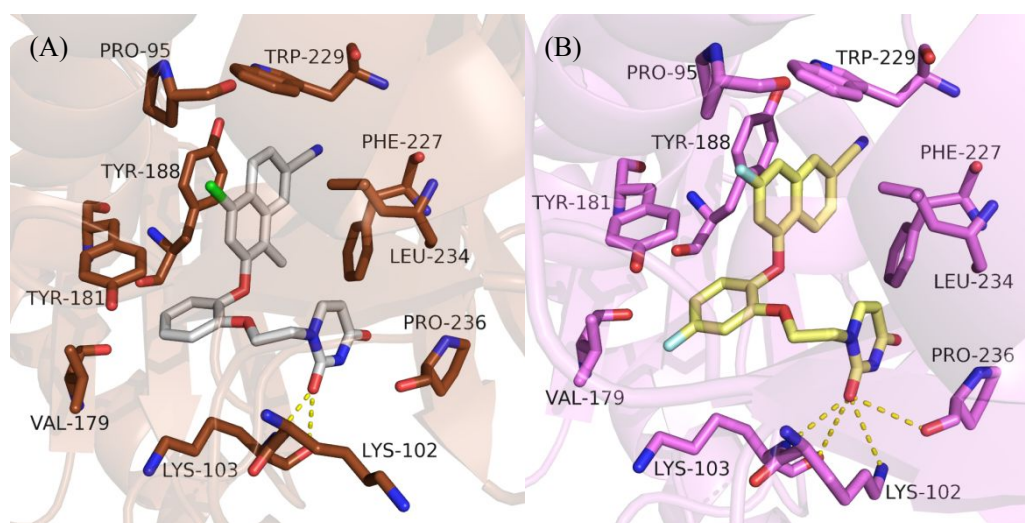


Figure 7. (A) Cocrystal structures of compound **11** (white) and WT RT (PDB code: 5TER). (B) Cocrystal structures of compound **12** (yellow) and WT RT (PDB code: 5TW3). Hydrogen bonds are shown as yellow dotted lines.

Further preclinical studies proved the significance of **12** with not only marked activity toward WT and mutant strains but also with desirable *in vivo* pharmacokinetic properties, no substantial cytotoxicity, and off-target effects (**Table 1**). Moreover, the

development of a long-acting nanoformulation of **12** allowed the plasma drug concentration and antiviral efficacy to be continuously maintained for nearly three weeks after a single-dose administration (**Figure 8**).⁴⁶ Considering the efficacy of **12** in HIV-1-infected humanized mice and synergistic antiretroviral potency with existing anti-AIDS drugs, it will likely become a promising candidate for preexposure prophylaxis (PrEP).

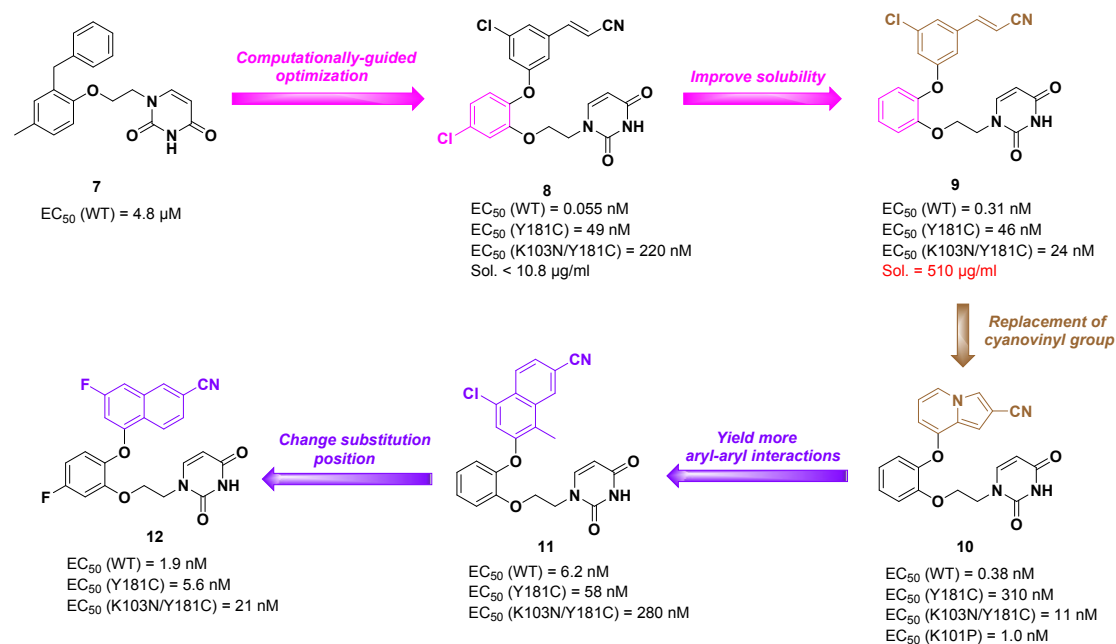


Figure 8. Discovery and optimization of a new class of catechol diether-based NNRTIs.

Table 1. Antiviral Activity and Cytotoxicity of Compounds **8–12**.

Compd	EC ₅₀ (nM) ^a			CC ₅₀ (μM) ^b
	WT	Y181C	K103N/Y181C	
8	0.055	49	220	10
9	0.31	46	24	18
10	0.38	310	11	>100
11	6.2	58	280	>100
12	1.9	5.6	21	>100
NVP ⁴²	110	>100000	>100000	>100

EFV ⁴²	2	10	30	15
ETV ⁴²	1	8	5	11
RPV ⁴²	0.67	0.65	2	8

^aEC₅₀: The EC₅₀ value is defined as the dose required to achieve 50% protection of the infected MT-2 cells by the MTT colorimetric method; antiviral curves were established from triplicate samples at each concentration.

^bCC₅₀: The CC₅₀ value is defined as the dose required to achieve 50% inhibition of MT-2 cell growth by the MTT colorimetric method; the toxicity curves were established from triplicate samples.

2.2. CuAAC Click Chemistry-Based Combinatorial Libraries

Rapid synthesis and direct screening of combinatorial compound libraries through copper(I)-catalyzed azide-alkyne cycloaddition (CuAAC) click chemistry proved to be an important approach for exploring SARs and identifying hit compounds.⁴⁷⁻⁵¹ As an extension of the click reaction concept, this method has the advantages of high chemoselectivity, convenient synthetic accessibility, and stability of triazole-containing products, enabling the successful implementation of rapid activity screening directly after parallel microplate-scale synthesis without isolation and purification.

Our group reported the rapid discovery of bioactive compounds by employing the miniaturized parallel CuAAC click reaction followed by direct biological screening (**Figure 9**).⁵² Specifically, six terminal alkyne fragments were constructed to fully exploit the chemical space within the binding sites. Furthermore, various aryl- and alkyl-substituted azide derivatives were designed to satisfy the needs of structural diversity. The RT inhibition screening of 156-member DAPY derivatives library in 96-well plates identified 22 hits from the compound library, with inhibition rates higher than those of the control drugs at a fixed concentration. Further cell-based biological

evaluation of the 22 hits led to the discovery of **13** as an interesting lead compound with potent anti-HIV activities.

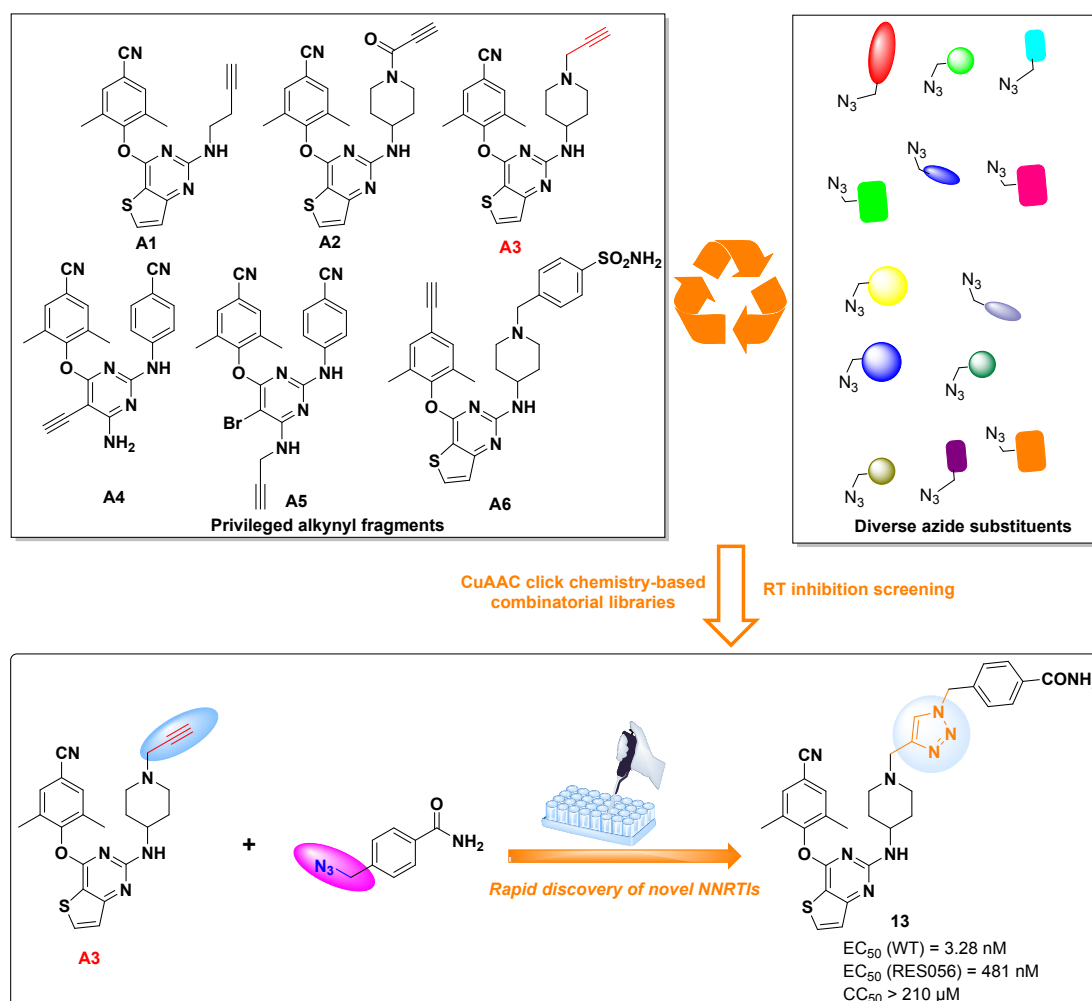


Figure 9. The rapid discovery of novel NNRTIs from CuAAC click chemistry-based combinatorial libraries.

3. STRUCTURAL OPTIMIZATION OF NNRTI LEADS

To identify promising candidates with both prominent antiviral activities and drug-like properties, classic medicinal chemistry strategies combined with structural biology have been applied in the lead optimization of diverse NNRTIs during recent decades.⁵³⁻

3.1. Scaffold Hopping

The main goal of scaffold hopping is to identify novel compounds containing topologically different backbones by replacing the pivotal structure of existing active compounds by considering key ligand–protein interactions.⁵⁷⁻⁶⁰

As the first class of NNRTIs discovered to act on HIV-1 RT specifically, iterative SAR research involving the 1-[(2-hydroxyethoxy)methyl]-6-(phenylthio)thymine (HEPT) family has developed promising derivatives **14** (MKC-442) and **15** (TNK-651) that share the uracil scaffold containing an isopropyl group. Recognizing the importance of the bulky isopropyl group in providing sufficient steric hindrance to regulate the conformation of the *ortho*-benzyl moiety to form an optimal π – π interaction with Y181, the replacement of the isopropyl group with various halogens of large atomic radii led to the discovery of iodine-bearing uracil analog **16** with potent activities in RT inhibition and antiviral assays.⁶¹ Encouraged by the robust potencies of these previously discovered compounds, the central uracil scaffold of TNK-651 was converted to a pyridinone ring, and methyl-substituted cyclohexane was introduced to promote the π – σ interaction with the conserved residue W229 rather than the readily mutated residue Y181, which eventually gave rise to compound **17** with an improved resistance profile (**Figure 10**). Then, the **17-cis** and **17-trans** diastereomers were prepared separately by the Mitsunobu stereoselective reaction to investigate the effect of the 2'-methyl configuration of cyclohexyl on the RT inhibitory potency. The biological results indicated that the activity of **17-trans** was approximately 400-fold greater than that of **17-cis**.⁶²

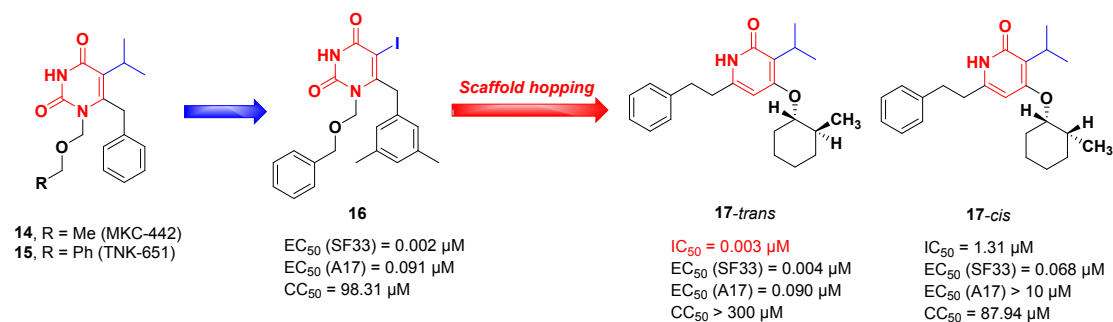


Figure 10. Optimization of HEPT-type NNRTIs by employing a scaffold hopping strategy.

A scaffold hopping strategy was also used to optimize the DAPY family to search for novel chemotypes that are structurally different from ETV, which resulted in identification of thiophene[3,2-*d*]pyrimidine derivatives in the hope that the sulfur atom with an electronic nature similar to that of the bromine atom could form strong electrostatic interactions with the surrounding residues (**Figure 11**). Peripheral substituent decoration culminated in the discovery of compound **18**, which contained a benzylsulfamide group with better activity and lower cytotoxicity than ETV, although it was somewhat weaker against RES056.⁶³ Following the structure-based design, the left cyano group of **18** was changed to a cyanovinyl group to target highly conserved residues in the hydrophobic channel, resulting in compound **19** with overall enhanced potency compared to that of **18**, especially against RES056.⁶⁴ Nevertheless, both **18** and **19** (Sol. < 1 μg/mL) were extremely difficult to dissolve owing to the introduction of aromatic rings. The cocrystal structures of **18** (**Figure 12A**) and **19** (**Figure 12B**) with RT illustrated that the conformational flexibility of molecules, multiple hydrophobic contacts, and the main chain hydrogen-bonding network explain their highly effective activities. Afterward, the thiophene ring was replaced with various aliphatic rings, resulting in the exceptionally potent dihydrofuro[3,4-*d*]pyrimidine derivative **20**, which

1
2
3
4 showed improved solubility.⁶⁵ Additionally, **20** showed favorable safety and PK
5
6 profiles with moderate bioavailability and a long half-life (**Table 2**). Recently, a series
7
8 of trisubstituted pyrimidine derivatives were discovered by opening the fused ring of
9
10 lead compound **18**.⁶⁶ Among them, the most promising compound **21**, bearing a
11
12 pyridyl-substituted pyrimidine scaffold, exhibited improved resistance profiles and
13
14 reduced cytotoxicity compared to ETV. In addition, **21** showed favorable safety
15
16 properties and PK profiles with a moderate oral bioavailability of 15.3% *in vivo*. The
17
18 cocrystal structures of RT/**21** indicated the critical role of the hydrogen bond network
19
20 mediated by water molecules around NNIBP in binding and resisting residue mutations
21
22 (**Figure 12C**).

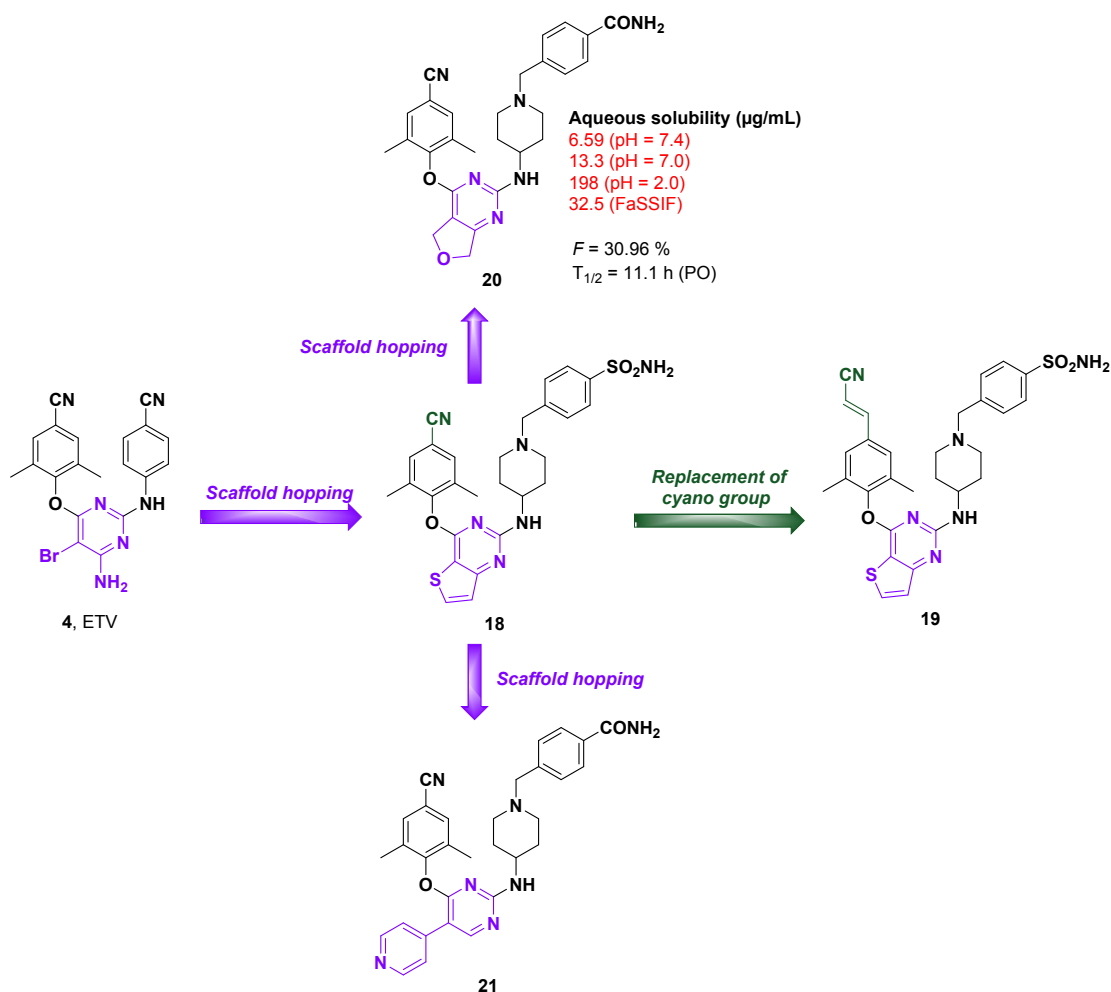


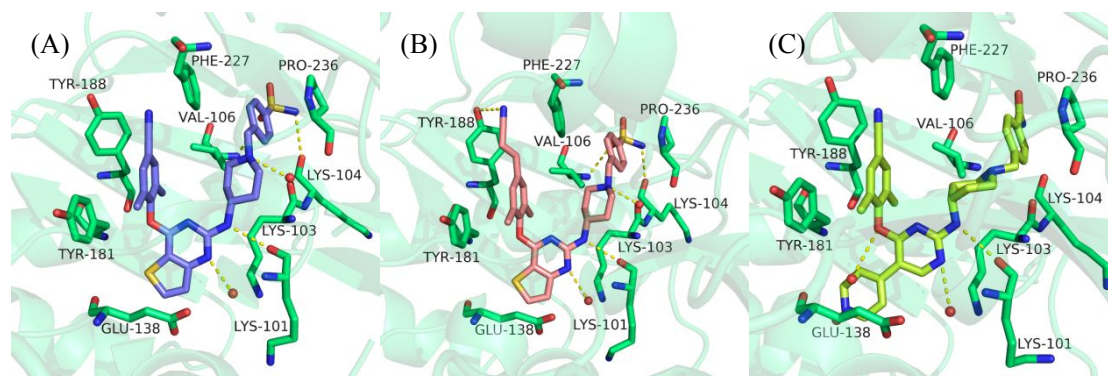
Figure 11. Development of DAPY-based NNRTIs *via* a scaffold hopping strategy in our group.

Figure 12. (A) Cocrystal structures of compound **18** (blue) and WT RT (PDB code: 6C0J); (B) Cocrystal structures of compound **19** (pink) and WT RT (PDB code: 6C0N); (C) Cocrystal structures of compound **21** (yellow) and WT RT (PDB code: 7KWU). Hydrogen bonds are shown as yellow dotted lines.

Table 2. Antiviral Activity and Cytotoxicity of Compounds **18–21**.

Compd	EC ₅₀ (nM) ^a								CC ₅₀ (μM) ^b
	WT	L100I	K103N	Y181C	Y188L	E138K	F227L/V106A	K103N/Y181C	
18	1.4±0.4	3.4±0.6	2.9	3.2±0.4	3.0±0.1	2.9	4.2±1.2	30.6±12	>227
19	1.22±0.26	1.34±0.50	0.96±0.07	5.00±0.11	5.45±0.20	4.74±0.16	2.70±1.74	5.50±0.81	2.30±0.47
20	1.6±0.4	2.4±0.2	0.9±0.1	4.4±1.1	8.4±3.6	7.0±2.5	19.0±2.2	41.5±9.9	>250
21	3.75±0.40	4.26±0.62	3.79±0.42	6.79±1.49	6.79±2.82	10.9±5.63	10.4±5.30	24.4±3.06	36.0±4.85
EFV ⁶³	5.03±2.12	115±8.28	80.1±2.68	8.20±1.03	514±51.5	5.19±0.63	348±58.2	308±164	>0.00633
ETV ⁶³	4.07±0.15	5.38±2.06	2.35±0.67	15.7±2.12	20.5±2.92	14.4±2.27	29.4±7.79	17.0±1.78	>0.00459

^aEC₅₀: The EC₅₀ value is defined as the dose required to achieve 50% protection of the infected MT-4 cells by the MTT colorimetric method; antiviral curves were established from triplicate samples at each concentration.

^bCC₅₀: The CC₅₀ value is defined as the dose required to achieve 50% inhibition of MT-4 cell growth by the MTT colorimetric method; the toxicity curves were established from triplicate samples.

3.2. Molecular Hybridization

1
2
3
4 Molecular hybridization has been widely applied to drug development processes
5
6 and represents a promising approach to improve binding affinity and overcome cross-
7
8 resistance.⁶⁷⁻⁶⁹ However, it is essential to note that hybrids generally have a larger
9
10 volume of molecules and pose challenges to the prediction of physicochemical
11
12 properties. Therefore, it is preferred to select the parent molecules with a high degree
13
14 of overlap and minimize the size of the hybrids as much as possible so that the final
15
16 combined ligands will not be too large to produce drug-like liabilities.⁷⁰
17
18
19
20
21

22 To remedy the drawbacks of the decreased susceptibility of EFV to the K103N
23
24 variant and the poor PK profiles of ETV, the hybridization of the chlorophenyl fragment
25
26 of EFV and the introduction of the cyanovinyl group of RPV led to the discovery of
27
28 compound **22** by employing the substituent decorating approach on the left-wing
29
30 (**Figure 13**). Subsequent removal of the chlorine atom from **22** afforded the quinazoline
31
32 derivative **23** with satisfactory liver microsome stability and PK properties, the potency
33
34 of which was slightly greater than or comparable to that of ETV and EFV.⁷¹
35
36 Alternatively, the superposition of the binding orientations of EFV and ETV motivated
37
38 the grafting of the 4-cyanoaniline moiety to the carbonyl group of EFV while retaining
39
40 other essential pharmacophores, leading to the discovery of a series of
41
42 dihydroquinazolin-2-amine derivatives, as exemplified by compound **24**.⁷²
43
44
45
46
47
48
49
50
51
52
53
54
55
56
57
58
59
60

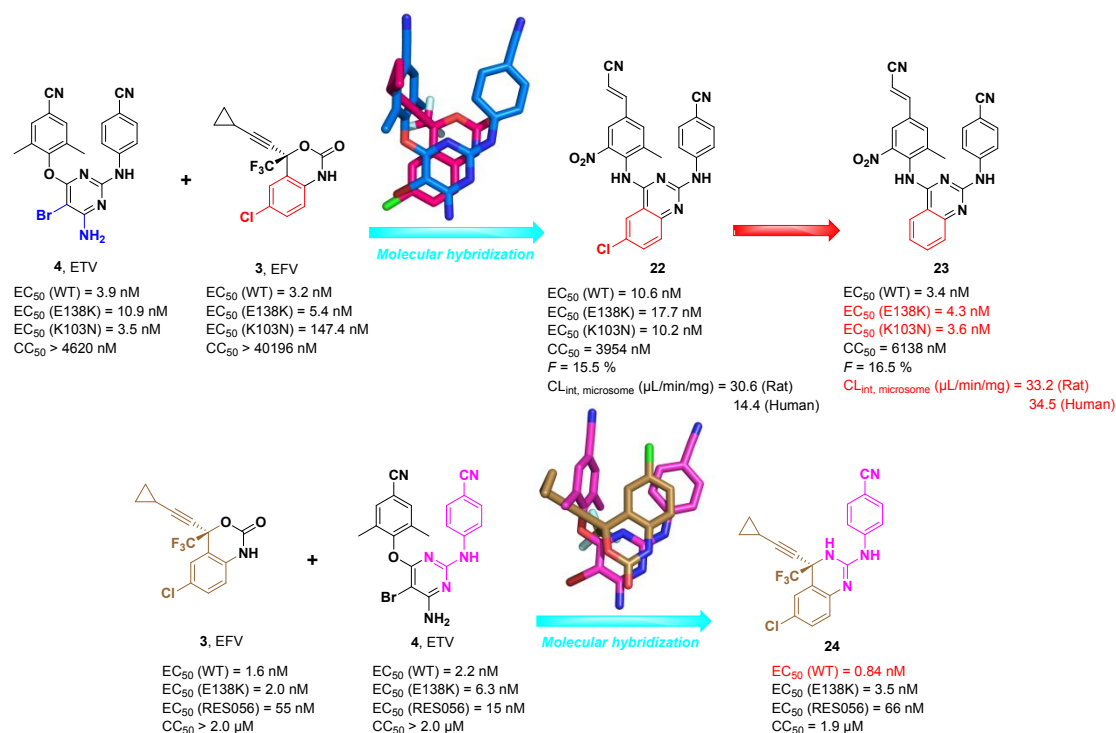


Figure 13. Molecular hybridization of the approved NNRTIs ETV and EFV. Overlay of cocrystal structures of ETV (**4**, blue) and EFV (**3**, red) with WT RT. Overlay of cocrystal structures of EFV (**3**, brown) and ETV (**4**, magenta) with WT RT (PDB codes: 1FK9 and 3MEC).

As shown in **Figure 14**, the discovery of doravirine began with the hit compound tetrazole thioacetanilide derivative **25**, which was identified *via* a high-throughput screening. However, **25** proved to be incapable of being orally bioavailable and was rapidly metabolized to the carboxylic acid form in rat plasma. Subsequent extensive SAR explorations were conducted by the combination of more stable substituents both on the anilide and the benzene linked to the tetrazole core, which resulted in compound **26**, with improved oral bioavailability and decreased plasma clearance.⁷³ Nonetheless, suboptimal PK results of the tetrazole thioacetanilide analogs prompted the evolution of the new scaffold.^{74, 75} Inspired by the overlap of the arylacetamide structures of compound **26** and the known NNRTI candidate **27** (GW678248),⁷⁶⁻⁷⁹ a novel class of

1
2
3
4 diaryl ethers was obtained *via* the molecular hybridization of **26** and **27** to optimize
5
6 interactions with the binding site. These diaryl ether phenoxyacetanilide derivatives
7
8 (exemplified by compound **28**) were rapidly eliminated *in vivo* because of the
9
10 occurrence of metabolic hydrolysis of the aniline moiety. Hence, a variety of isosteric
11
12 heterocycles were introduced to replace the metabolizable aniline group, yielding the
13
14 indazol-containing compound **29**.⁸⁰ However, the poor solubility and low
15
16 bioavailability ($F = 3.3\%$) of **29** hindered its further development. Since the
17
18 crystallographic studies indicated that the lower edge of the indazole ring was located
19
20 at the protein–solvent interface, subsequent efforts have focused on replacing the
21
22 phenyl moiety of the indazolyl group with a solubilizing pyridyl moiety to improve the
23
24 physicochemical properties. Further refinement resulted in the identification of **30**,
25
26 which was labeled MK-4965, as a drug candidate, exhibiting excellent activity against
27
28 various HIV-1 strains and improved bioavailability ($F = 52\%$).^{81, 82}
29
30
31
32
33
34
35
36
37

38 The follow-up optimizations adopt the methylene linker of another compound
39
40 **31**,⁸³⁻⁸⁵ in which the side chain was truncated and a pyridone platform was introduced
41
42 instead of the *meta*-resorcinol moiety, leading to 4-chloro pyridone compound **32** with
43
44 superior anti-resistance profiles.⁸⁶ To improve the exposure and plasma half-life after
45
46 oral administration of **32** ($T_{1/2} = 2.2$ h), the tolerant exploration of various small
47
48 lipophilic substituents (such as alkyl, halogen, and fluorinated alkyl) at the 4-position
49
50 of pyridone led to the discovery of 4-trifluoromethyl analog **33** with improved plasma
51
52 stability and a prolonged half-life ($T_{1/2} = 7.0$ h). Owing to the strong intermolecular
53
54 hydrogen bonds of the pyrazolopyridyl moiety, compound **33** suffers from poor
55
56
57
58
59
60

solubility (Sol. = 1.1 μM) and oral bioavailability ($F = 15\%$).⁸⁷ In parallel with this effort, the bioisosteric replacement of pyrazolopyridine was also conducted to disrupt intermolecular interactions, resulting in the discovery of methyltriazolinone compound **6** (MK-1439, doravirine) with improved solubility (Sol. = 45 μM) and a favorable pharmacokinetic profile ($F = 57\%$).⁸⁷

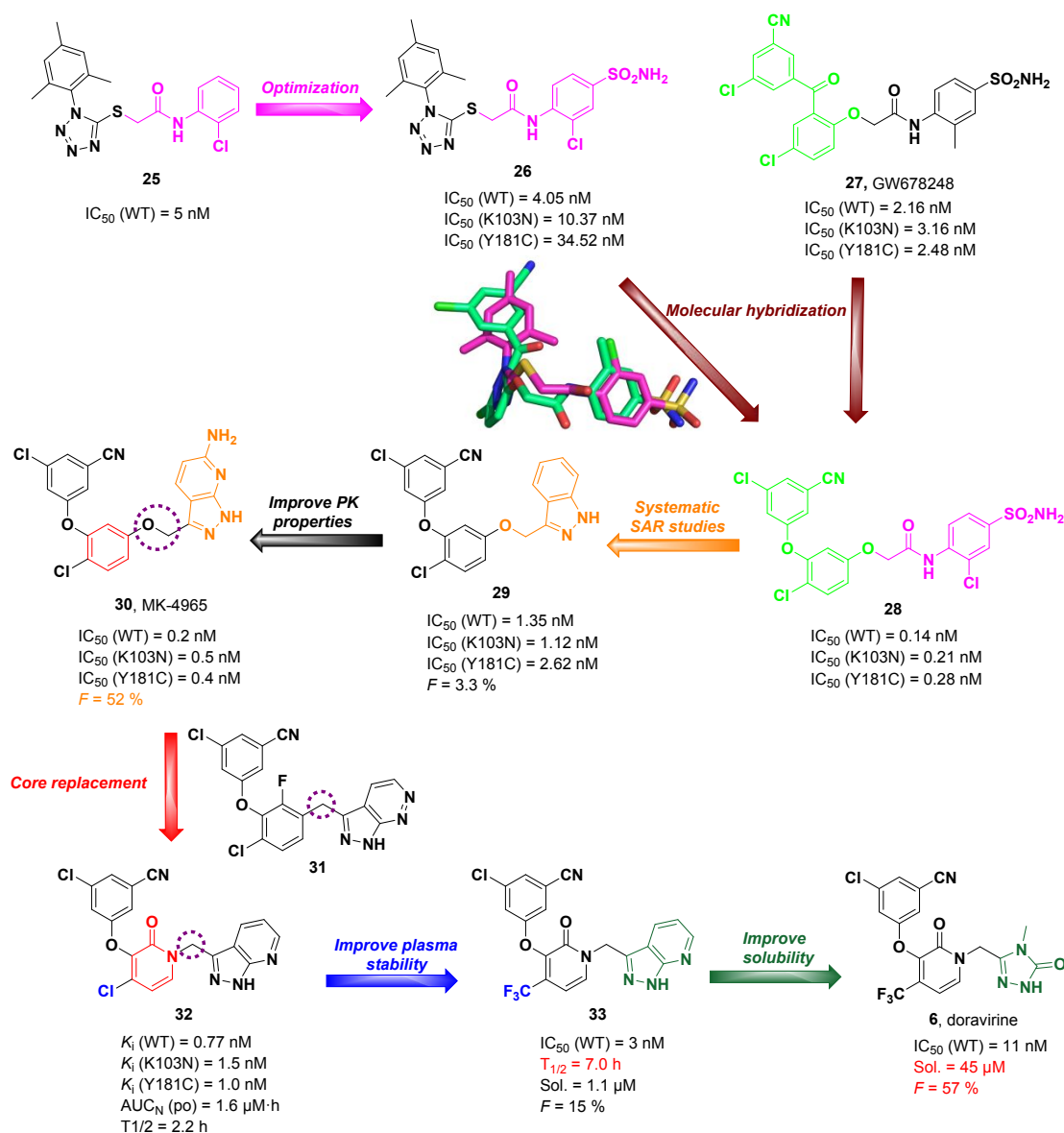


Figure 14. Illustration of the development process of doravirine. Overlay of the cocrystal structures of compound **26** (magenta) and GW678248 (**27**, green) with K103N RT (PDB code: 3DOK).

Given the current landscape of available antiretroviral agents for HIV-1 infections,

1
2
3
4 the development of novel and highly effective NNRTIs is an arduous campaign. Many
5
6 positive attributes of the NNRTI class, such as high potency and long plasma half-life,
7
8 make them attractive targets for drug discovery. However, more than two decades of
9
10 optimization attempts on NNRTIs have failed to provide ideal clinical efficacy
11
12 compared with existing treatment options. DOR has become the only NNRTI that has
13
14 successfully obtained U.S. FDA approval in recent years.⁸⁸⁻⁹⁰
15
16
17
18

19 The emergence of DOR alleviates the known deficiencies related to other drugs,
20
21 including the reduced susceptibility to the mutant strains K103N, Y181C, and G190A
22
23 that are associated with more than 90% of NNRTI resistance; the neuropsychiatric side
24
25 effects of EFV; and the cardiotoxicity, food restriction, and high viral load limitation
26
27 of RPV. In addition, DOR exhibits a more favorable drug–drug interaction profile than
28
29 earlier NNRTIs, as it does not affect the expression of CYP or other major drug-
30
31 metabolizing enzymes or drug transporters. The long half-life of DOR allows for its
32
33 once-daily administration as a single tablet or the fixed-dose combination.⁹¹⁻⁹³
34
35
36
37
38
39

40 Overall, the complementary advantages of structural biology, *in vitro* resistance
41
42 characterization, and multiple medicinal chemistry strategies facilitated the discovery
43
44 of DOR with distinct anti-resistance profiles and good safety properties.^{94, 95} Currently,
45
46 the most recent DHHS guidelines recommend the use of DOR-containing therapy under
47
48 specific treatment conditions due to the lack of sufficient clinical experience. DOR is
49
50 expected to be reintroduced as a first-line treatment option on behalf of the NNRTI
51
52 class as a result of the accumulation of clinical experience and positive patient outcomes.
53
54
55
56
57

58 **3.3. Bioisosteric Replacement**

59
60

1
2
3
4 The bioisosteric replacement strategy allows the adjustment of the
5 physicochemical properties while retaining their efficient target engagement. Classic
6 bioisosteres with the same atomic number are required to be isoelectronic; otherwise,
7 nonclassical bioisosteres are likely to differ significantly in the number of atoms and
8 valence electrons but induce similar biological activities.⁹⁶⁻⁹⁸

9
10
11
12
13
14
15
16
17 The replacement of the pyrimidine moiety of ETV with an aminobenzene moiety
18 to compensate for the key hydrogen-bonding interactions between pyrimidine and
19 K101 led to the identification of the potent diarylaniline derivative **34**.⁹⁹ Then
20 introduction of the cyanovinyl group at the cyano position of **34** for insertion into the
21 hydrophobic region resulted in a more active compound **35** with subnanomolar EC₅₀
22 values.¹⁰⁰ Thereafter, to overcome the poor solubility and low permeability of **35**,
23 compound **36** was discovered by allowing substituent modifications at the cyanovinyl
24 and nitro positions of **35**. As expected, the incorporation of the hydroxymethyl group
25 could promote the dissolution of **36**, which was far more soluble than **35** and equivalent
26 to RPV.¹⁰¹ However, due to the relatively low metabolic stability and high clearance
27 rate of **36**, subsequent optimization was carried out to maintain a balance between anti-
28 HIV activity and multiple physicochemical properties; this effort culminated in
29 compound **37**, which showed significantly improved solubility and metabolic stability
30 compared to RPV while maintaining excellent antiviral activity (**Figure 15**).¹⁰²

31
32
33
34
35
36
37
38
39
40
41
42
43
44
45
46
47
48
49
50
51
52
53
54
55
56
57
58
59
60

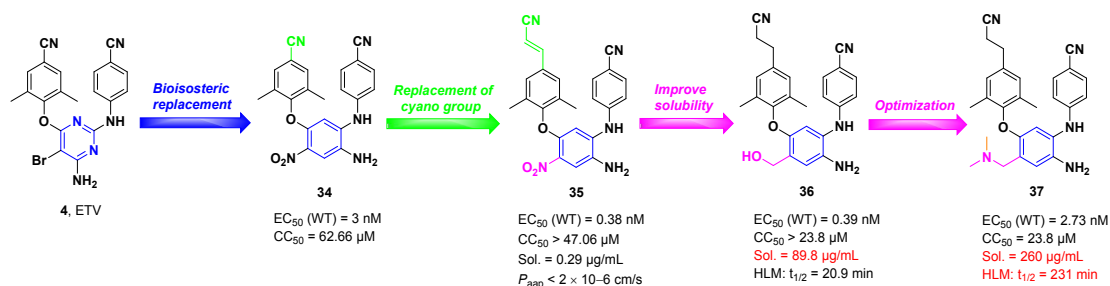


Figure 15. Optimization of novel diarylaniline derivatives.

With **19** as the lead compound, novel thiophene[2,3-*d*]pyrimidine derivatives were identified *via* the structure-based bioisosterism strategy to reduce the toxicity and improve the druggability profile (**Figure 16**).¹⁰³ Compared to **19**, the most potent compound **38** showed comparable activities and much better drug-like properties (**Table 3**). In addition, it was obvious that the RT inhibitory activities (IC₅₀) of **19** and **38** differ significantly from their antiviral activities (EC₅₀), possibly due to the distinct testing methods of the two biological evaluation screening systems (**Table 4**). In the enzyme inhibition assay, the RT inhibitory activities are related to the amount of biotin deoxyuridine triphosphate and RT. In the anti-HIV-1 assay, the antiviral activities are related to the amount of MT-4 cells and HIV-1, the replication round, and the serum protein used to indicate the protein binding of test compounds. Notably, the HIV-1 WT strain was passaged in MT-4 cell culture with increasing concentrations of compound **38** to select for HIV-1 mutant strains. Furthermore, no phenotypic cross-resistance toward NRTIs was observed in the selected mutations that were resistant to **38**.

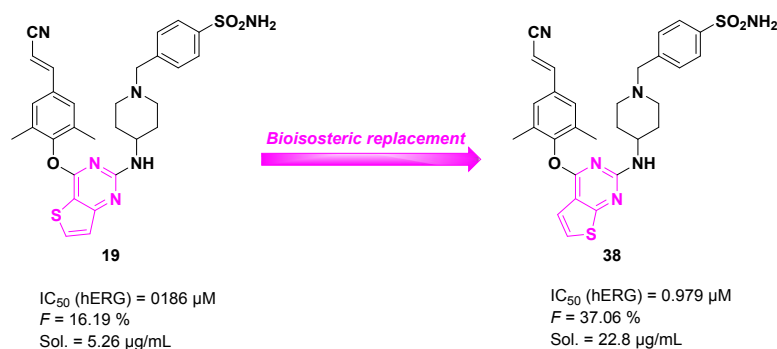


Figure 16. Bioisosteric replacement of the thiophene[3,2-*d*]pyrimidine compound **19**.

Table 3. Antiviral Activity and Cytotoxicity of Compound **38**.

Compd	EC ₅₀ (nM) ^a								CC ₅₀ (μM) ^b
	WT	L100I	K103N	Y181C	Y188L	E138K	F227L/V106A	K103N/Y181C	
38	3.24±2.15	2.05±0.58	2.34±0.82	6.57±0.33	7.59±0.46	6.70±0.49	4.81±0.84	6.45±0.49	10.1±3.28
19	1.22±0.26	1.34±0.50	0.96±0.07	5.00±0.11	5.45±0.20	4.74±0.16	2.70±1.74	5.50±0.81	2.30±0.47
RPV ¹⁰³	1.00±0.27	1.54±0.00	1.31±0.36	4.73±0.48	79.4±0.77	5.75±0.11	81.6±21.2	10.7±7.96	3.98
ETV ¹⁰³	4.07±0.15	5.38±2.06	2.35±0.67	15.7±2.12	20.5±2.92	14.4±2.27	29.4±7.79	17.0±1.78	>4.59

^aEC₅₀: The EC₅₀ value is defined as the dose required to achieve 50% protection of the infected MT-4 cells by the

MTT colorimetric method; antiviral curves were established from triplicate samples at each concentration.

^bCC₅₀: The CC₅₀ value is defined as the dose required to achieve 50% inhibition of MT-4 cell growth by the MTT

colorimetric method; the toxicity curves were established from triplicate samples.

Table 4. Inhibitory Activity against WT and Mutant RT of Compound **38**.

Compd	IC ₅₀ (μM) ^a							
	WT	L100I	K103N	Y181C	Y188L	E138K	F227L/V106A	K103N/Y181C
38	0.114±0.029	0.228±0.090	0.222±0.010	0.141±0.003	0.452±0.083	0.374±0.203	0.130±0.013	0.120±0.057
19	0.101±0.015	0.099±0.040	0.191±0.022	0.149±0.005	0.301±0.071	0.350±0.120	0.106±0.040	0.107±0.052
RPV ¹⁰³	0.015±0.001	0.024±0.012	0.027±0.000	0.021±0.002	0.084±0.038	0.041±0.021	0.015±0.004	0.023±0.014
ETV ¹⁰³	0.012±0.002	0.013±0.004	0.025±0.002	0.017±0.002	0.046±0.009	0.032±0.011	0.008±0.002	0.019±0.008

^aIC₅₀: The IC₅₀ value is defined as the concentration required to achieve 50% inhibition of the incorporation of biotin

deoxyuridine triphosphate (biotin-dUTP) into HIV-1 RT.

3.4. Conformational Restriction

Conformational restriction of ligand flexibility has attracted considerable attention in novel drug discovery, as it can enhance activity by reducing entropic loss during ligand–receptor binding and by stabilizing the preferential conformation, as well as improve metabolic stability by introducing specific structural constraints to block metabolically sensitive sites.^{104, 105}

The distinct conformation of the oxymethylene linker presented in the cocrystal structures of **30** (MK-4965) prompted exploration of the functionality of conformational restriction (**Figure 17**). Therefore, cyclization of the central benzene ring with five-membered aromatic heterocycles was performed to improve the metabolic stability by weakening the oxidative dealkylation of the pyrazolopyridyl group; this campaign resulted in the confirmation of indazolyl as the best cyclic substituent and generated MK-6186 (**39**) and MK-7445 (**40**) with a good combination of antiviral activity and PK profile.¹⁰⁶

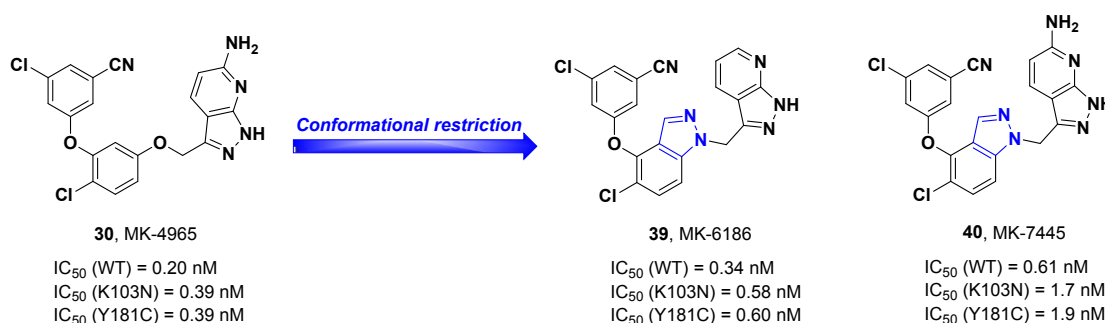


Figure 17. Optimization of MK-4965 *via* a conformational restriction approach.

The application of conformational restriction strategies was also observed in the research process of DAPY derivatives (**Figure 18**). DAPYs are characterized by torsional flexibility (“wiggling”) and repositioning (“jiggling”) due to the rotatable *O*

or *NH* linker on both sides of the central core. The cyclization of the pyrimidine ring with the left or right NH group of RPV by introducing the fused ring structure afforded the potent 2,9-purine analogs **41** and **42**.^{107, 108}

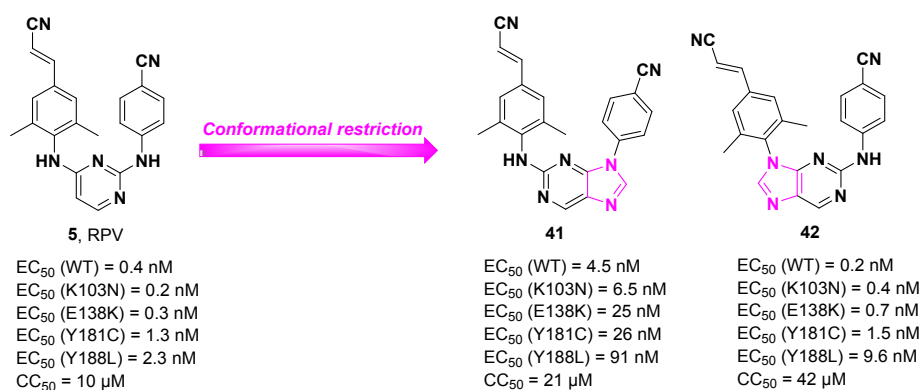


Figure 18. Discovery of novel conformationally restricted DAPY derivatives.

Conformational restriction can often lead to improved potency and decreased drug metabolism, but inherent conformational flexibility is critical to the favorable anti-resistance profile of NNRTIs.¹⁰⁹⁻¹¹¹ Notably, the inherent flexibility of NNRTIs enables them to continually adjust their conformation in the NNIBP, contributing to maintaining binding affinity for various resistant RT mutations.¹¹²⁻¹¹⁴ Therefore, the trade-off between conformational flexibility and restriction appears to be particularly important in the application of the conformational restriction strategy for the optimization of NNRTIs. After all, only a suitable conformation that matches well with the binding pocket can produce the optimal potency.

4. MEDICINAL CHEMISTRY STRATEGIES TO OVERCOME DRUG RESISTANCE

Drug resistance causes major challenges for drug design against mutated proteins

1
2
3
4 and impedes the performance of existing therapies in clinical practice. Due to the lack
5
6 of mechanisms for detecting and repairing potential base mismatches, the frequent
7
8 emergence of HIV-1 resistant mutations against approved antiretroviral drugs
9
10 necessitates the continued search for novel NNRTIs by utilizing alternative drug design
11
12 strategies.¹¹⁵⁻¹¹⁷ Although resistance may not be avoided entirely, designing new
13
14 inhibitors based on the medicinal chemistry strategies discussed here could alleviate the
15
16 prevalence of drug resistance.¹¹⁸
17
18
19
20
21

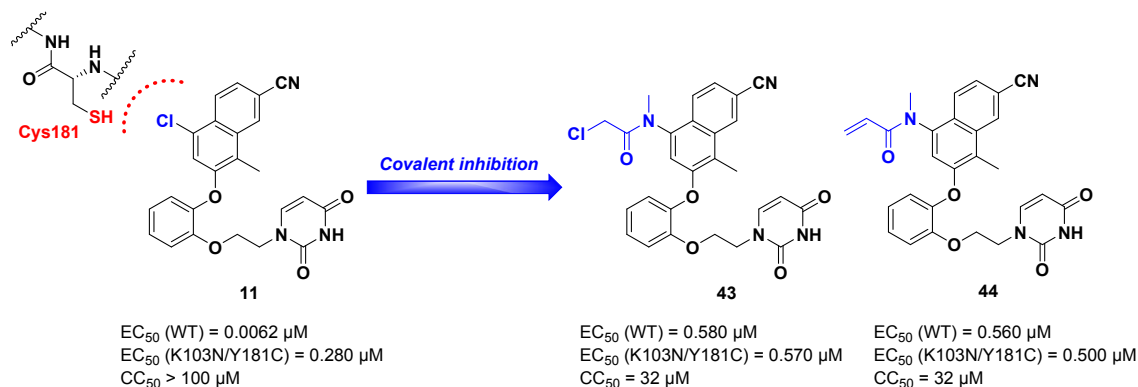
22 **4.1. Covalent Binding Strategy**

23
24

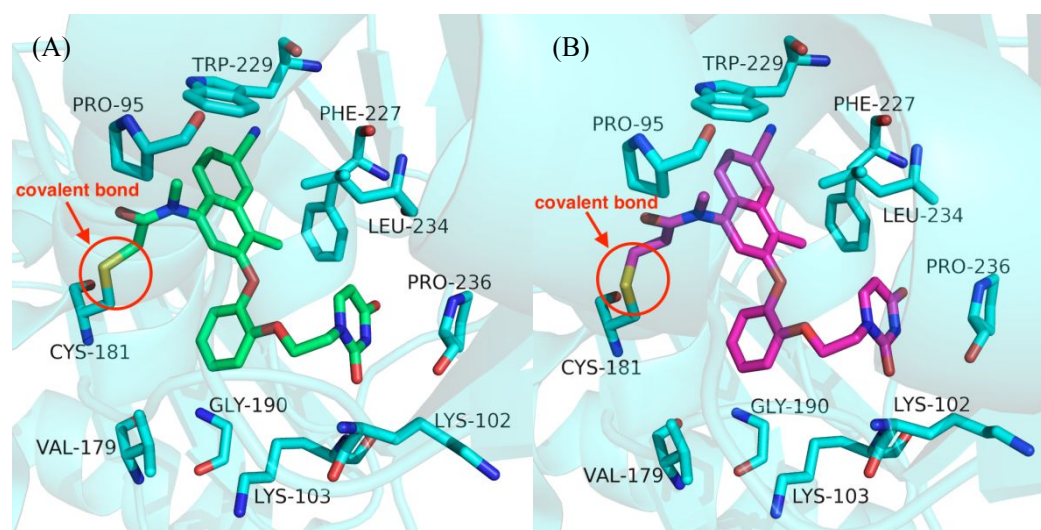
25 Covalent inhibitors exert their biological functions by reacting irreversibly or
26
27 reversibly with nucleophilic groups of proteins.¹¹⁹⁻¹²¹ The covalent binding strategy
28
29 enables the discovery of highly efficient, selective, and long-acting chemical molecules.
30
31

32 Y181C substitution is the most prevalent mutation after treatment with NNRTIs,
33
34 especially for NVP and EFV. To address this problem, novel NNRTIs targeting the
35
36 Y181C mutation were discovered *via* the covalent binding design strategy (**Figure 19**).
37
38 By analyzing the cocrystal structures of **11** and WT RT (**Figure 7A**), the chlorine atom
39
40 on the naphthalene ring of **11** points to the amino acid at position 181.¹²² Using **11** as a
41
42 lead compound, two types of relatively less reactive electrophilic substituents were
43
44 chosen to replace the chlorine atom, including haloamides and acrylamides. The
45
46 inhibitory ability of chloromethylamide **43** and the acrylamide **44** on variants
47
48 containing Cys181 presented a time-dependent characteristic; that is, the potency was
49
50 enhanced with increasing incubation time. Notably, after 48 h of incubation, the IC₅₀
51
52 values of compounds **43** and **44** against the variants were in the range of 0.14 to 0.19
53
54
55
56
57
58
59
60

1
2
3
4 μM , approximately 10 times lower than that against the WT strain. Time-dependent
5
6
7 inhibition kinetic analyses confirmed that compound **44** completely suppressed the
8
9
10 catalytic activity of Y181C RT after 72 h due to irreversible covalent binding. In
11
12
13 addition, mass spectrometry experiments revealed a single shifted peak on the p66
14
15
16 subunit of Y181C RT, and the added value was fully consistent with the molecular
17
18
19 weight of the corresponding inhibitors. Most importantly, the covalent bond between
20
21
22 the electrophilic warhead and Cys181 was visible in the cocrystal structures of **43** or **44**
23
24 and Y181C RT (**Figure 20**).



38 **Figure 19.** Identification of novel 2-naphthyl catechol diether derivatives as covalent NNRTIs by
39
40 targeting Cys181.



60 **Figure 20.** (A) Cocrystal structures of compound **43** (green) and Y181C RT (PDB code: 5VQX).

1
2
3
4 (B) Cocrystal structures of compound **44** (magenta) and Y181C RT (PDB code: 5VQV). The
5
6 covalent bond is shown as a yellow line.
7
8

9
10 Distinct from the covalent modification of the Y181C mutant protein, the design
11
12 of covalent inhibitors targeting WT RT seems more complicated due to the lack of
13
14 cysteine. Although NNIBP contains numerous lysine residues, they are located in the
15
16 solvent-exposed region and do not have sufficient nucleophilicity. In contrast, tyrosine
17
18 residues become preferred through potential covalent binding of the side chain phenolic
19
20 hydroxyl. Therefore, based on the cocrystal structures of **8** and WT RT (**Figure 4**), a
21
22 series of fluorosulfate-bearing derivatives of compound **8** were designed in light of the
23
24 stability of fluorosulfate and its relatively modest electrophilicity (**Figure 21**). As a
25
26 result, compounds **45–47** were identified as covalent inhibitors by the crystallographic
27
28 studies.¹²³ As shown in **Figure 22**, these compounds covalently modified Tyr181 to
29
30 form biaryl sulfate between tyrosine and the fluorosulfate group. Generally, the
31
32 inhibitory potency of covalent inhibitors improves with the extension of the incubation
33
34 time, and non-covalent inhibitors are not affected. However, the known covalent
35
36 inhibitors **45–47** did not show a typical time-dependent effect, while the potency of
37
38 other non-covalent inhibitors decreased significantly over time. The tested inhibitor
39
40 may have been partially degraded during the assay, as indicated by the decreasing
41
42 potency of the non-covalent inhibitor, but this effect was counteracted by the
43
44 irreversible binding of the covalent inhibitor to the enzyme. Moreover, the activity of
45
46 all of these compounds was substantially inferior to that of compound **8**, presumably
47
48 because the fluorosulfate group with increased bulk and polarity caused steric conflict
49
50
51
52
53
54
55
56
57
58
59
60

with Lys101 and weakened the binding affinity. Notably, mass spectrometry was used to confirm the covalent modifications, and an accurate mass increase was observed only for the p66 catalytic subunit.

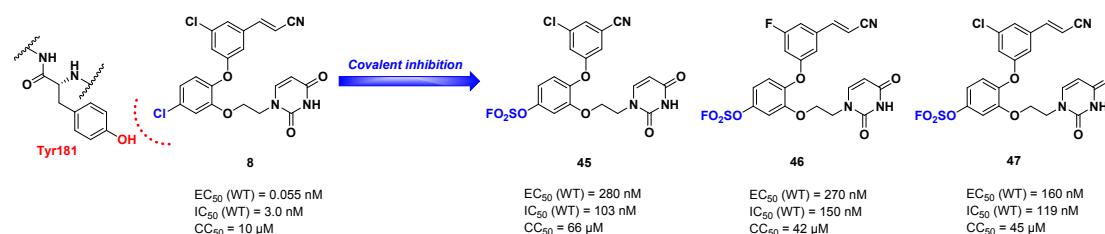


Figure 21. Identification of novel fluorosulfate-bearing derivatives as covalent NNRTIs by targeting Tyr181.

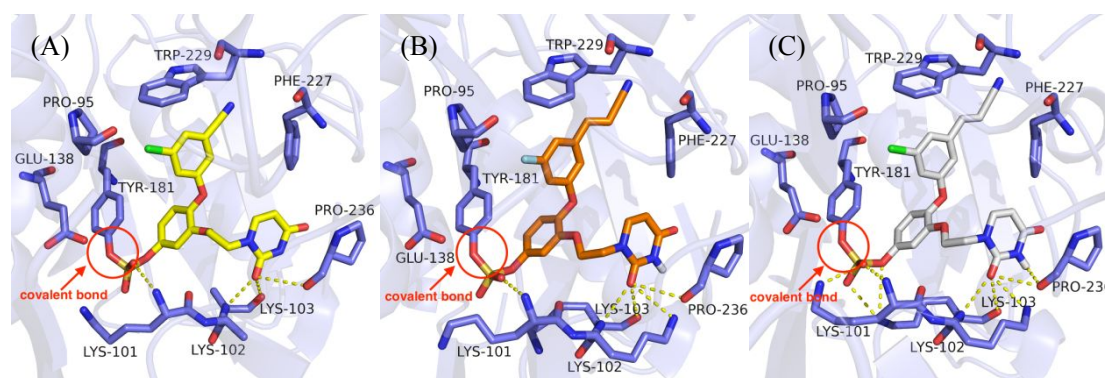


Figure 22. (A) Cocystal structures of compound **45** (yellow) and WT RT (PDB code: 7KRD). (B) Cocystal structures of compound **46** (orange) and WT RT (PDB code: 7KRF). (C) Cocystal structures of compound **47** (white) and WT RT (PDB code: 7KRC). The covalent bond is shown as a red line.

4.2. Targeting Highly Conserved Regions

Analysis of the nature of the amino acids in the binding site revealed that mutations occurred less frequently on highly conserved residues. Therefore, designing inhibitors that specifically interact with highly conserved residues while reducing the dependence on potentially variable residues holds promise as an alternative strategy for the treatment of constantly emerging mutants.^{124, 125}

1
2
3
4 The cyanovinyl moiety of RPV extends into the hydrophobic channel formed by
5
6 residues Tyr181, Tyr188, Phe227, and Trp229, contributing to an improvement in drug
7
8 resistance profiles. However, the electrophilic cyanovinyl group may lead to potential
9
10 covalent modification and high cytotoxicity as a Michael acceptor.¹²⁶ Therefore, to
11
12 extend the left-wing conjugation system, diverse biphenyl moieties were introduced to
13
14 increase the degree of aromaticity and stretch into the hydrophobic channel to
15
16 strengthen interactions with the highly conserved region (**Figure 23**); this work resulted
17
18 in the discovery of compound **48** bearing a 3,5-dimethyl-[1,1'-biphenyl]-4'-carbonitrile
19
20 substituent, which could strongly suppress the whole panel of viral strains.¹²⁷ Afterward,
21
22 a series of nondimethylphenyl DAPYs were identified to overcome the high
23
24 cytotoxicity of **48**, and the most active 3,5-difluoro biphenyl derivative **49** showed
25
26 prominent inhibitory activity and no apparent cytotoxicity.¹²⁸ Further addition of a
27
28 methyl group to the central scaffold yielded compound **50** with better *in vitro* metabolic
29
30 stability.¹²⁹ In addition, a variety of aromatic heterocycles were introduced on the
31
32 terminal benzonitrile of **49** by using the fragment-based replacement strategy, leading
33
34 to the identification of compound **51** bearing a pyridinyl group with excellent
35
36 druggability (**Table 5**).¹³⁰
37
38
39
40
41
42
43
44
45
46
47
48
49
50
51
52
53
54
55
56
57
58
59
60

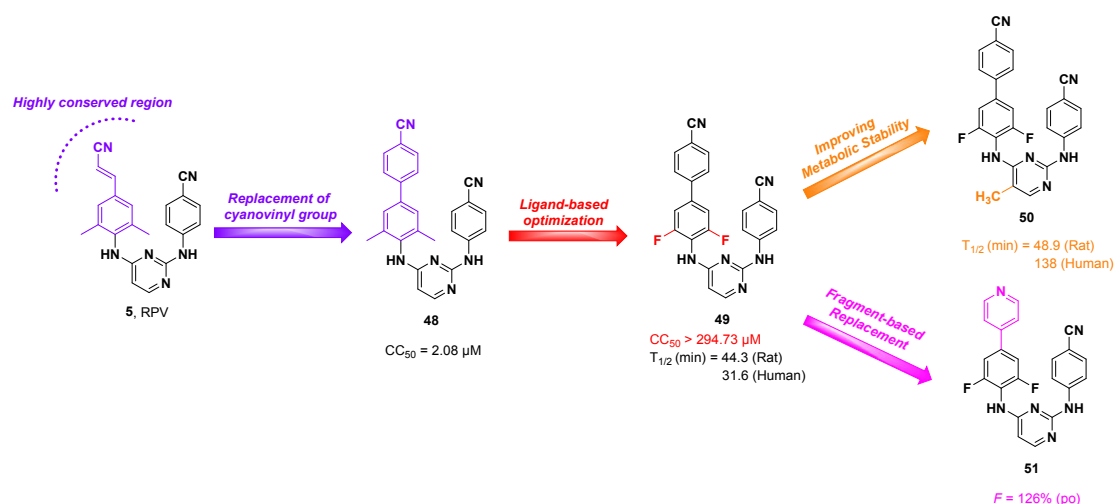


Figure 23. Development of DAPY-type NNRTIs bearing a biphenyl moiety.

Table 5. Antiviral Activity and Cytotoxicity of Compounds **48–51**.

Compd	EC ₅₀ (nM) ^a						CC ₅₀ (μM) ^b
	WT	L100I	K103N	Y181C	Y188L	E138K	
48	1±0.6	1.3±0.1	0.84±0.66	1.5±0.0	11±1	2±0.6	2.08±0.72
49	1.3±0	10.8±5	2.6±0	6.1±1	130±12	1.9±1	>294.73
50	1±0.32	16.3±5.3	5.4±1.8	11.2±1.9	-	8.3±1.5	>285
51	1.0±0	20.4±3.7	8±1.1	15±0.9	417±39	4±1.8	>313
EFV¹³⁰	4±1.5	44.7±12.6	91.5±23.6	5.4±1.2	269±31.2	7.5±0.54	>6.33
ETV¹³⁰	4±0.68	10.7±4.6	3.4±0.34	18.9±5.9	29.3±9.3	17.5±7.7	>4.60

^aEC₅₀: The EC₅₀ value is defined as the dose required to achieve 50% protection of the infected MT-4 cells by the MTT colorimetric method; antiviral curves were established from triplicate samples at each concentration.

^bCC₅₀: The CC₅₀ value is defined as the dose required to achieve 50% inhibition of MT-4 cell growth by the MTT colorimetric method; the toxicity curves were established from triplicate samples.

4.3. Targeting an Additional Binding Site

According to the classic concept of receptor–ligand interactions, an efficient NNRTI should interact with NNIBP and additional binding sites within RT as much as possible. The extraordinary advantage of this strategy lies in the interactions of the

1
2
3
4 molecule with other sites that can compensate for the decreased affinity caused by
5
6 specific amino acid mutations at one binding site, ensuring that the inhibitor is less
7
8 sensitive to variants.^{131, 132} Here, we demonstrated the application of this design strategy
9
10 in the following representative cases.
11
12

13
14 The NNRTI-adjacent binding site spanning the palm and connection domains was
15
16 identified as an unexploited new site approximately 14.46 Å from the NNIBP.¹³³ Based
17
18 on crystallographic studies, our group initially attempted to design dual-site NNRTIs
19
20 occupying both the NNIBP and NNRTI-adjacent binding sites (**Figure 24**). With ETV
21
22 as the lead compound, diverse substituents varying in volume and electronic nature
23
24 were incorporated into the sulfur atom or sulfone group of the central scaffold through
25
26 different linkers to fully explore the chemical space of the NNRTI-adjacent binding site
27
28 (**Figure 25**). Notably, the most potent compound **52** bearing a morpholine ring showed
29
30 superior activity and decreased cytotoxicity compared with ETV.¹³⁴ In the follow-up
31
32 optimization work, olefinic bonds with steric positioning advantages were creatively
33
34 introduced to ensure that the terminal moiety accurately stretched to the NNRTI-
35
36 adjacent binding site, as exemplified by the two most effective compounds **53** and **54**
37
38
39
40
41
42
43
44
45 (**Table 6**).¹³⁵
46
47
48
49
50
51
52
53
54
55
56
57
58
59
60

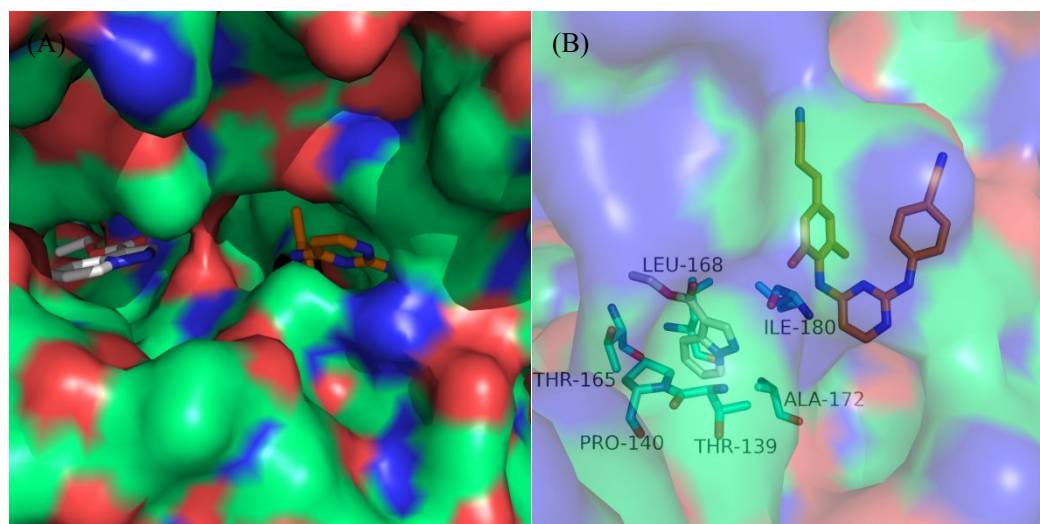


Figure 24. (A) Protein/solvent interface of NNIBP and the NNRTI-adjacent binding pocket (PDB code: 4KFB). (B) Cocystal structures of RPV and the NNRTI-adjacent fragment with WT RT (PDB code: 4KFB).

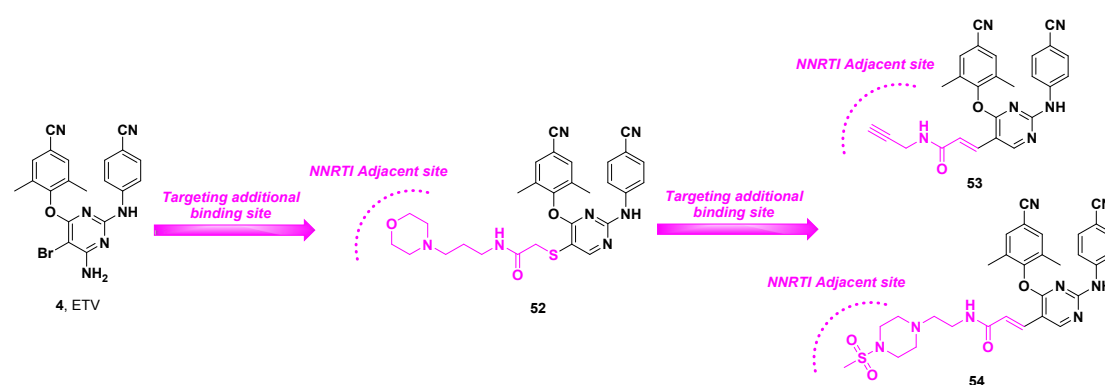


Figure 25. Design of novel NNRTIs by targeting the NNIBP and NNRTI-adjacent binding sites.

Table 6. Antiviral Activity and Cytotoxicity of Compounds 52–54.

Compd	EC ₅₀ (nM) ^a								CC ₅₀ (μM) ^b
	WT	L100I	K103N	Y181C	Y188L	E138K	F227L/V106A	K103N/Y181C	
52	2.6±1.1	6.5±2.2	1.4±0.3	11.6±1.0	16.2±2.6	6.0±0.6	105.9±20.9	345.2±69.7	27.2±4.6
53	5.20±1.50	113±33.4	10.4±0.60	61.8±13.2	64.5±15.6	10.6±3.00	402±313	1291±290	141±37.7
54	6.10±1.30	78.6±31.4	8.70±3.10	48.6±13.1	101±24.3	20.9±0.80	251±91.7	808±180	5.90±0.800
EFV ¹³⁴	5.2±0.9	81.0±16.6	98.8±24.4	6.7±1.4	370.8±43.9	6.3±2.4	218.5±85.1	225.4±113.2	>6.3
ETV ¹³⁴	4.0±0.3	20.1±7.29	3.3±0.6	17.6±4.5	34.1±12.2	16.9±10.0	27.6±3.0	35.0±12.9	2.2±0.1

^aEC₅₀: The EC₅₀ value is defined as the dose required to achieve 50% protection of the infected MT-4 cells by the

1
2
3
4 MTT colorimetric method; antiviral curves were established from triplicate samples at each concentration.
5

6 ^bCC₅₀: The CC₅₀ value is defined as the dose required to achieve 50% inhibition of MT-4 cell growth by the MTT
7
8
9 colorimetric method; the toxicity curves were established from triplicate samples.
10

11
12 As an important complement to NNRTIs, NRTIs cause chain termination during
13
14 DNA strand elongation rather than inhibit polymerase activity. Notably, the proximity
15
16 of the respective NRTI and NNRTI binding sites enabled the simultaneous occupation
17
18 of two sites and the rationality of developing novel chimeric inhibitors to achieve the
19
20 of two sites and the rationality of developing novel chimeric inhibitors to achieve the
21
22 synergistic inhibition of RT. Based on the available structural biology information,
23
24 chimeric NRTI/NNRTI bifunctional inhibitors connected by a flexible joint were
25
26 designed, and the positions of the anchor and the optimal length of the connecting linker
27
28 were determined with the aid of computer modeling (**Figure 26**). Specifically, the 2',3'-
29
30 dideohydrothymidine (d4T) was selected as an NRTI given its high binding affinity to
31
32 RT comparable to that of natural analogs. Accordingly, the conformational flexibility
33
34 of DAPY-type NNRTI (TMC-derivative) with retained basic pharmacophores was
35
36 utilized to accommodate the addition of the conjugate moiety. On the other hand, a
37
38 flexible PEG linker was used to connect the two moieties because of its favorable water
39
40 solubility and significant lipophilicity. Earlier efforts on chimera inhibitors
41
42 demonstrated that most of them are inactive, probably due to the failure of
43
44 phosphorylation of the nucleoside portion catalyzed by cellular kinases. Therefore, the
45
46 metabolically active triphosphate form was prepared directly in this work to bypass the
47
48 prerequisite pathway for catalysis to the phosphorylation requirement. Incorporation
49
50 assays indicated that the triphosphate form compound 4TTP-4PEG-TMC (**55**) could
51
52
53
54
55
56
57
58
59
60

1
2
3
4 bind to the active site and be incorporated as a substrate in a base-specific manner by
5
6 HIV-1 RT. In the biological evaluation *via* a steady-state competition assay, **55**
7
8 displayed the best activity against HIV-1 RT ($IC_{50} = 3$ nM), which was approximately
9
10 4.3 times more active than the TMC-derivative ($IC_{50} = 13$ nM) and 4300 times more
11
12 potent than d4T ($IC_{50} = 13000$ nM).¹³⁶
13
14
15

16
17 Similarly, in continued studies, connecting thymidine (THY) and TMC-derivative
18
19 through a polymethylene linker (ALK) produced a novel bifunctional inhibitor. In
20
21 particular, compounds THYHP-ALK-TMC (**56**) and THYTP-ALK-TMC (**57**)
22
23 exhibited higher enzymatic inhibition activity ($IC_{50} = 4.3$ and 6.0 nM, respectively),
24
25 with approximately 3- and 2-fold improvement compared to the parent TMC-derivative
26
27 ($IC_{50} = 13$ nM). Furthermore, compounds THY-ALK-TMC (**58**) and **56** were effective
28
29 against the WT strain with EC_{50} values of 0.12 and 0.22 μ M, respectively, being 30-
30
31 and 16-fold superior to that of d4T ($EC_{50} = 3.6$ μ M). Compounds **58** ($CC_{50} = 2.2$ μ M)
32
33 and **56** ($CC_{50} = 6$ μ M) showed moderate cytotoxicity equivalent to those of TMC-
34
35 derivative ($CC_{50} = 1.9$ μ M) and ddC ($CC_{50} = 4$ μ M).¹³⁷
36
37
38
39
40
41
42
43
44
45
46
47
48
49
50
51
52
53
54
55
56
57
58
59
60

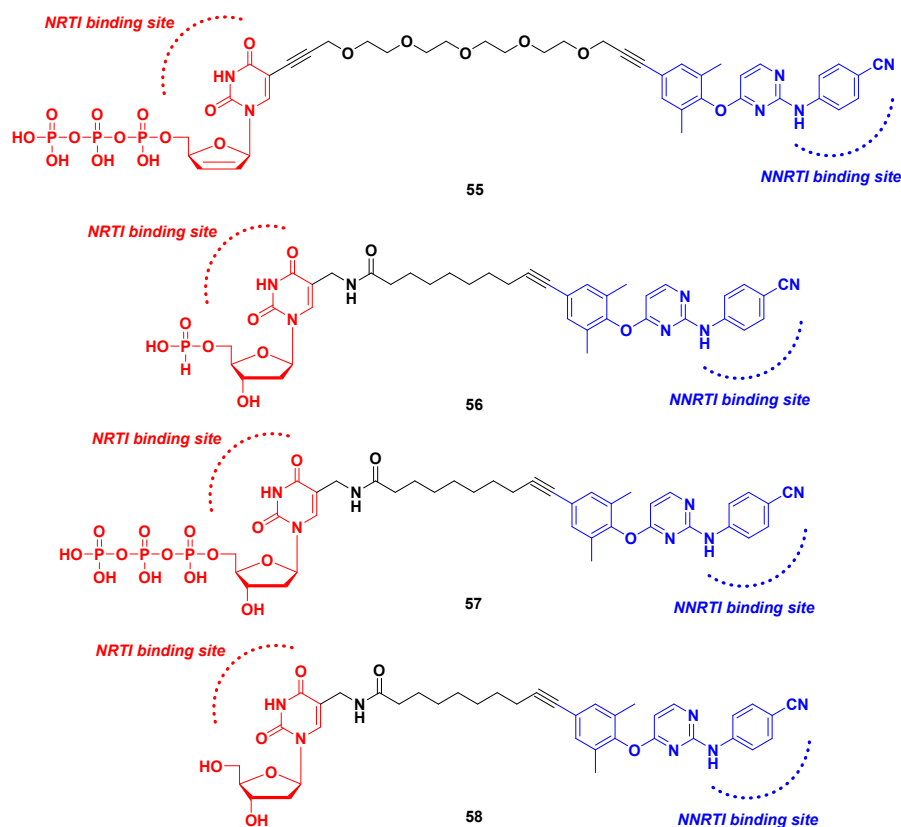


Figure 26. Discovery of novel chimeric NRTI/NNRTI bifunctional inhibitors.

To sum up, these encouraging results paved the way for the establishment of proof-of-concept and the design of highly effective bifunctional molecules. Since intracellular phosphorylation is indispensable, future research directions may include embedding bifunctional inhibitors in biodegradable nanogels for drug delivery or using alternative nucleotide-competing RT inhibitors (NcRTIs) that do not require activation by cellular kinases.

5. MEDICINAL CHEMISTRY STRATEGIES TO IMPROVE AQUEOUS SOLUBILITY

Drug solubility is a crucial physicochemical property required to characterize the active pharmaceutical ingredient during formulation selection and drug delivery.^{138, 139}

1
2
3
4 Because frequent daily medication remains an intractable issue in the clinical
5
6 application of NNRTIs due to poor aqueous solubility, there is still a need to search for
7
8 novel structural analogs that can achieve improved solubility without sacrificing the
9
10 original efficacy.
11
12

13 14 **5.1. Prodrug Approach**

15
16
17 The prodrug strategy proved to be an expedient approach to balance both potency
18
19 and drug-like profiles.^{140, 141} Notably, the propionylation modification of the
20
21 sulfonamide group was effectively confirmed as a potential prodrug strategy, such as
22
23 the COX-2 inhibitors valdecoxib and parecoxib.¹⁴² GW678248 (**27**), as a novel
24
25 benzophenone NNRTI, exhibits potent anti-HIV-1 activities toward mutant strains
26
27 associated with NVP and EFV (**Figure 27**).⁷⁹ Its *N*-acylated prodrug form designated
28
29 GW695634 (**59**) was developed as a potential drug candidate with significantly
30
31 improved aqueous solubility (Sol. = 92 mg/mL) compared to GW678248 (Sol. = 0.18
32
33 µg/mL).¹⁴³ GW695634 can be converted into the active metabolite GW678248 by
34
35 endogenous proteinases.^{79, 144} However, GW695634 did not achieve the expected
36
37 favorable outcome after the phase II trial. In addition, drug-related adverse events
38
39 including rash, nausea, and diarrhea, were observed in patients. Therefore, by January
40
41 2006, the development of GW695634 was discontinued due to safety issues.¹⁴⁵
42
43
44
45
46
47
48
49

50
51 In addition, the *N*-propionyl sulfonamide prodrug strategy was successfully
52
53 applied in the development of elsulfavirine (**61**), a prodrug that received approval in
54
55 Russia to treat HIV infection and was generated by propionylation of the small
56
57 molecule selective NNRTI VM-1500A (**60**) terminal sulfonamide group
58
59
60

(Figure 27).¹⁴⁶ The orally formulated prodrug elsulfavirine can be transformed into the active parent drug VM-1500A through hydrolysis and loss of propionic acid. Elsulfavirine showed excellent tolerability, a favorable safety profile, and high efficacy. The recommended combination regimen includes elsulfavirine, plus two NRTIs, tenofovir disoproxil fumarate and emtricitabine, which was shown to be equally efficacious to EFV-based therapy with fewer adverse CNS and skin adverse events.¹⁴⁷⁻

149

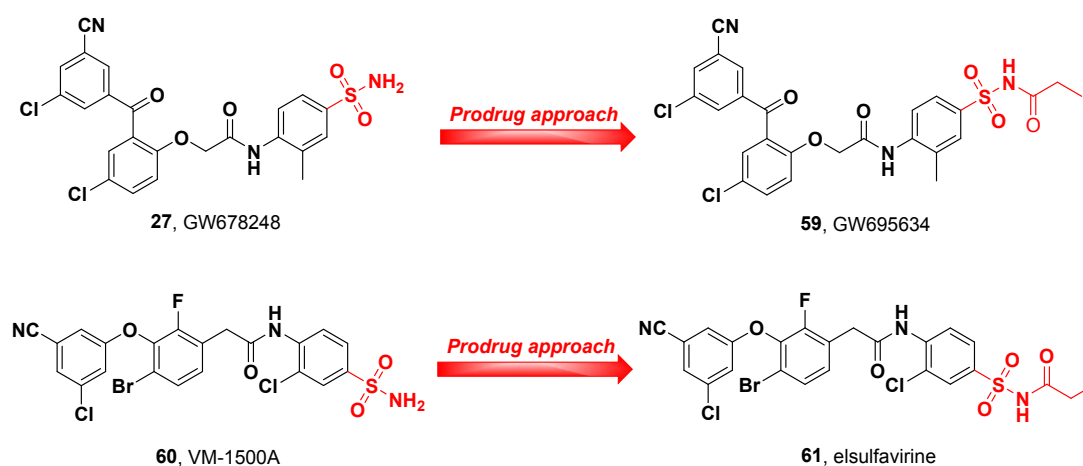
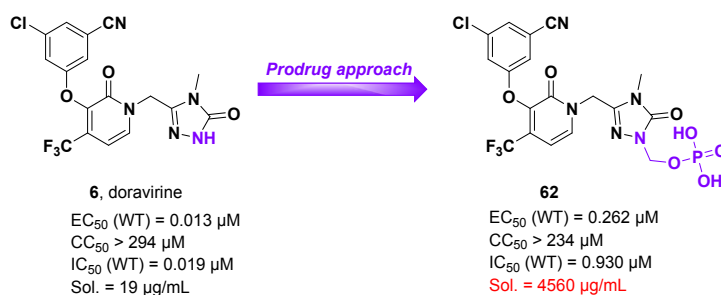


Figure 27. Application of the prodrug strategy in GW695634 and elsulfavirine.

By utilizing the prodrug strategy, the replacement of the methylene phosphate group with the *NH* of the DOR triazole ring yielded prodrug **62** with acceptable potency in antiviral and RT inhibitory assays. The aqueous solubility of **62** was 4560 $\mu\text{g/mL}$, while that of DOR was only 19 $\mu\text{g/mL}$ under the same conditions of pH 7.0. Compound **62** also displayed sufficient chemical stability *in vitro*. All these specific examples suggest the availability and versatility of the prodrug strategy to increase the aqueous solubility of insoluble compounds (Figure 28).¹⁵⁰



13 **Figure 28.** Optimization of doravirine *via* a prodrug approach.

14
15
16 **5.2. Introducing Hydrophilic Groups into the Solvent-Exposed Region**

17
18 Solvent-exposed regions, as broad modification spaces, are expected to effectively
19 accommodate different kinds of chemical structures and participate in the formation of
20 additional interactions.¹⁵¹ In addition to the commonly used prodrug strategies, the
21 introduction of solubilizing substituents into the solvent-exposed region has been
22 proven to be equally effective for improving solubility-limited physicochemical
23 properties.
24
25
26
27
28
29
30
31
32

33
34 To enhance the antiviral potency of the previously discovered morpholine-
35 containing compound **63** and maintain its good solubility, the introduction of a
36 hydrophilic methylsulfonyl-substituted piperazine moiety yielded compound **64** with
37 moderate activities and improved solubility (**Figure 29**).¹⁵² Thereafter, with a focus on
38 the substituted piperazine fragment pointing toward the solvent-exposed region, the
39 incorporation of dominant scaffolds of **19** and **38** led to the discovery of compounds **65**
40 and **66**, featuring the same sulfonamide group with substantially increased solubility
41 and without severe loss of potency.¹⁵³ Currently, the fraction of sp³ carbon atoms is
42 introduced as a parameter to determine the saturation and complexity of spatial
43 structures.^{154, 155} Guided by this design assumption, different saturated polar groups
44 were introduced to enrich the SARs around the solvent-exposed region, leading to the
45
46
47
48
49
50
51
52
53
54
55
56
57
58
59
60

identification of compound **67**, which displayed improved drug resistance profiles against several single mutant strains and favorable water solubility (**Table 7**).¹⁵⁶

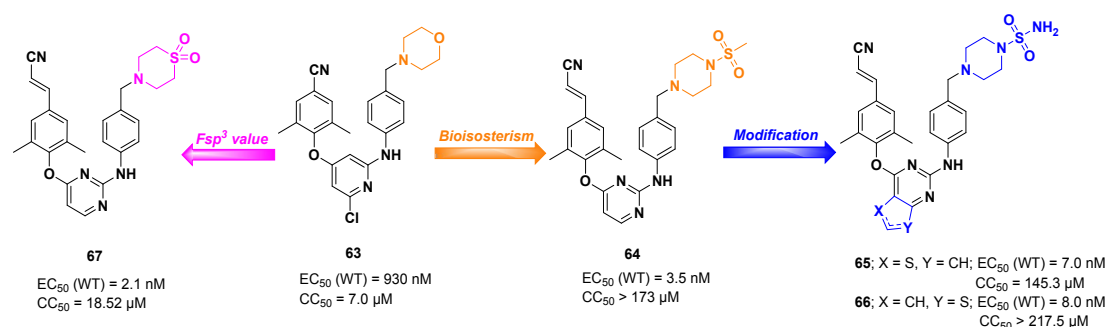


Figure 29. Improve the aqueous solubility by introducing hydrophilic substituents into the solvent-exposed region.

Table 7. Aqueous Solubility of Compounds **64–67**.

Compd	64	65	66	67	ETV ¹⁵³
pH = 7.4 (μ g/mL) ^a	-	39.5	38.9	-	<1
pH = 7.0 (μ g/mL) ^a	30.92	49.7	49.3	34.0	<1
pH = 2.0 (μ g/mL) ^a	-	73.1	64.9	-	127

^aAqueous solubility: The aqueous solubility of the test compound was determined under different pH values. The assay was measured at least in duplicate.

6. MULTITARGET-DIRECTED LIGANDS

In the last few decades, the "one target, one compound" paradigm has achieved unprecedented success in the pharmaceutical industry. However, with the advancement of the pathogenesis of multifactorial disease research, it is evident that this single-target drug does not always guarantee satisfactory efficacy. Although the mixed dose of multiple drugs featuring complementary mechanisms of action may be a quicker and more flexible approach for multitarget therapeutics, such combination is often hindered

1
2
3
4 by poor patient compliance and unpredictable PK profiles.^{157, 158} An alternative
5
6 approach, termed the multitarget-directed ligand (MTDL) strategy, considers
7
8 developing drugs that can interact with more than one biological target involved in
9
10 complex diseases.¹⁵⁹ Currently, the rational design of multifunctional ligands by subtly
11
12 combining the essential pharmacophores of multiple drugs acting on various targets is
13
14 attracting significant attention.¹⁶⁰ The concept of the MTDL strategy is particularly
15
16 applicable to HIV-1 inhibitor design, with the apparent virtue of simultaneously
17
18 modulating multiple targets during the virus replication process.
19
20
21
22
23

24
25 Integrase (IN) is responsible for catalyzing the essential process of viral DNA
26
27 integration into host DNA. Since IN has no homologous enzyme in humans, both IN
28
29 and RT are regarded as validated targets for developing anti-HIV drugs. Moreover, the
30
31 high structural and functional analogies between RT and IN led to the similarity of the
32
33 pharmacophores required by inhibitors, providing the foundation for the intentional
34
35 design of dual inhibitors.^{161, 162} Introducing the aryl diketoacid moiety of IN inhibitor
36
37 **68** at the *N*-1 position of HEPT-type NNRTI TNK-651 (**15**) afforded four hybrid
38
39 inhibitors (**Figure 30**). The enzyme inhibition assay results showed that the activity of
40
41 all the dual inhibitors was greater than or similar to that of **15** against RT, indicating
42
43 that the open channel surrounding the *N*-1 phenyl could accommodate structural
44
45 modifications. All tested compounds also potently inhibited IN at low micromolar
46
47 concentrations, at least one order of magnitude lower than that of **68**. The best
48
49 compound **69** displayed excellent potency against HIV-1 ($EC_{50} = 9.7$ nM) and a high
50
51 selectivity index ($SI > 1000$).¹⁶³ The discrepancy between the RT and IN inhibitory
52
53
54
55
56
57
58
59
60

activities prompted a detailed exploration of SARs by systematic modification of compound **70**, including the insertion of benzyl into the N-1 linker, the extension of the N-1 linker, and the incorporation of a diketoacid group into the C-2 or N-3 linker. However, four subseries of compounds exhibited weak or lost potency against RT and IN.¹⁶⁴ On the other hand, substituting the diketoacid functionality at the C-5 or C-7 position of the approved drug delavirdine's indole ring to replace the original methyl sulfonamide group yielded a series of delavirdine derivatives. The biological activity results showed that the C-5 substitution was preferred over the C-7 substitution, probably because the angular conformation of the latter might not be conducive for binding to IN and partially reduce the electrostatic interactions with K103 and K104 in RT. It was also observed that substituting a halogen at indole significantly decreased the RT-inhibition potency and slightly increased the IN-inhibition potency, achieving the equilibrium activities toward RT and IN of compounds **71** and **72**.¹⁶⁵

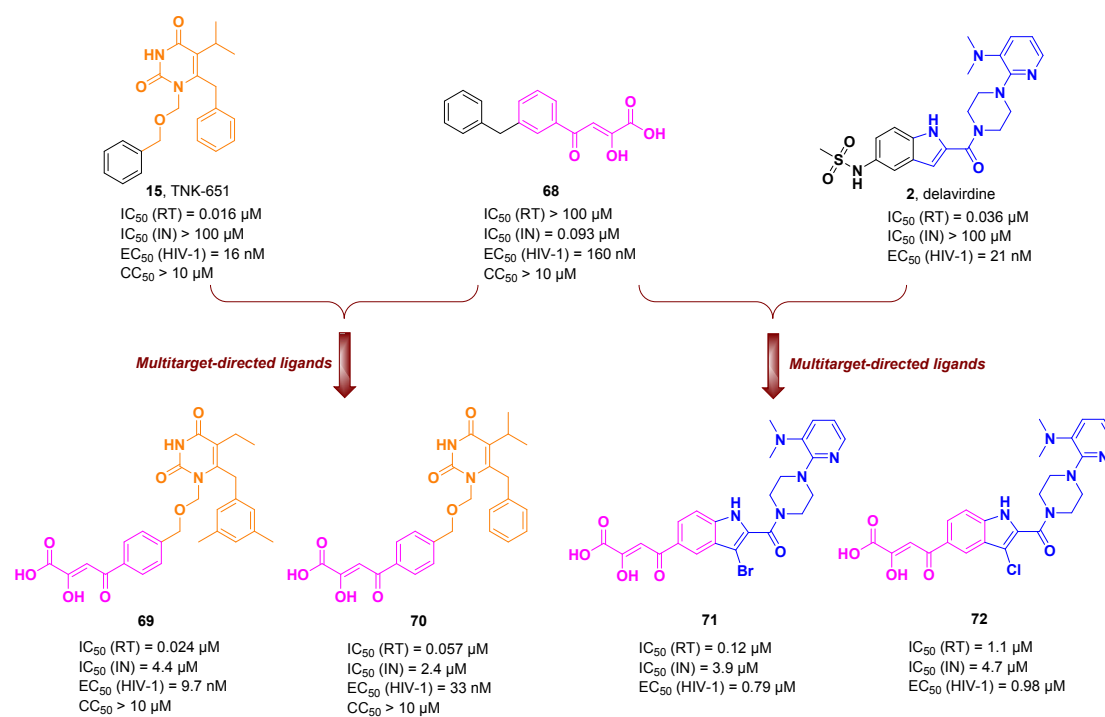


Figure 30. Design of multitarget-directed ligands as RT/IN dual inhibitors.

The simplified pharmacophore model revealed that IN binding requires a minimum of two magnesium ions chelating triad and one hydrophobic benzyl group. *N*-3 hydroxylation of the HEPT analog afforded a series of pyrimidine-2,4-dione derivatives. The development of this series was encouraged by molecular docking into NNIBP and the IN catalytic core domain (CCD). The new hydroxy group could maintain the key hydrogen bonding between the ligand and K101 in NNIBP to avoid significantly compromising the affinity with RT. The C(2)O–N(3)OH–C(4)O acts as a functional group to chelate two metal ions and, together with the benzyl moiety, meets the basic pharmacophore requirements. SAR analysis indicated that the OH group at *N*-3 was indispensable for the inhibitory effect on IN and that the oxybenzyl moiety at *N*-1 was also important for IN inhibition (**Figure 31**). The most potent compound **74** was able to dually inhibit IN and RT, and **74** also displayed equipotent antiviral potency compared to TNK-651 ($EC_{50} = 13$ nM).¹⁶⁶ After the discovery of potent dual inhibitor **74** with a novel chemotype for an IN inhibitor, further optimizations focused on the three structural features around lead **74**, namely, the aromatic and chelating domains, linker domain, and hydrophobic domain. The SARs results can be summarized as follows: further improvement in anti-IN activity can be achieved by halogen substitution of the *N*-1 benzyl under the premise of keeping the *N*-3 OH group unchanged. The length and atomic nature of the linker affect the affinity of the molecule to IN by controlling the spatial orientation between the chelating functionality and *N*-1 oxybenzyl moiety, and the optimal linker should include a carbon chain of 3 to 4 atoms.

The hydrophobic domain has an elusive influence on IN inhibition, and this region predominantly affects the activity in cooperation with the linker domain. This study resulted in the discovery of compounds **73–75**, featuring a CH₂OCH₂ linker offering both high IN-inhibitory activity and favorable anti-HIV potency for further development.¹⁶⁷

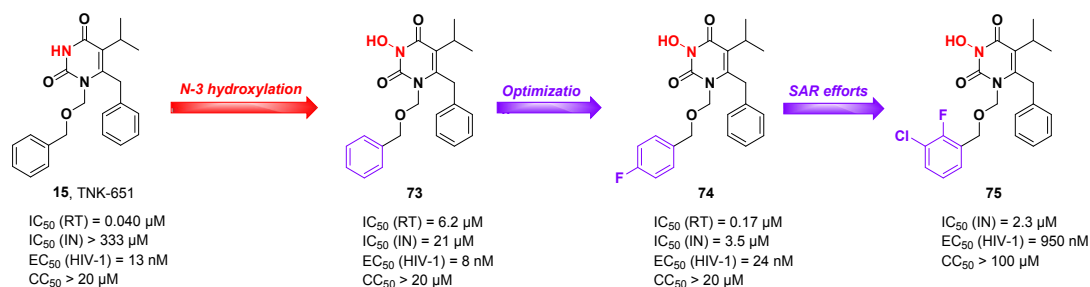


Figure 31. Optimization of TNK-651 as an RT/IN dual inhibitor.

7. CONCLUDING REMARKS AND FUTURE PERSPECTIVES

Since the first clinical identification of AIDS in the 1980s, significant scientific progress has been made in exploring related therapeutic treatments. However, the growing number of HIV-infected people reminds us that AIDS continues to be a severe pandemic disease throughout the world, and unremitting efforts are still needed to develop novel anti-HIV agents due to the lack of vaccines.

Drug discovery is a complex, expensive, and lengthy endeavor that includes a range of procedures from hit compound discovery to preclinical evaluation to clinical verification, especially when searching for pioneering drugs that target novel and unproven therapeutically relevant mechanisms. The elusiveness of therapeutically beneficial targets has prompted medicinal chemists to exploit validated targets thoroughly. In contrast, follow-up campaigns seem to be more economical and safer for

1
2
3
4 generating potential chemical entities with clinical application differentiation by
5
6 optimizing known bioactive molecules. Therefore, due to its unique mechanism of
7
8 action and well-known 3D structure, RT has attracted much attention as a validated
9
10 target in drug design and spawned potent NNRTIs as a major component of the HAART
11
12 regimen.
13
14
15

16
17 Significant progress has been achieved in the lead discovery and lead optimization
18
19 of different classes of NNRTIs by applying classical medicinal chemistry strategies, as
20
21 reviewed above. However, despite the success of many approved NNRTIs, drug
22
23 resistance still cannot be prevented due to the evolution of HIV-1 strains, especially
24
25 under drug selective pressure, and key amino acid mutations in NNIBP may greatly
26
27 affect the binding affinity between inhibitors and RT. In addition, there is little evidence
28
29 that any mutation can reduce the sensitivity to only one drug, so almost all mutations
30
31 confer a high level of cross-resistance to NNRTIs. Notably, precise sequence detection
32
33 of mutated amino acids has proven to be a prerequisite for successfully overcoming
34
35 drug resistance. This is an arduous multidisciplinary task, and it is reasonable to
36
37 cooperate closely with structural biologists while applying traditional medicinal
38
39 chemistry as the core component.
40
41
42
43
44
45
46
47

48 Currently, a new technology termed proteolysis targeting chimera (PROTAC)
49
50 takes advantage of the intracellular mechanism of the ubiquitin–proteasome system to
51
52 specifically degrade and eliminate proteins related to human diseases by simultaneously
53
54 binding the target of interest and the E3 ubiquitin ligase.^{168, 169} The PROTAC strategy
55
56 has been successfully used to identify effective molecules that inhibit and induce
57
58
59
60

1
2
3
4 hepatitis C virus (HCV) protease degradation.¹⁷⁰ However, it is now clear that HIV-1
5
6 reverse transcription takes place within the intact capsid in infected cells.^{171, 172} The
7
8 capsid plays important roles in the virus replication cycle, maintaining RT and genetic
9
10 material in the internal environment and thereby increasing the efficiency of reverse
11
12 transcription. Thus, we wish to point out that RT will not be an accessible target for
13
14 ubiquitination or degradation using a PROTAC strategy, as the E3 ligase ligand moiety
15
16 of the PROTAC molecule cannot normally recruit the E3 ubiquitin ligase in the host
17
18 cell to induce ubiquitination and degradation.
19
20
21
22
23
24

25 As diverse modern drug discovery strategies continue to mature and improve, the
26
27 development of novel NNRTIs will move from fortuitous discovery and trial-and-error
28
29 approaches to an elaborate design. In this regard, we discussed potential design
30
31 strategies for the rational optimization of new generation NNRTIs from the perspective
32
33 of medicinal chemistry.
34
35
36

37 **7.1. Advantages of Conformational Flexibility**

38
39
40 Resistance to first-generation drugs has developed rapidly because the structural
41
42 rigidity of these drugs prevents them from adapting to amino acid mutations. In contrast,
43
44 the intrinsic features of second-generation NNRTIs ETV and RPV with torsional
45
46 flexibility (“wiggling”) and repositioning ability (“jiggling”) allow them to adjust to
47
48 changes in the mutated NNIBP and minimize the loss of binding stabilization.^{109, 111}
49
50
51 ETV and RPV, with a more flexible horseshoe conformation, can be accommodated
52
53 well within variational NNIBP based on molecular movements and tiny side chain
54
55 rearrangements. More importantly, crystallographic studies revealed that RPV can
56
57
58
59
60

1
2
3
4 induce localized changes in NNIBP by using the structural flexibility of RT, thereby
5
6 establishing interactions with Y183 to compensate for the weakened π - π stacking
7
8 interactions after Y181C substitution.¹¹² It is evident that conformational flexibility and
9
10 positional adaptability ensure efficient binding and account for their maintained
11
12 potency in the presence of resistant mutations. Therefore, the exploitation of more
13
14 flexible inhibitors while taking advantage of the potential flexibility of RT within a
15
16 reasonable range raises a new opportunity to overcome drug resistance by adopting
17
18 multiple conformations to adapt for the mutated binding pockets.
19
20
21
22
23

24 **7.2. Targeting Highly Conserved Residues**

25
26
27 Earlier-generation NNRTIs mainly relied on the π - π stacking interaction with
28
29 aromatic residues Y181 and Y188, which were lost when tyrosine was replaced by non-
30
31 aromatic cysteine or leucine, resulting in drug resistance to these inhibitors.^{30, 31} The
32
33 design of novel NNRTIs should minimize the dependence on the interactions with the
34
35 readily mutated residues Y181 and Y188 while strengthening the interaction with the
36
37 highly conserved region composed of F227, W229, and L234, which are less prone to
38
39 mutation. Analysis of the mutation nature of residues and identification of highly
40
41 conserved residues within NNIBP are essential for rational design.
42
43
44
45
46
47

48 **7.3. Developing Main Chain Hydrogen Bonds**

49
50 The pyrimidinyl nitrogen and the right imino linker of ETV and RPV form the
51
52 “signature” dual hydrogen bonds with the K101 backbone that are necessary to
53
54 maintain binding affinity.¹⁷³ In addition, the left imino linker of RPV participates in
55
56 hydrogen-bonding interactions with the E138 main chain *via* a bridging water molecule.
57
58
59
60

1
2
3
4 Similarly, it can be observed that DOR is involved in a key hydrogen bond between the
5
6 methyltriazolone moiety and the K103 backbone.⁸⁷ The extensive hydrogen-bonding
7
8 network between ligands and the amino acid main chain greatly contributes to the free
9
10 energy for target binding, and it will continue to be maintained regardless of the side
11
12 chain mutations.
13
14
15

16 17 **7.4. Targeting Solvent-Exposed Regions** 18

19
20 The solvent-exposed region provides potential chemical space for substantial
21
22 modifications of known bioactive compounds, commonly by introducing charged and
23
24 polar groups to enhance binding affinity with the protein or introducing additional
25
26 pharmacophores to construct multifunctional ligands. Consistently, NNRTIs are mostly
27
28 hydrophobic, so the introduction of hydrophilic groups can also improve the
29
30 pharmacokinetic profiles for oral administration.
31
32
33

34 35 **7.5. Designing Covalent Inhibitors** 36

37
38 The covalent drug design strategy offers potential gains such as higher potency,
39
40 reduced drug resistance, and prolonged duration of target engagement. In addition to
41
42 the common acrylamide and sulfonyl fluoride that have been successfully applied, boric
43
44 and boronic acids are able to be used as functional groups in the construction of covalent
45
46 inhibitors.¹⁷⁴ The distinction between boron atoms and carbon atoms lies in the presence
47
48 of an empty p-type atomic orbital that allows the reversible formation of covalent bonds
49
50 with oxygen nucleophilic residues. The development of specific warheads chemically
51
52 reactive to certain residues is expected to provide new covalent NNRTIs with high
53
54 activity and few off-target effects. In addition to the rational selection of warheads to
55
56
57
58
59
60

1
2
3
4 modulate optimal covalent reactions, continuous attempts should be made to enhance
5
6 non-covalent and specific binding to target proteins reversibly.
7
8

9 **7.6. Introducing Privileged Halogen Atoms**

10
11 The optimization of EFV suggested that the trifluoromethyl group can reduce the
12
13 molecular pKa value and increase the affinity with NNIBP through strong hydrogen-
14
15 bonding interactions.¹⁷⁵ Furthermore, the introduction of trifluoromethyl to the
16
17 pyridone scaffold of DOR led to improved plasma stability and a prolonged half-life.⁸⁷
18
19 In addition to fluorine, the bromine atom of ETV contributes to the formation of
20
21 electrostatic interactions with L100 and V179 to enhance antiviral activity.¹⁰⁹ As
22
23 privileged substituents in NNRTI design, halogen atoms play an important role in
24
25 improving metabolic stability and optimizing pharmacological parameters such as
26
27 lipophilicity and permeability. In addition, the steric effects of halogens allow these
28
29 bulky atoms to fully occupy the chemical space of the target. More recently, halogen
30
31 bonds involving an electrophilic region of the halogen atom with a nucleophilic region
32
33 of the halogen-bonding acceptor have been recognized to be beneficial for the stability
34
35 of molecule–protein interactions.
36
37
38
39
40
41
42
43
44

45 **7.7. Exploiting Unconventional Binding Sites**

46
47 The discovery of NNRTIs acting at newly emerging binding sites contributes to
48
49 the exploration of potential interactions and enhancement of binding affinity to the
50
51 target as much as possible. Fragment screening based on crystallographic studies
52
53 identified seven novel binding sites of RT, three of which (knuckles, NNRTI-adjacent,
54
55 and incoming nucleotide binding) proved to be inhibitory in enzymatic assays.¹³³
56
57
58
59
60

1
2
3
4 Further crystallographic studies of 2,4,5-trisubstituted pyrimidines revealed that the
5
6 pyridine ring extends from the NNIBP toward the NNRTI-adjacent site, allowing the
7
8 design of dual-site NNRTIs through fragment linking or merging.⁶⁶ Moreover, the
9
10 proximity of the NRTI-binding pocket and the NNRTI-binding pocket enabled the
11
12 simultaneous occupation of two sites to achieve synergistic inhibition of RT. Very
13
14 recently, cocrystal structures of RT and gp120 antagonists indicated that they can
15
16 inhibit RT by linking the NRTI-binding pocket and the NNRTI-binding pocket.¹⁷⁶
17
18
19 Notably, the rational design of bifunctional NNRTIs as an alternative strategy to
20
21 enhance activity and alleviate drug resistance needs to take into account the
22
23 simplification of individual pharmacophores, the positions of attachment points on
24
25 multiple ligands, and the nature and length of the specific linker that orient the ligands
26
27 in an appropriate binding conformation.
28
29
30
31
32
33

34 **7.8. Targeting Host Factors involved in Reverse Transcription**

35
36
37 In addition to the interactions between viral proteins and ligands, host factors
38
39 closely related to pathogenic targets need to be considered seriously.¹⁷⁷ Compared to
40
41 drugs targeting viral proteins, host-targeting antiviral agents possess broad-spectrum
42
43 antiviral activities and higher genetic barriers, providing new insights for overcoming
44
45 drug resistance.¹⁷⁸ Host-derived RNA helicase A (RHA) is involved in many key stages
46
47 of the viral replication process and can be assembled together with the viral RNA
48
49 genome into the capsid core.^{179, 180} RHA, as an RT processivity factor, promotes reverse
50
51 transcription efficiency, so viruses lacking RHA are less infectious due to the reduced
52
53 DNA synthesis rate generated from genomic RNA.¹⁸¹ Since viruses are less likely to
54
55
56
57
58
59
60

1
2
3
4 mutate to replace missing host cell functions needed for viral replication, the possibility
5
6 of selecting resistant mutants toward host-directed agents is reduced. Nonetheless,
7
8 continued application of host-targeting drugs may facilitate viral switching to bind
9
10 alternative host factors or enhance viral efficiency to replicate optimally under limited
11
12 host factors; for example, emerged strains with partial maraviroc resistance may use
13
14 alternate co-receptors CXCR4 or alter its binding affinity with CCR5.¹⁸²⁻¹⁸⁴ Therefore,
15
16 the key to developing antiviral drugs that target host factors (such as RHA) involved in
17
18 reverse transcription is to clearly elucidate the internal connection and mechanism of
19
20 action between the host cell and HIV-1.
21
22
23
24
25

26 27 **7.9. Long-Acting Formulations and Preexposure Prophylaxis Agents** 28 29

30 Poor compliance leads to irregular drug concentrations and incomplete viral
31
32 suppression that in turn readily induces drug resistance and treatment failure.
33
34 Consequently, the application of alternative long-acting formulations should be
35
36 conducive to overcoming patient compliance challenges that lead to drug resistance.
37
38 The new long-acting regimen containing extended release injectable nanosuspensions
39
40 of cabotegravir plus rilpivirine was approved by the U.S. FDA in 2021 as the first
41
42 injectable complete regimen (Cabenuva[®]) due to its good tolerance, lack of adverse
43
44 reactions, and non-inferiority to the current standard oral therapy.¹⁸⁵⁻¹⁸⁷
45
46
47
48
49

50 In particular, we wish to emphasize that the fight against AIDS is a long-term
51
52 campaign, so the use of PrEP agents in high-risk individuals and the popularization of
53
54 related prevention knowledge are also particularly important. Another promising
55
56 DAPY-type NNRTI dapivirine, which was developed in the form of a vaginal
57
58
59
60

1
2
3
4 microbicide, was approved by the European Medicines Agency (EMA) in 2020 as an
5
6 effective PrEP agent for HIV-1 prevention.¹⁸⁸⁻¹⁹⁰ As prescriptions and treatments
7
8 become more personalized, the application of precision medicine based on individual
9
10 patient information may be promising in the future, despite being relatively advanced
11
12 in the field of antiviral therapy.
13
14
15

16 **7.10. Prediction and Evaluation of ADMET Properties**

17
18
19 Finally, most promising drug candidates are eventually forced to be suspended at
20
21 the late stage of drug development due to their toxicity or poor PK profiles rather than
22
23 efficacy. For example, fosdevirine (GSK2248761) is a potent and selective NNRTI
24
25 drug candidate previously developed by the GSK team.¹⁹¹ However, the high incidence
26
27 of delayed seizures after administration and persistent seizures after withdrawal
28
29 observed in treatment-experienced individuals ultimately led to the failure of its
30
31 development after a phase IIb clinical trial.¹⁹² The predominant cysteine-conjugated
32
33 metabolite derived from the Michael addition of the electrophilic cyanovinylphenyl
34
35 group of fosdevirine with glutathione was considered to be the cause of CNS toxicity.¹²⁶
36
37 In addition, animal toxicity, a high oxidative metabolism rate, and poor effects of the
38
39 combination therapy caused the development of capravirine (S-1153, AG1549) to be
40
41 suspended after phase IIb clinical trials.^{193, 194} Therefore, in the optimization process of
42
43 NNRTIs, more attention should be given to early drug-likeness research, especially the
44
45 prediction and evaluation of ADMET properties.
46
47
48
49
50
51
52
53
54

55
56 However, the testing capabilities of *in vivo* and *in vitro* ADMET assay seem
57
58 stretched thin in the face of large amounts of screening efforts. Currently, *in silico*
59
60

1
2
3
4 ADMET prediction platforms have been developed to evaluate these properties in an
5
6 economical and efficient way. Available open-access tools such as admetSAR 2.0¹⁹⁵
7
8 and ADMETlab 2.0¹⁹⁶ are fully integrated with ADMET prediction platforms that are
9
10 capable of excluding undesirable drug candidates, which can predict ADMET from
11
12 their chemical structure before practical synthesis. The accuracy of an *in silico* ADMET
13
14 prediction tool depends on the quality of the experimental data in the database, the
15
16 validation criteria and the design ideas of the developed model. To obtain reliable
17
18 predictions, researchers should use different *in silico* tools for comparison, followed by
19
20 identifying the most likely prediction results.
21
22
23
24
25

26
27 Currently, the development of antiviral drugs with low toxicity and high
28
29 tolerability to improve patient compliance remains a challenging task. Therefore, the
30
31 application of a drug repositioning strategy to screen anti-HIV hits from available drugs
32
33 with reliable physicochemical properties and safety will also demonstrate great
34
35 potential, which has been proven to be valuable and powerful in the prompt treatment
36
37 of the recent large-scale outbreak of the infectious virus SARS-CoV-2.^{197, 198}
38
39
40
41
42

43 In summary, this article describes the molecular structure and discovery campaign
44
45 of novel representative NNRTIs while elaborating significant bioactive compound
46
47 optimization strategies associated with the solution of intractable scientific issues.
48
49 Overall, there is still a continuing demand for synergistic collaboration between
50
51 medicinal chemistry strategies, crystallographic studies, and computer-aided tools to
52
53 achieve the ultimate goal of obtaining new NNRTIs with improved genetic barriers,
54
55 desirable pharmacokinetic profiles, and excellent safety properties.
56
57
58
59
60

AUTHOR INFORMATION

Corresponding Authors

Erik De Clercq – *Rega Institute for Medical Research, Laboratory of Virology and Chemotherapy, K. U. Leuven, Leuven B-3000, Belgium; orcid.org/0000-0002-2985-8890; Phone: 32-(0)16-321674; Email: erik.declercq@kuleuven.be*

Dongwei Kang – *Department of Medicinal Chemistry, Key Laboratory of Chemical Biology (Ministry of Education), School of Pharmaceutical Sciences, Cheeloo College of Medicine, Shandong University, Jinan, Shandong 250012, PR China; China-Belgium Collaborative Research Center for Innovative Antiviral Drugs of Shandong Province, Jinan, Shandong 250012, PR China; orcid.org/0000-0001-9232-953X; Phone: 086-531-88382005; Email: kangdongwei@sdu.edu.cn*

Peng Zhan – *Department of Medicinal Chemistry, Key Laboratory of Chemical Biology (Ministry of Education), School of Pharmaceutical Sciences, Cheeloo College of Medicine, Shandong University, Jinan, Shandong 250012, PR China; China-Belgium Collaborative Research Center for Innovative Antiviral Drugs of Shandong Province, Jinan, Shandong 250012, PR China; orcid.org/0000-0002-9675-6026; Phone: 086-531-88382005; Email: zhanpeng1982@sdu.edu.cn*

Xinyong Liu – *Department of Medicinal Chemistry, Key Laboratory of Chemical Biology (Ministry of Education), School of Pharmaceutical Sciences, Cheeloo College of Medicine, Shandong University, Jinan, Shandong 250012, PR China; China-Belgium Collaborative Research Center for Innovative Antiviral Drugs of Shandong*

Province, Jinan, Shandong 250012, PR China; orcid.org/0000-0002-7302-2214; Phone:
086-531-88380270; Email: xinyongl@sdu.edu.cn

Notes

The authors declare no competing financial interest.

Biographies

Zhao Wang received his B.S. degree from the School of Pharmaceutical Sciences, Shandong University, in 2017. He is currently pursuing a Ph.D. degree in the Department of Medicinal Chemistry, School of Pharmaceutical Sciences, Shandong University, working under the supervision of Professor Xinyong Liu and Professor Peng Zhan. His research interests focus on rational design, synthesis, and biological evaluation of novel potent reverse transcriptase inhibitors of human immunodeficiency virus.

Srinivasulu Cherukupalli received his B.S. and M.S. degrees from Sri Venkateswara University, India, in 2009 and 2012. Then he obtained his Ph.D. from the University of KwaZulu-Natal, South Africa, in 2018. He is currently working as a postdoctoral fellow in the research group of Professor Xinyong Liu at Shandong University. His research interests focus on the discovery of novel potent antiviral agents.

Minghui Xie completed her B.S. degree at Shandong First Medical University in 2020. She is studying for her M.S. degree at Shandong University, working under the supervision of Professor Xinyong Liu, Professor Peng Zhan, and Professor Dongwei Kang. Her current research focuses on the discovery of anti-AIDS drugs.

Wenbo Wang received his B.S. degree from the School of Pharmaceutical Sciences in

1
2
3
4 Shandong University in 2017. He is studying for his M.S. degree in Shandong
5
6 University, working under the supervision of Professor Xinyong Liu. His research
7
8 focuses on rational design, synthesis, and biological evaluation of novel potent anti-
9
10 AIDS drugs.
11
12

13
14 **Xiangyi Jiang** was born in 1996 in Dezhou, Shandong Province, China. He received
15
16 his B.S. and M.S. degrees from the School of Pharmaceutical Sciences, Shandong
17
18 University, in 2018 and 2021. He is currently studying for a Ph.D. degree in the
19
20 Department of Medicinal Chemistry, School of Pharmaceutical Sciences in Shandong
21
22 University. His research interests focus on the discovery of novel anti-HIV-1 and anti-
23
24 SARS-CoV-2 lead compounds.
25
26
27
28

29
30 **Ruifang Jia** obtained her bachelor's degree in pharmacy from Shandong University
31
32 (Wei Hai), China, in 2016. Currently, she is working in the School of Pharmaceutical
33
34 Sciences of Shandong University as a Ph.D. candidate, supervised by Professor
35
36 Xinyong Liu. Her research interests focus on the discovery of novel anti-influenza
37
38 drugs.
39
40
41

42
43 **Christophe Pannecouque** graduated in pharmaceutical sciences at the Rega Institute
44
45 for Medical Research of the Katholieke Universiteit Leuven in 1990. He obtained his
46
47 Ph.D. in medicinal chemistry at the same university in 1995 and joined the group of
48
49 Professor Erik De Clercq as a postdoctoral fellow. In 2003, he became an associate
50
51 professor. In the field of virological research, he has unravelled the modes of action of
52
53 several classes of new products with anti-HIV activity. Recently, his research has been
54
55 focused on cellular targets interfering with HIV replication and on regulation of the
56
57
58
59
60

1
2
3
4 (cyto)pathogenicity of the virus.
5

6 **Erik De Clercq** has MD and Ph.D. degrees and has taught at the Katholieke
7
8
9 Universiteit Leuven (and Kortrijk) Medical School, Belgium, where he was Chairman
10
11 of the Department of Microbiology and Immunology until September 2006. He is
12
13 currently Emeritus Professor of K.U. Leuven University, Member of the Belgian
14
15 (Flemish) Royal Academy of Medicine and the Academia Europaea, and Fellow of the
16
17 American Association for the Advancement of Science. In 2008, he was elected
18
19 European Inventor of the Year (Lifetime Achievement Award), and in 2010, he,
20
21 together with Dr. A. S. Fauci, was Laureate of the Dr. Paul Janssen Award for
22
23 Biomedical Research. He is the (co)inventor of a number of antiviral drugs (valaciclovir,
24
25 brivudin, cidofovir, adefovir, and tenofovir).
26
27
28
29
30
31

32 **Dongwei Kang** received his B.S. degree from Hebei University of Technology in 2012,
33
34 M.S. and Ph.D. degrees from Shandong University, in 2015 and 2018. From 2018 to
35
36 2020, he worked as a postdoctoral fellow in the research group of Professor Xinyong
37
38 Liu in Shandong University. Currently he is a Professor in the Institute of Medicinal
39
40 Chemistry, Shandong University. His research is devoted to discovering novel antiviral
41
42 inhibitors and immunomodulators.
43
44
45
46
47

48 **Peng Zhan** obtained his B.S. degree from Shandong University, China, in 2005. Then
49
50 he earned his M.S. degree and Ph.D. in medicinal chemistry from Shandong University
51
52 in 2008 and 2010, respectively. He subsequently joined the research group of Professor
53
54 Xinyong Liu as a Lecturer (2010–2012). From 2012 to 2014, he worked as a
55
56 Postdoctoral Fellow funded by JSPS (Japan Society for the Promotion of Science) in
57
58
59
60

1
2
3
4 the Graduate School of Medical Science, Kyoto Prefectural University of Medicine,
5
6 Japan. He is currently a full professor in the Department of Medicinal Chemistry,
7
8 Shandong University. His research interests involve the discovery of novel antiviral
9
10 (HIV, HBV, influenza, coronavirus, *etc*), anti-gout and anticancer agents based on
11
12 rational drug design and combinatorial chemistry approaches.
13
14

15
16 **Xinyong Liu** received his B.S. and M.S. degrees from Shandong University, in 1984
17
18 and 1991, respectively. From 1997 to 1999, he worked at the Instituto de Quimica
19
20 Medica (CSIC) in Spain as a senior visiting scholar. He obtained his Ph.D. from
21
22 Shandong University in 2004. He is currently a full Professor of Shandong University.
23
24 His research interests include rational drug design, synthesis, and antiviral evaluation
25
26 of various molecules that interact with specific enzymes and receptors in the viral life
27
28 cycle (HIV, HBV, influenza, SARS-CoV-2, *etc*). Other ongoing programs include
29
30 studies of the molecular modification and structure–activity relationships of synthetic
31
32 small molecule and natural products used to treat gout, cardiovascular diseases, and
33
34 neurodegenerative diseases, as well as drug delivery research using PEGylated small-
35
36 molecular agents.
37
38
39
40
41
42
43
44
45
46
47

48 **ACKNOWLEDGMENTS**

49
50 We gratefully acknowledge the financial support from the National Natural Science
51
52 Foundation of China (NSFC nos. 81973181, 81903453), the Key Project of NSFC for
53
54 International Cooperation (no. 81420108027), National Science and Technology Major
55
56 Projects for "Major New Drugs Innovation and Development" (2019ZX09301126),
57
58
59
60

1
2
3
4 Science Foundation for Outstanding Young Scholars of Shandong Province
5
6 (ZR2020JQ31), Science Foundation for Excellent Young Scholars of Shandong
7
8 Province (ZR2020YQ61), Foreign cultural and educational experts Project
9
10 (GXL20200015001), Shandong Provincial Natural Science Foundation
11
12 (ZR2019BH011), Shandong Provincial Key research and development project (nos.
13
14 2017CXGC1401, 2019JZZY021011), Qilu Young Scholars Program of Shandong
15
16 University and the Taishan Scholar Program at Shandong Province.
17
18
19
20
21
22
23
24

25 **ABBREVIATIONS**

26
27 AIDS, acquired immune deficiency syndrome; CC_{50} , 50% cytotoxicity concentration;
28
29 CCD, catalytic core domain; CL, clearance rate; CuAAC, copper(I)-catalyzed azide-
30
31 alkyne cycloaddition; CYP, cytochrome P450; d4T, 2',3'-didehydrothymidine; DAPY,
32
33 diarylpyrimidine; DLV, delavirdine; DOR, doravirine; EC_{50} , 50% effective
34
35 concentration; EFV, efavirenz; ETV, etravirine; FDA, Food and Drug Administration;
36
37 FEP, free energy perturbation; HAART, highly active antiretroviral therapy; HIV-1,
38
39 human immunodeficiency virus-1; IC_{50} , 50% inhibition concentration; IN, integrase;
40
41 MTDL, multitarget-directed ligand; NcRTIs, nucleotide-competing reverse
42
43 transcriptase inhibitors; NNIBP, NNRTI-binding pocket; NNRTIs, nonnucleoside
44
45 reverse transcriptase inhibitors; NRTIs, nucleoside reverse transcriptase inhibitors;
46
47 NVP, nevirapine; PDB, protein data bank; PK, pharmacokinetics; PrEP, preexposure
48
49 prophylaxis; RPV, rilpivirine; RT, reverse transcriptase; SARs, structure–activity
50
51 relationships; $T_{1/2}$, half-life; UNAIDS, the Joint United Nations Programme on
52
53
54
55
56
57
58
59
60

1
2
3
4 HIV/AIDS; WT, wild-type.
5
6
7
8

9 **REFERENCES**

- 10
11 1. Fauci, A. S.; Lane, H. C. Four decades of HIV/AIDS - much accomplished, much to
12 do. *N. Engl. J. Med.* **2020**, *383*, 1–4.
13
14
15 2. Margolis, D. M.; Archin, N. M.; Cohen, M. S.; Eron, J. J.; Ferrari, G.; Garcia, J. V.;
16 Gay, C. L.; Goonetilleke, N.; Joseph, S. B.; Swanstrom, R.; Turner, A. W.; Wahl, A.
17 Curing HIV: seeking to target and clear persistent infection. *Cell* **2020**, *181*, 189–206.
18
19
20 3. Shattock, R. J.; Warren, M.; McCormack, S.; Hankins, C. A. AIDS. Turning the tide
21 against HIV. *Science* **2011**, *333*, 42–43.
22
23
24 4. Shafer, R. W.; Vuitton, D. A. Highly active antiretroviral therapy (HAART) for the
25 treatment of infection with human immunodeficiency virus type 1. *Biomed.*
26 *Pharmacother.* **1999**, *53*, 73–86.
27
28
29 5. Mehellou, Y.; De Clercq, E. Twenty-six years of anti-HIV drug discovery: where do
30 we stand and where do we go? *J. Med. Chem.* **2010**, *53*, 521–538.
31
32
33 6. Beyrer, C.; Pozniak, A. HIV drug resistance - an emerging threat to epidemic control.
34 *N. Engl. J. Med.* **2017**, *377*, 1605–1607.
35
36
37 7. Larsen, K. P.; Mathiharan, Y. K.; Kappel, K.; Coey, A. T.; Chen, D. H.; Barrero, D.;
38 Madigan, L.; Puglisi, J. D.; Skiniotis, G.; Puglisi, E. V. Architecture of an HIV-1
39 reverse transcriptase initiation complex. *Nature* **2018**, *557*, 118–122.
40
41
42 8. Reynolds, C.; de Koning, C. B.; Pelly, S. C.; van Otterlo, W. A.; Bode, M. L. In
43 search of a treatment for HIV—current therapies and the role of non-nucleoside reverse
44
45
46
47
48
49
50
51
52
53
54
55
56
57
58
59
60

- 1
2
3
4 transcriptase inhibitors (NNRTIs). *Chem. Soc. Rev.* **2012**, *41*, 4657–4670.
5
6
7 9. Tavassoli, A. Targeting the protein-protein interactions of the HIV lifecycle. *Chem.*
8
9 *Soc. Rev.* **2011**, *40*, 1337–1346.
10
11 10. Flexner, C. HIV drug development: the next 25 years. *Nat. Rev. Drug Discov.* **2007**,
12
13 *6*, 959–966.
14
15
16 11. Bec, G.; Meyer, B.; Gerard, M. A.; Steger, J.; Fauster, K.; Wolff, P.; Burnouf, D.;
17
18 Micura, R.; Dumas, P.; Ennifar, E. Thermodynamics of HIV-1 reverse transcriptase in
19
20 action elucidates the mechanism of action of non-nucleoside inhibitors. *J. Am. Chem.*
21
22 *Soc.* **2013**, *135*, 9743–9752.
23
24
25 12. Li, D.; Zhan, P.; De Clercq, E.; Liu, X. Strategies for the design of HIV-1 non-
26
27 nucleoside reverse transcriptase inhibitors: lessons from the development of seven
28
29 representative paradigms. *J. Med. Chem.* **2012**, *55*, 3595–3613.
30
31
32 13. Cilento, M. E.; Kirby, K. A.; Sarafianos, S. G. Avoiding drug resistance in HIV
33
34 reverse transcriptase. *Chem. Rev.* **2021**, *121*, 3271–3296.
35
36
37 14. Zhan, P.; Pannecouque, C.; De Clercq, E.; Liu, X. Anti-HIV drug discovery and
38
39 development: current innovations and future trends. *J. Med. Chem.* **2016**, *59*,
40
41 2849–2878.
42
43
44 15. Zhan, P.; Chen, X.; Li, D.; Fang, Z.; De Clercq, E.; Liu, X. HIV-1 NNRTIs:
45
46 structural diversity, pharmacophore similarity, and implications for drug design. *Med.*
47
48 *Res. Rev.* **2013**, *33*, No. E1–E72.
49
50
51 16. De Clercq, E. Fifty years in search of selective antiviral drugs. *J. Med. Chem.* **2019**,
52
53 *62*, 7322–7339.
54
55
56
57
58
59
60

- 1
2
3
4 17. Domingo, P.; Mateo, M. G.; Gutierrez, M. D. M.; Vidal, F. Tolerability of current
5
6 antiretroviral single-tablet regimens. *AIDS Rev.* **2018**, *20*, 141–149.
7
8
9 18. Blair, H. A. Dolutegravir/Rilpivirine: a review in HIV-1 infection. *Drugs* **2018**, *78*,
10
11 1741–1750.
12
13
14 19. Llibre, J. M.; Hung, C. C.; Brinson, C.; Castelli, F.; Girard, P. M.; Kahl, L. P.; Blair,
15
16 E. A.; Angelis, K.; Wynne, B.; Vandermeulen, K.; Underwood, M.; Smith, K.; Gartland,
17
18 M.; Aboud, M. Efficacy, safety, and tolerability of dolutegravir-rilpivirine for the
19
20 maintenance of virological suppression in adults with HIV-1: phase 3, randomised,
21
22 non-inferiority SWORD-1 and SWORD-2 studies. *Lancet* **2018**, *391*, 839–849.
23
24
25 20. Pozniak, A. L.; Arribas, J. R. Dolutegravir-rilpivirine for virological suppression.
26
27
28
29
30
31
32
33
34
35
36
37
38
39
40
41
42
43
44
45
46
47
48
49
50
51
52
53
54
55
56
57
58
59
60
60
Lancet HIV **2019**, *6*, e560–e561.
21. Namasivayam, V.; Vanangamudi, M.; Kramer, V. G.; Kurup, S.; Zhan, P.; Liu, X.;
Kongsted, J.; Byrareddy, S. N. The journey of HIV-1 non-nucleoside reverse
transcriptase inhibitors (NNRTIs) from lab to clinic. *J. Med. Chem.* **2019**, *62*,
4851–4883.
22. Battini, L.; Bollini, M. Challenges and approaches in the discovery of human
immunodeficiency virus type-1 non-nucleoside reverse transcriptase inhibitors. *Med.*
Res. Rev. **2019**, *39*, 1235–1273.
23. Feng, M.; Wang, D.; Grobler, J. A.; Hazuda, D. J.; Miller, M. D.; Lai, M. T. In vitro
resistance selection with doravirine (MK-1439), a novel nonnucleoside reverse
transcriptase inhibitor with distinct mutation development pathways. *Antimicrob.*
Agents Chemother. **2015**, *59*, 590–598.

- 1
2
3
4 24. Tantillo, C.; Ding, J. P.; Jacobomolina, A.; Nanni, R. G.; Boyer, P. L.; Hughes, S.
5
6 H.; Pauwels, R.; Andries, K.; Janssen, P. A. J.; Arnold, E. Locations of anti-AIDS drug
7
8 binding sites and resistance mutations in the three-dimensional structure of HIV-1
9
10 reverse transcriptase. Implications for mechanisms of drug inhibition and resistance. *J.*
11
12 *Mol. Biol.* **1994**, *243*, 369–387.
13
14
15
16
17 25. Das, K.; Arnold, E. HIV-1 reverse transcriptase and antiviral drug resistance. Part
18
19 1. *Curr. Opin. Virol.* **2013**, *3*, 111–118.
20
21
22 26. Das, K.; Arnold, E. HIV-1 reverse transcriptase and antiviral drug resistance. Part
23
24 2. *Curr. Opin. Virol.* **2013**, *3*, 119–128.
25
26
27 27. Sarafianos, S. G.; Das, K.; Hughes, S. H.; Arnold, E. Taking aim at a moving target:
28
29 designing drugs to inhibit drug-resistant HIV-1 reverse transcriptases. *Curr. Opin.*
30
31 *Struc. Biol.* **2004**, *14*, 716–730.
32
33
34
35 28. Hsiou, Y.; Ding, J.; Das, K.; Clark Jr, A. D.; Hughes, S. H.; Arnold, E. Structure of
36
37 unliganded HIV-1 reverse transcriptase at 2.7 Å resolution: implications of
38
39 conformational changes for polymerization and inhibition mechanisms. *Structure* **1996**,
40
41 *4*, 853–860.
42
43
44
45 29. Ding, J. P.; Das, K.; Moereels, H.; Koymans, L.; Andries, K.; Janssen, P. A.;
46
47 Hughes, S. H.; Arnold, E. Structure of HIV-1 RT/TIBO R 86183 complex reveals
48
49 similarity in the binding of diverse nonnucleoside inhibitors. *Nat. Struct. Biol.* **1995**, *2*,
50
51 407–415.
52
53
54
55 30. Hsiou, Y.; Das, K.; Ding, J.; Clark Jr, A. D.; Kleim, J. P.; Rösner, M.; Winkler, I.;
56
57 Riess, G.; Hughes, S. H.; Arnold, E. Structures of Tyr188Leu mutant and wild-type
58
59
60

1
2
3
4 HIV-1 reverse transcriptase complexed with the non-nucleoside inhibitor HBY 097:
5
6 inhibitor flexibility is a useful design feature for reducing drug resistance. *J. Mol. Biol.*
7
8
9 **1998**, *284*, 313–323.

10
11 31. Das, K.; Sarafianos, S. G.; Clark Jr, A. D.; Boyer, P. L.; Hughes, S. H.; Arnold, E.
12
13 Crystal structures of clinically relevant Lys103Asn/Tyr181Cys double mutant HIV-1
14
15 reverse transcriptase in complexes with ATP and non-nucleoside inhibitor HBY 097.
16
17
18
19 *J. Mol. Biol.* **2007**, *365*, 77–89.

20
21
22 32. Raymer, B.; Bhattacharya, S. K. Lead-like drugs: a perspective. *J. Med. Chem.* **2018**,
23
24
25 *61*, 10375–10384.

26
27 33. Wu, G.; Zhao, T.; Kang, D.; Zhang, J.; Song, Y.; Namasivayam, V.; Kongsted, J.;
28
29
30 Pannecouque, C.; De Clercq, E.; Poongavanam, V.; Liu, X.; Zhan, P. Overview of
31
32 recent strategic advances in medicinal chemistry. *J. Med. Chem.* **2019**, *62*, 9375–9414.

33
34
35 34. Bergström, F.; Lindmark, B. Accelerated drug discovery by rapid candidate drug
36
37
38 identification. *Drug Discov. Today* **2019**, *24*, 1237–1241.

39
40 35. Yang, Z. Y.; He, J. H.; Lu, A. P.; Hou, T. J.; Cao, D. S. Application of negative
41
42
43 design to design a more desirable virtual screening library. *J. Med. Chem.* **2020**, *63*,
44
45
46 4411–4429.

47
48 36. Tanrikulu, Y.; Kruger, B.; Proschak, E. The holistic integration of virtual screening
49
50
51 in drug discovery. *Drug Discov. Today* **2013**, *18*, 358–364.

52
53 37. Zheng, M.; Zhao, J.; Cui, C.; Fu, Z.; Li, X.; Liu, X.; Ding, X.; Tan, X.; Li, F.; Luo,
54
55
56 X.; Chen, K.; Jiang, H. Computational chemical biology and drug design: Facilitating
57
58
59 protein structure, function, and modulation studies. *Med. Res. Rev.* **2018**, *38*, 914–950.
60

- 1
2
3
4 38. Nichols, S. E.; Domaoal, R. A.; Thakur, V. V.; Tirado-Rives, J.; Anderson, K. S.;
5
6 Jorgensen, W. L. Discovery of wild-type and Y181C mutant non-nucleoside HIV-1
7
8 reverse transcriptase inhibitors using virtual screening with multiple protein structures.
9
10
11 *J. Chem. Inf. Model.* **2009**, *49*, 1272–1279.
12
13
14 39. Bollini, M.; Domaoal, R. A.; Thakur, V. V.; Gallardo-Macias, R.; Spasov, K. A.;
15
16 Anderson, K. S.; Jorgensen, W. L. Computationally-guided optimization of a docking
17
18 hit to yield catechol diethers as potent anti-HIV agents. *J. Med. Chem.* **2011**, *54*,
19
20 8582–8591.
21
22
23
24 40. Frey, K. M.; Bollini, M.; Mislak, A. C.; Cisneros, J. A.; Gallardo-Macias, R.;
25
26 Jorgensen, W. L.; Anderson, K. S. Crystal structures of HIV-1 reverse transcriptase
27
28 with picomolar inhibitors reveal key interactions for drug design. *J. Am. Chem. Soc.*
29
30 **2012**, *134*, 19501–19503.
31
32
33
34 41. Frey, K. M.; Puleo, D. E.; Spasov, K. A.; Bollini, M.; Jorgensen, W. L.; Anderson,
35
36 K. S. Structure-based evaluation of non-nucleoside inhibitors with improved potency
37
38 and solubility that target HIV reverse transcriptase variants. *J. Med. Chem.* **2015**, *58*,
39
40 2737–2745.
41
42
43
44 42. Lee, W. G.; Gallardo-Macias, R.; Frey, K. M.; Spasov, K. A.; Bollini, M.; Anderson,
45
46 K. S.; Jorgensen, W. L. Picomolar inhibitors of HIV reverse transcriptase featuring
47
48 bicyclic replacement of a cyanovinylphenyl group. *J. Am. Chem. Soc.* **2013**, *135*,
49
50 16705–16713.
51
52
53
54 43. Gray, W. T.; Frey, K. M.; Laskey, S. B.; Mislak, A. C.; Spasov, K. A.; Lee, W. G.;
55
56 Bollini, M.; Siliciano, R. F.; Jorgensen, W. L.; Anderson, K. S. Potent inhibitors active
57
58
59
60

1
2
3
4 against HIV reverse transcriptase with K101P, a mutation conferring rilpivirine
5
6 resistance. *ACS Med. Chem. Lett.* **2015**, *6*, 1075–1079.

7
8
9 44. Lee, W. G.; Chan, A. H.; Spasov, K. A.; Anderson, K. S.; Jorgensen, W. L. Design,
10
11 conformation, and crystallography of 2-naphthyl phenyl ethers as potent anti-HIV
12
13 agents. *ACS Med. Chem. Lett.* **2016**, *7*, 1156–1160.

14
15
16 45. Lee, W. G.; Frey, K. M.; Gallardo-Macias, R.; Spasov, K. A.; Bollini, M.; Anderson,
17
18 K. S.; Jorgensen, W. L. Picomolar inhibitors of HIV-1 reverse transcriptase: design and
19
20 crystallography of naphthyl phenyl ethers. *ACS Med. Chem. Lett.* **2014**, *5*, 1259–1262.

21
22
23 46. Kudalkar, S. N.; Beloor, J.; Quijano, E.; Spasov, K. A.; Lee, W. G.; Cisneros, J. A.;
24
25 Saltzman, W. M.; Kumar, P.; Jorgensen, W. L.; Anderson, K. S. From in silico hit to
26
27 long-acting late-stage preclinical candidate to combat HIV-1 infection. *Proc. Natl.*
28
29 *Acad. Sci. U.S.A.* **2018**, *115*, E802–E811.

30
31
32 47. Wang, X.; Huang, B.; Liu, X.; Zhan, P. Discovery of bioactive molecules from
33
34 CuAAC click-chemistry-based combinatorial libraries. *Drug Discov. Today* **2016**, *21*,
35
36 118–132.

37
38
39 48. Hu, X.; Manetsch, R. Kinetic target-guided synthesis. *Chem. Soc. Rev.* **2010**, *39*,
40
41 1316–1324.

42
43
44 49. Bosc, D.; Camberlein, V.; Gealageas, R.; Castillo-Aguilera, O.; Deprez, B.; Deprez-
45
46 Poulain, R. Kinetic target-guided synthesis: reaching the age of maturity. *J. Med. Chem.*
47
48 **2020**, *63*, 3817–3833.

49
50
51 50. Mamidyala, S. K.; Finn, M. G. In situ click chemistry: probing the binding
52
53 landscapes of biological molecules. *Chem. Soc. Rev.* **2010**, *39*, 1252–1261.
54
55
56
57
58
59
60

- 1
2
3
4 51. Sharpless, K. B.; Manetsch, R. In situ click chemistry: a powerful means for lead
5
6 discovery. *Expert Opin. Drug Discov.* **2006**, *1*, 525–538.
7
8
9 52. Kang, D.; Feng, D.; Jing, L.; Sun, Y.; Wei, F.; Jiang, X.; Wu, G.; De Clercq, E.;
10
11 Pannecouque, C.; Zhan, P.; Liu, X. In situ click chemistry-based rapid discovery of
12
13 novel HIV-1 NNRTIs by exploiting the hydrophobic channel and tolerant regions of
14
15 NNIBP. *Eur. J. Med. Chem.* **2020**, *193*, 112237.
16
17
18
19 53. Chatterjee, A. K. Cell-based medicinal chemistry optimization of high-throughput
20
21 screening (HTS) hits for orally active antimalarials. Part 1: challenges in potency and
22
23 absorption, distribution, metabolism, excretion/pharmacokinetics (ADME/PK). *J. Med.*
24
25 *Chem.* **2013**, *56*, 7741–7749.
26
27
28
29 54. Copeland, R. A.; Pompliano, D. L.; Meek, T. D. Drug-target residence time and its
30
31 implications for lead optimization. *Nat. Rev. Drug Discov.* **2006**, *5*, 730–739.
32
33
34
35 55. Mignani, S.; Rodrigues, J.; Tomas, H.; Jalal, R.; Singh, P. P.; Majoral, J. P.;
36
37 Vishwakarma, R. A. Present drug-likeness filters in medicinal chemistry during the hit
38
39 and lead optimization process: how far can they be simplified? *Drug Discov. Today*
40
41 **2018**, *23*, 605–615.
42
43
44
45 56. Xiao, Z.; Morris-Natschke, S. L.; Lee, K. H. Strategies for the optimization of
46
47 natural leads to anticancer drugs or drug candidates. *Med. Res. Rev.* **2016**, *36*, 32–91.
48
49
50
51 57. Bohm, H. J.; Flohr, A.; Stahl, M. Scaffold hopping. *Drug Discov. Today Technol.*
52
53 **2004**, *1*, 217–224.
54
55
56 58. Zhao, H. Scaffold selection and scaffold hopping in lead generation: a medicinal
57
58 chemistry perspective. *Drug Discov. Today* **2007**, *12*, 149–155.
59
60

- 1
2
3
4 59. Hu, Y.; Stumpfe, D.; Bajorath, J. Recent advances in scaffold hopping. *J. Med.*
5
6
7 *Chem.* **2017**, *60*, 1238–1246.
8
9 60. Sun, H.; Tawa, G.; Wallqvist, A. Classification of scaffold-hopping approaches.
10
11 *Drug Discov. Today* **2012**, *17*, 310–324.
12
13 61. Wang, X.; Zhang, J.; Huang, Y.; Wang, R.; Zhang, L.; Qiao, K.; Li, L.; Liu, C.;
14
15 Ouyang, Y.; Xu, W.; Zhang, Z.; Zhang, L.; Shao, Y.; Jiang, S.; Ma, L.; Liu, J. Design,
16
17 synthesis, and biological evaluation of 1-[(2-benzyloxy/alkoxy)methyl]-5-halo-6-
18
19 aryluracils as potent HIV-1 non-nucleoside reverse transcriptase inhibitors with an
20
21 improved drug resistance profile. *J. Med. Chem.* **2012**, *55*, 2242–2250.
22
23 62. Li, A.; Ouyang, Y.; Wang, Z.; Cao, Y.; Liu, X.; Ran, L.; Li, C.; Li, L.; Zhang, L.;
24
25 Qiao, K.; Xu, W.; Huang, Y.; Zhang, Z.; Tian, C.; Liu, Z.; Jiang, S.; Shao, Y.; Du, Y.;
26
27 Ma, L.; Wang, X.; Liu, J. Novel pyridinone derivatives as non-nucleoside reverse
28
29 transcriptase inhibitors (NNRTIs) with high potency against NNRTI-resistant HIV-1
30
31 strains. *J. Med. Chem.* **2013**, *56*, 3593–3608.
32
33 63. Kang, D.; Fang, Z.; Li, Z.; Huang, B.; Zhang, H.; Lu, X.; Xu, H.; Zhou, Z.; Ding,
34
35 X.; Daelemans, D.; De Clercq, E.; Pannecouque, C.; Zhan, P.; Liu, X. Design, synthesis,
36
37 and evaluation of thiophene[3,2-d]pyrimidine derivatives as HIV-1 non-nucleoside
38
39 reverse transcriptase inhibitors with significantly improved drug resistance profiles. *J.*
40
41 *Med. Chem.* **2016**, *59*, 7991–8007.
42
43 64. Kang, D.; Fang, Z.; Huang, B.; Lu, X.; Zhang, H.; Xu, H.; Huo, Z.; Zhou, Z.; Yu,
44
45 Z.; Meng, Q.; Wu, G.; Ding, X.; Tian, Y.; Daelemans, D.; De Clercq, E.; Pannecouque,
46
47 C.; Zhan, P.; Liu, X. Structure-based optimization of thiophene[3,2-d]pyrimidine
48
49
50
51
52
53
54
55
56
57
58
59
60

1
2
3
4 derivatives as potent HIV-1 non-nucleoside reverse transcriptase inhibitors with
5
6 improved potency against resistance-associated variants. *J. Med. Chem.* **2017**, *60*,
7
8 4424–4443.
9

10
11 65. Kang, D.; Zhang, H.; Wang, Z.; Zhao, T.; Ginex, T.; Luque, F. J.; Yang, Y.; Wu,
12
13 G.; Feng, D.; Wei, F.; Zhang, J.; De Clercq, E.; Pannecouque, C.; Chen, C. H.; Lee, K.
14
15 H.; Murugan, N. A.; Steitz, T. A.; Zhan, P.; Liu, X. Identification of dihydrofuro[3,4-
16
17 d]pyrimidine derivatives as novel HIV-1 non-nucleoside reverse transcriptase
18
19 inhibitors with promising antiviral activities and desirable physicochemical properties.
20
21 *J. Med. Chem.* **2019**, *62*, 1484–1501.
22
23
24

25
26 66. Kang, D.; Ruiz, F. X.; Sun, Y.; Feng, D.; Jing, L.; Wang, Z.; Zhang, T.; Gao, S.;
27
28 Sun, L.; De Clercq, E.; Pannecouque, C.; Arnold, E.; Zhan, P.; Liu, X. 2,4,5-
29
30 trisubstituted pyrimidines as potent HIV-1 NNRTIs: rational design, synthesis, activity
31
32 evaluation, and crystallographic studies. *J. Med. Chem.* **2021**, *64*, 4239–4256.
33
34
35

36
37 67. Xiao, J.; Sun, Z.; Kong, F.; Gao, F. Current scenario of ferrocene-containing hybrids
38
39 for antimalarial activity. *Eur. J. Med. Chem.* **2020**, *185*, 111791.
40
41

42
43 68. Zhang, S.; Zhang, J.; Gao, P.; Sun, L.; Song, Y.; Kang, D.; Liu, X.; Zhan, P.
44
45 Efficient drug discovery by rational lead hybridization based on crystallographic
46
47 overlay. *Drug Discov. Today* **2019**, *24*, 805–813.
48
49

50
51 69. Jing, L.; Wu, G.; Kang, D.; Zhou, Z.; Song, Y.; Liu, X.; Zhan, P. Contemporary
52
53 medicinal-chemistry strategies for the discovery of selective butyrylcholinesterase
54
55 inhibitors. *Drug Discov. Today* **2019**, *24*, 629–635.
56
57

58
59 70. Ivasiv, V.; Albertini, C.; Goncalves, A. E.; Rossi, M.; Bolognesi, M. L. Molecular
60

1
2
3
4 hybridization as a tool for designing multitarget drug candidates for complex diseases.

5
6
7 *Curr. Top. Med. Chem.* **2019**, *19*, 1694–1711.

8
9 71. Han, S.; Sang, Y. L.; Wu, Y.; Tao, Y.; Pannecouque, C.; De Clercq, E.; Zhuang, C.

10
11 L.; Che, F. E. Molecular hybridization-inspired optimization of diarylbenzopyrimidines

12
13 as HIV-1 nonnucleoside reverse transcriptase inhibitors with improved activity against

14
15 K103N and E138K mutants and pharmacokinetic profiles. *Acs Infect. Dis.* **2020**, *6*,

16
17
18
19
20 787–801.

21
22 72. Jin, K.; Sang, Y.; Han, S.; De Clercq, E.; Pannecouque, C.; Meng, G.; Chen, F.

23
24 Synthesis and biological evaluation of dihydroquinazoline-2-amines as potent non-

25
26
27
28
29 nucleoside reverse transcriptase inhibitors of wild-type and mutant HIV-1 strains. *Eur.*

30
31
32
33
34
35
36
37
38
39
40
41
42
43
44
45
46
47
48
49
50
51
52
53
54
55
56
57
58
59
60 *J. Med. Chem.* **2019**, *176*, 11–20.

73. Muraglia, E.; Kinzel, O. D.; Laufer, R.; Miller, M. D.; Moyer, G.; Munshi, V.;

Orvieto, F.; Palumbi, M. C.; Pescatore, G.; Rowley, M.; Williarns, P. D.; Summa, V.

Tetrazole thioacetanilides: potent non-nucleoside inhibitors of WT HIV reverse

transcriptase and its K103N mutant. *Bioorg. Med. Chem. Lett.* **2006**, *16*, 2748–2752.

74. De La Rosa, M.; Kim, H. W.; Gunic, E.; Jenket, C.; Boyle, U.; Koh, Y. H.;

Korboukh, I.; Allan, M.; Zhang, W. J.; Chen, H. M.; Xu, W.; Nilar, S.; Yao, N. H.;

Hamatake, R.; Lang, S. A.; Hong, Z.; Zhang, Z. J.; Girardet, J. L. Tri-substituted

triazoles as potent non-nucleoside inhibitors of the HIV-1 reverse transcriptase. *Bioorg.*

Med. Chem. Lett. **2006**, *16*, 4444–4449.

75. Gagnon, A.; Amad, M. H.; Bonneau, P. R.; Coulombe, R.; Deroy, P. L.; Doyon, L.;

Duan, J.; Garneau, M.; Guse, I.; Jakalian, A.; Jolicoeur, E.; Landry, S.; Malenfant, E.;

1
2
3
4 Simoneau, B.; Yoakim, C. Thiotetrazole alkynylacetanilides as potent and bioavailable
5
6 non-nucleoside inhibitors of the HIV-1 wild type and K103N/Y181C double mutant
7
8 reverse transcriptases. *Bioorg. Med. Chem. Lett.* **2007**, *17*, 4437–4441.

9
10
11 76. Wyatt, P. G.; Bethell, R. C.; Cammack, N.; Charon, D.; Dodic, N.; Dumaitre, B.;
12
13 Evans, D. N.; Green, D. V. S.; Hopewell, P. L.; Humber, D. C.; Lamont, R. B.; Orr, D.
14
15 C.; Plested, S. J.; Ryan, D. M.; Sollis, S. L.; Storer, R.; Weingarten, G. G.
16
17 Benzophenone derivatives: a novel series of potent and selective inhibitors of human
18
19 immunodeficiency virus type 1 reverse transcriptase. *J. Med. Chem.* **1995**, *38*,
20
21 1657–1665.

22
23
24 77. Chan, J. H.; Freeman, G. A.; Tidwell, J. H.; Romines, K. R.; Schaller, L. T.; Cowan,
25
26 J. R.; Gonzales, S. S.; Lowell, G. S.; Andrews, C. W.; Reynolds, D. J.; St Clair, M.;
27
28 Hazen, R. J.; Ferris, R. G.; Creech, K. L.; Roberts, G. B.; Short, S. A.; Weaver, K.;
29
30 Koszalka, G. W.; Boone, L. R. Novel benzophenones as non-nucleoside reverse
31
32 transcriptase inhibitors of HIV-1. *J. Med. Chem.* **2004**, *47*, 1175–1182.

33
34
35 78. Romines, K. R.; Freeman, G. A.; Schaller, L. T.; Cowan, J. R.; Gonzales, S. S.;
36
37 Tidwell, J. H.; Andrews, C. W.; Stammers, D. K.; Hazen, R. J.; Ferris, R. G.; Short, S.
38
39 A.; Chan, J. H.; Boone, L. R. Structure-activity relationship studies of novel
40
41 benzophenones leading to the discovery of a potent, next generation HIV nonnucleoside
42
43 reverse transcriptase inhibitor. *J. Med. Chem.* **2006**, *49*, 727–739.

44
45
46 79. Ferris, R. G.; Hazen, R. J.; Roberts, G. B.; Clair, M. H. S.; Chan, J. H.; Romines,
47
48 K. R.; Freeman, G. A.; Tidwell, J. H.; Schaller, L. T.; Cowan, J. R.; Short, S. A.; Weaver,
49
50 K. L.; Selleseth, D. W.; Moniri, K. R.; Boone, L. R. Antiviral activity of GW678248, a
51
52
53
54
55
56
57
58
59
60

1
2
3
4 novel benzophenone nonnucleoside reverse transcriptase inhibitor. *Antimicrob. Agents*
5
6 *Chemother.* **2005**, *49*, 4046–4051.

7
8
9 80. Tucker, T. J.; Saggar, S.; Sisko, J. T.; Tynebor, R. M.; Williams, T. M.; Felock, P.
10
11 J.; Flynn, J. A.; Lai, M. T.; Liang, Y.; McGaughey, G.; Liu, M.; Miller, M.; Moyer, G.;
12
13 Munshi, V.; Perlow-Poehnelt, R.; Prasad, S.; Sanchez, R.; Torrent, M.; Vacca, J. P.;
14
15 Wan, B. L.; Yan, Y. The design and synthesis of diaryl ether second generation HIV-1
16
17 non-nucleoside reverse transcriptase inhibitors (NNRTIs) with enhanced potency
18
19 versus key clinical mutations. *Bioorg. Med. Chem. Lett.* **2008**, *18*, 2959–2966.

20
21
22 81. Tucker, T. J.; Sisko, J. T.; Tynebor, R. M.; Williams, T. M.; Felock, P. J.; Flynn, J.
23
24 A.; Lai, M. T.; Liang, Y. X.; McGaughey, G.; Liu, M. Q.; Miller, M.; Moyer, G.;
25
26 Munshi, V.; Perlow-Poehnelt, R.; Prasad, S.; Reid, J. C.; Sanchez, R.; Torrent, M.;
27
28 Vacca, J. P.; Wan, B. L.; Yan, Y. W. Discovery of 3-{5-[(6-amino-1H-pyrazolo[3,4-
29
30 b]pyridine-3-yl)methoxy]-2-chlorophenoxy}-5-chlorobenzonitrile (MK-4965): a
31
32 potent, orally bioavailable HIV-1 non-nucleoside reverse transcriptase inhibitor with
33
34 improved potency against key mutant viruses. *J. Med. Chem.* **2008**, *51*, 6503–6511.

35
36
37 82. Lai, M. T.; Munshi, V.; Touch, S.; Tynebor, R. M.; Tucker, T. J.; McKenna, P. M.;
38
39 Williams, T. M.; DiStefano, D. J.; Hazuda, D. J.; Miller, M. D. Antiviral activity of
40
41 MK-4965, a novel nonnucleoside reverse transcriptase inhibitor. *Antimicrob. Agents*
42
43 *Chemother.* **2009**, *53*, 2424–2431.

44
45
46 83. Sweeney, Z. K.; Dunn, J. P.; Li, Y.; Heilek, G.; Dunten, P.; Elworthy, T. R.; Han,
47
48 X.; Harris, S. F.; Hirschfeld, D. R.; Hogg, J. H.; Huber, W.; Kaiser, A. C.; Kertesz, D.
49
50 J.; Kim, W.; Mirzadegan, T.; Roepel, M. G.; Saito, Y. D.; Silva, T. M.; Swallow, S.;
51
52
53
54
55
56
57
58
59
60

1
2
3
4 Tracy, J. L.; Villasenor, A.; Vora, H.; Zhou, A. S.; Klumpp, K. Discovery and
5
6 optimization of pyridazinone non-nucleoside inhibitors of HIV-1 reverse transcriptase.

7
8
9 *Bioorg. Med. Chem. Lett.* **2008**, *18*, 4352–4354.

10
11 84. Sweeney, Z. K.; Acharya, S.; Briggs, A.; Dunn, J. P.; Elworthy, T. R.; Fretland, J.;
12
13 Giannetti, A. M.; Heilek, G.; Li, Y.; Kaiser, A. C.; Martin, M.; Saito, Y. D.; Smith, M.;
14
15 Suh, J. M.; Swallow, S.; Wu, J.; Hang, J. Q.; Zhou, A. S.; Klumpp, K. Discovery of
16
17 triazolinone non-nucleoside inhibitors of HIV reverse transcriptase. *Bioorg. Med. Chem.*
18
19 *Lett.* **2008**, *18*, 4348–4351.

20
21
22 85. Sweeney, Z. K.; Harris, S. F.; Arora, S. F.; Javanbakht, H.; Li, Y.; Fretland, J.;
23
24 Davidson, J. P.; Billedeau, J. R.; Gleason, S. K.; Hirschfeld, D.; Kennedy-Smith, J. J.;
25
26 Mirzadegan, T.; Roetz, R.; Smith, M.; Sperry, S.; Suh, J. M.; Wu, J.; Tsing, S.;
27
28 Villasenor, A. G.; Paul, A.; Su, G.; Heilek, G.; Hang, J. Q.; Zhou, A. S.; Jernelius, J.
29
30 A.; Zhang, F. J.; Klumpp, K. Design of annulated pyrazoles as inhibitors of HIV-1
31
32 reverse transcriptase. *J. Med. Chem.* **2008**, *51*, 7449–7458.

33
34
35 86. Gomez, R.; Jolly, S.; Williams, T.; Tucker, T.; Tynebor, R.; Vacca, J.; McGaughey,
36
37 G.; Lai, M. T.; Felock, P.; Munshi, V.; DeStefano, D.; Touch, S.; Miller, M.; Yan, Y.
38
39 W.; Sanchez, R.; Liang, Y. X.; Paton, B.; Wan, B. L.; Anthony, N. Design and synthesis
40
41 of pyridone inhibitors of non-nucleoside reverse transcriptase. *Bioorg. Med. Chem. Lett.*
42
43 **2011**, *21*, 7344–7350.

44
45 87. Cote, B.; Burch, J. D.; Asante-Appiah, E.; Bayly, C.; Bedard, L.; Blouin, M.;
46
47 Campeau, L. C.; Cauchon, E.; Chan, M.; Chefson, A.; Coulombe, N.; Cromlish, W.;
48
49 Debnath, S.; Deschenes, D.; Dupont-Gaudet, K.; Falguyret, J. P.; Forget, R.; Gagne,
50
51
52
53
54
55
56
57
58
59
60

- 1
2
3
4 S.; Gauvreau, D.; Girardin, M.; Guiral, S.; Langlois, E.; Li, C. S.; Nguyen, N.; Papp,
5
6 R.; Plamondon, S.; Roy, A.; Roy, S.; Seliniotakis, R.; St-Onge, M.; Ouellet, S.; Tawa,
7
8 P.; Truchon, J. F.; Vacca, J.; Wrona, M.; Yan, Y. W.; Ducharme, Y. Discovery of MK-
9
10 1439, an orally bioavailable non-nucleoside reverse transcriptase inhibitor potent
11
12 against a wide range of resistant mutant HIV viruses. *Bioorg. Med. Chem. Lett.* **2014**,
13
14 *24*, 917–922.
15
16
17
18
19 88. Colombier, M. A.; Molina, J. M. Doravirine: a review. *Curr. Opin. HIV AIDS* **2018**,
20
21 *13*, 308–314.
22
23
24
25 89. Deeks, E. D. Doravirine: first global approval. *Drugs* **2018**, *78*, 1643–1650.
26
27
28 90. Hwang, C.; Lai, M. T.; Hazuda, D. Rational design of doravirine: from bench to
29
30 patients. *Acs Infect. Dis.* **2020**, *6*, 64–73.
31
32
33 91. Molina, J. M.; Squires, K.; Sax, P. E.; Cahn, P.; Lombaard, J.; DeJesus, E.; Lai, M.
34
35 T.; Xu, X.; Rodgers, A.; Lupinacci, L.; Kumar, S.; Sklar, P.; Nguyen, B. Y.; Hanna, G.
36
37 J.; Hwang, C.; DRIVE-FORWARD Study Group. Doravirine versus ritonavir-boosted
38
39 darunavir in antiretroviral-naive adults with HIV-1 (DRIVE-FORWARD): 48-week
40
41 results of a randomised, double-blind, phase 3, non-inferiority trial. *Lancet HIV* **2018**,
42
43 *5*, e211–e220.
44
45
46
47 92. Molina, J. M.; Squires, K.; Sax, P. E.; Cahn, P.; Lombaard, J.; DeJesus, E.; Lai, M.
48
49 T.; Rodgers, A.; Lupinacci, L.; Kumar, S.; Sklar, P.; Hanna, G. J.; Hwang, C.; Martin,
50
51 E. A.; DRIVE-FORWARD trial group. Doravirine versus ritonavir-boosted darunavir
52
53 in antiretroviral-naive adults with HIV-1 (DRIVE-FORWARD): 96-week results of a
54
55 randomised, double-blind, non-inferiority, phase 3 trial. *Lancet HIV* **2020**, *7*, e16–e26.
56
57
58
59
60

- 1
2
3
4 93. Martin, E. A.; Lai, M. T.; Ngo, W.; Feng, M. Z.; Graham, D.; Hazuda, D. J.; Kumar,
5
6
7 S.; Hwang, C.; Sklar, P.; Asante-Appiah, E. Review of doravirine resistance patterns
8
9 identified in participants during clinical development. *J. Acquir. Immune. Defic. Syndr.*
10
11 **2020**, *85*, 635–642.
12
13
14 94. Blevins, S. R.; Hester, E. K.; Chastain, D. B.; Cluck, D. B. Doravirine: a return of
15
16 the NNRTI class? *Ann. Pharmacother.* **2020**, *54*, 64–74.
17
18
19 95. Stockdale, A. J.; Khoo, S. Doravirine: its role in HIV treatment. *Curr. Opin. HIV*
20
21 *AIDS* **2022**, *17*, 4–14.
22
23
24 96. Langdon, S. R.; Ertl, P.; Brown, N. Bioisosteric replacement and scaffold hopping
25
26 in lead generation and optimization. *Mol. Inform.* **2010**, *29*, 366–385.
27
28
29 97. Dick, A.; Cocklin, S. Bioisosteric replacement as a tool in anti-HIV drug design.
30
31 *Pharmaceuticals-Base.* **2020**, *13*, 36.
32
33
34 98. Showell, G. A.; Mills, J. S. Chemistry challenges in lead optimization: silicon
35
36 isosteres in drug discovery. *Drug Discov. Today* **2003**, *8*, 551–556.
37
38
39 99. Qin, B.; Jiang, X.; Lu, H.; Tian, X.; Barbault, F.; Huang, L.; Qian, K.; Chen, C. H.;
40
41 Huang, R.; Jiang, S.; Lee, K. H.; Xie, L. Diarylaniline derivatives as a distinct class of
42
43 HIV-1 non-nucleoside reverse transcriptase inhibitors. *J. Med. Chem.* **2010**, *53*,
44
45 4906–4916.
46
47
48 100. Tian, X.; Qin, B.; Wu, Z.; Wang, X.; Lu, H.; Morris-Natschke, S. L.; Chen, C. H.;
49
50
51 Jiang, S.; Lee, K. H.; Xie, L. Design, synthesis, and evaluation of diarylpyridines and
52
53 diarylanilines as potent non-nucleoside HIV-1 reverse transcriptase inhibitors. *J. Med.*
54
55 *Chem.* **2010**, *53*, 8287–8297.
56
57
58
59
60

- 1
2
3
4 101. Sun, L. Q.; Zhu, L.; Qian, K.; Qin, B.; Huang, L.; Chen, C. H.; Lee, K. H.; Xie, L.
5
6 Design, synthesis, and preclinical evaluations of novel 4-substituted 1,5-diarylanilines
7
8 as potent HIV-1 non-nucleoside reverse transcriptase inhibitor (NNRTI) drug
9
10 candidates. *J. Med. Chem.* **2012**, *55*, 7219–7229.
11
12
13
14 102. Liu, N.; Wei, L.; Huang, L.; Yu, F.; Zheng, W.; Qin, B.; Zhu, D. Q.; Morris-
15
16 Natschke, S. L.; Jiang, S.; Chen, C. H.; Lee, K. H.; Xie, L. Novel HIV-1 non-nucleoside
17
18 reverse transcriptase inhibitor agents: optimization of diarylanilines with high potency
19
20 against wild-type and rilpivirine-resistant E138K mutant virus. *J. Med. Chem.* **2016**,
21
22
23
24
25 *59*, 3689–3704.
26
27
28 103. Kang, D.; Feng, D.; Sun, Y.; Fang, Z.; Wei, F.; De Clercq, E.; Pannecouque, C.;
29
30 Liu, X.; Zhan, P. Structure-based bioisosterism yields HIV-1 NNRTIs with improved
31
32 drug-resistance profiles and favorable pharmacokinetic properties. *J. Med. Chem.* **2020**,
33
34
35
36
37 *63*, 4837–4848.
38
39
40 104. Gao, C.; Park, M. S.; Stern, H. A. Accounting for ligand conformational restriction
41
42 in calculations of protein-ligand binding affinities. *Biophys. J.* **2010**, *98*, 901–910.
43
44
45 105. Fang, Z.; Song, Y.; Zhan, P.; Zhang, Q.; Liu, X. Conformational restriction: an
46
47 effective tactic in 'follow-on'-based drug discovery. *Future Med. Chem.* **2014**, *6*,
48
49
50
51 106. Gomez, R.; Jolly, S. J.; Williams, T.; Vacca, J. P.; Torrent, M.; McGaughey, G.;
52
53
54
55
56
57
58
59
60
Lai, M. T.; Felock, P.; Munshi, V.; Distefano, D.; Flynn, J.; Miller, M.; Yan, Y.; Reid,
J.; Sanchez, R.; Liang, Y.; Paton, B.; Wan, B. L.; Anthony, N. Design and synthesis of
conformationally constrained inhibitors of non-nucleoside reverse transcriptase. *J. Med.*

1
2
3
4 *Chem.* **2011**, *54*, 7920–7933.
5

6 107. Johnson, B. C.; Pauly, G. T.; Rai, G.; Patel, D.; Bauman, J. D.; Baker, H. L.; Das,
7 K.; Schneider, J. P.; Maloney, D. J.; Arnold, E.; Thomas, C. J.; Hughes, S. H. A
8
9 comparison of the ability of rilpivirine (TMC278) and selected analogues to inhibit
10
11 clinically relevant HIV-1 reverse transcriptase mutants. *Retrovirology* **2012**, *9*, 99.
12
13
14

15
16 108. Smith, S. J.; Pauly, G. T.; Akram, A.; Melody, K.; Rai, G.; Maloney, D. J.;
17
18 Ambrose, Z.; Thomas, C. J.; Schneider, J. T.; Hughes, S. H. Rilpivirine analogs potently
19
20 inhibit drug-resistant HIV-1 mutants. *Retrovirology* **2016**, *13*, 11.
21
22
23

24
25 109. Das, K.; Clark, A. D.; Lewi, P. J.; Heeres, J.; de Jonge, M. R.; Koymans, L. M.
26
27 H.; Vinkers, H. M.; Daeyaert, F.; Ludovici, D. W.; Kukla, M. J.; De Corte, B.; Kavash,
28
29 R. W.; Ho, C. Y.; Ye, H.; Lichtenstein, M. A.; Andries, K.; Pauwels, R.; de Bethune,
30
31 M. P.; Boyer, P. L.; Clark, P.; Hughes, S. H.; Janssen, P. A. J.; Arnold, E. Roles of
32
33 conformational and positional adaptability in structure-based design of TMC125-
34
35 R165335 (etravirine) and related non-nucleoside reverse transcriptase inhibitors that
36
37 are highly potent and effective against wild-type and drug-resistant HIV-1 variants. *J.*
38
39
40
41
42
43 *Med. Chem.* **2004**, *47*, 2550–2560.
44

45
46 110. Das, K.; Lewi, P. J.; Hughes, S. H.; Arnold, E. Crystallography and the design of
47
48 anti-AIDS drugs: conformational flexibility and positional adaptability are important in
49
50 the design of non-nucleoside HIV-1 reverse transcriptase inhibitors. *Prog. Biophys.*
51
52
53 *Mol. Bio.* **2005**, *88*, 209–231.
54

55
56 111. Paris, K. A.; Haq, O.; Felts, A. K.; Das, K.; Arnold, E.; Levy, R. M.
57
58 Conformational landscape of the human immunodeficiency virus type 1 reverse
59
60

1
2
3
4 transcriptase non-nucleoside inhibitor binding pocket: lessons for inhibitor design from
5
6 a cluster analysis of many crystal structures. *J. Med. Chem.* **2009**, *52*, 6413–6420.

7
8
9 112. Das, K.; Bauman, J. D.; Clark, A. D.; Frenkel, Y. V.; Lewi, P. J.; Shatkin, A. J.;
10
11 Hughes, S. H.; Arnold, E. High-resolution structures of HIV-1 reverse
12
13 transcriptase/TMC278 complexes: strategic flexibility explains potency against
14
15 resistance mutations. *Proc. Natl. Acad. Sci. U.S.A.* **2008**, *105*, 1466–1471.

16
17
18
19 113. Bauman, J. D.; Das, K.; Ho, W. C.; Baweja, M.; Himmel, D. M.; Clark, A. D.;
20
21 Oren, D. A.; Boyer, P. L.; Hughes, S. H.; Shatkin, A. J.; Arnold, E. Crystal engineering
22
23 of HIV-1 reverse transcriptase for structure-based drug design. *Nucleic Acids Res.* **2008**,
24
25 *36*, 5083–5092.

26
27
28
29 114. Frenkel, Y. V.; Gallicchio, E.; Das, K.; Levy, R. M.; Arnold, E. Molecular
30
31 dynamics study of non-nucleoside reverse transcriptase inhibitor 4-[[4-[[4-[(E)-2-
32
33 cyanoethenyl]-2,6-dimethylphenyl]amino]-2-pyrimidinyl]amino]benzotrile
34
35 (TMC278/rilpivirine) aggregates: correlation between amphiphilic properties of the
36
37 drug and oral bioavailability. *J. Med. Chem.* **2009**, *52*, 5896–5905.

38
39
40
41
42 115. Agnello, S.; Brand, M.; Chellat, M. F.; Gazzola, S.; Riedl, R. A structural view on
43
44 medicinal chemistry strategies against drug resistance. *Angew. Chem., Int. Ed.* **2019**, *58*,
45
46 3300–3345.

47
48
49
50 116. Hayes, J. D.; Wolf, C. R. Molecular mechanisms of drug resistance. *Biochem. J.*
51
52 **1990**, *272*, 281–295.

53
54
55
56 117. Kyrochristos, I. D.; Ziogas, D. E.; Roukos, D. H. Drug resistance: origins,
57
58 evolution and characterization of genomic clones and the tumor ecosystem to optimize
59
60

- 1
2
3
4 precise individualized therapy. *Drug Discov. Today* **2019**, *24*, 1281–1294.
- 5
6
7 118. Ma, Y.; Frutos-Beltran, E.; Kang, D.; Pannecouque, C.; De Clercq, E.; Menendez-
8
9 Arias, L.; Liu, X.; Zhan, P. Medicinal chemistry strategies for discovering antivirals
10
11 effective against drug-resistant viruses. *Chem. Soc. Rev.* **2021**, *50*, 4514–4540.
- 12
13
14 119. Pettinger, J.; Jones, K.; Cheeseman, M. D. Lysine-targeting covalent inhibitors.
15
16
17 *Angew. Chem., Int. Ed.* **2017**, *56*, 15200–15209.
- 18
19
20 120. Lonsdale, R.; Ward, R. A. Structure-based design of targeted covalent inhibitors.
21
22
23 *Chem. Soc. Rev.* **2018**, *47*, 3816–3830.
- 24
25 121. Gehringer, M.; Laufer, S. A. Emerging and re-emerging warheads for targeted
26
27 covalent inhibitors: applications in medicinal chemistry and chemical biology. *J. Med.*
28
29
30 *Chem.* **2019**, *62*, 5673–5724.
- 31
32
33 122. Chan, A. H.; Lee, W. G.; Spasov, K. A.; Cisneros, J. A.; Kudalkar, S. N.; Petrova,
34
35
36
37
38
39
40
41
42 Z. O.; Buckingham, A. B.; Anderson, K. S.; Jorgensen, W. L. Covalent inhibitors for
43
44
45 eradication of drug-resistant HIV-1 reverse transcriptase: From design to protein
46
47
48
49
50
51
52 crystallography. *Proc. Natl. Acad. Sci. U.S.A.* **2017**, *114*, 9725–9730.
- 53
54
55 123. Ippolito, J. A.; Niu, H.; Bertolotti, N.; Carter, Z. J.; Jin, S.; Spasov, K. A.; Cisneros,
56
57
58
59
60 J. A.; Valhondo, M.; Cutrona, K. J.; Anderson, K. S.; Jorgensen, W. L. Covalent
inhibition of wild-type HIV-1 reverse transcriptase using a fluorosulfate warhead. *ACS*
Med. Chem. Lett. **2021**, *12*, 249–255.
124. Hao, G. F.; Yang, G. F.; Zhan, C. G. Structure-based methods for predicting target
mutation-induced drug resistance and rational drug design to overcome the problem.
Drug Discov. Today **2012**, *17*, 1121–1126.

- 1
2
3
4 125. Zhan, P.; Liu, X.; Li, Z.; Pannecouque, C.; De Clercq, E. Design strategies of novel
5
6 NNRTIs to overcome drug resistance. *Curr. Med. Chem.* **2009**, *16*, 3903–3917.
7
8
9 126. Castellino, S.; Groseclose, M. R.; Sigafos, J.; Wagner, D.; de Serres, M.; Polli, J.
10
11 W.; Romach, E.; Myer, J.; Hamilton, B. Central nervous system disposition and
12
13 metabolism of Fosdevirine (GSK2248761), a non-nucleoside reverse transcriptase
14
15 inhibitor: an LC-MS and Matrix-assisted laser desorption/ionization imaging MS
16
17 investigation into central nervous system toxicity. *Chem. Res. Toxicol.* **2013**, *26*,
18
19 241–251.
20
21
22
23
24 127. Jin, K.; Yin, H.; De Clercq, E.; Pannecouque, C.; Meng, G.; Chen, F. Discovery
25
26 of biphenyl-substituted diarylpyrimidines as non-nucleoside reverse transcriptase
27
28 inhibitors with high potency against wild-type and mutant HIV-1. *Eur. J. Med. Chem.*
29
30 **2018**, *145*, 726–734.
31
32
33
34 128. Sang, Y.; Han, S.; Pannecouque, C.; De Clercq, E.; Zhuang, C.; Chen, F. Ligand-
35
36 based design of nondimethylphenyl-diarylpyrimidines with improved metabolic
37
38 stability, safety, and oral pharmacokinetic profiles. *J. Med. Chem.* **2019**, *62*,
39
40 11430–11436.
41
42
43
44 129. Ding, L.; Pannecouque, C.; De Clercq, E.; Zhuang, C. L.; Chen, F. E. Hydrophobic
45
46 pocket occupation design of difluoro-biphenyl-diarylpyrimidines as non-nucleoside
47
48 HIV-1 reverse transcriptase inhibitors: from N-alkylation to methyl hopping on the
49
50 pyrimidine ring. *J. Med. Chem.* **2021**, *64*, 5067–5081.
51
52
53
54
55 130. Ding, L.; Pannecouque, C.; De Clercq, E.; Zhuang, C. L.; Chen, F. E. Improving
56
57 druggability of novel diarylpyrimidine NNRTIs by a fragment-based replacement
58
59
60

1
2
3
4 strategy: from biphenyl-DAPYs to heteroaromatic-biphenyl-DAPYs. *J. Med. Chem.*
5
6 **2021**, *64*, 10297–10311.
7

8
9 131. Borsari, C.; Trader, D. J.; Tait, A.; Costi, M. P. Designing Chimeric Molecules for
10 Drug Discovery by Leveraging Chemical Biology. *J. Med. Chem.* **2020**, *63*, 1908–1928.
11

12
13 132. Song, Y.; Zhan, P.; Li, X.; Rai, D.; De Clercq, E.; Liu, X. Multivalent agents: a
14 novel concept and preliminary practice in Anti-HIV drug discovery. *Curr. Med. Chem.*
15
16 **2013**, *20*, 815–832.
17
18

19
20 133. Bauman, J. D.; Patel, D.; Dharia, C.; Fromer, M. W.; Ahmed, S.; Frenkel, Y.;
21 Vijayan, R. S.; Eck, J. T.; Ho, W. C.; Das, K.; Shatkin, A. J.; Arnold, E. Detecting
22 allosteric sites of HIV-1 reverse transcriptase by X-ray crystallographic fragment
23 screening. *J. Med. Chem.* **2013**, *56*, 2738–2746.
24
25

26
27 134. Huo, Z.; Zhang, H.; Kang, D.; Zhou, Z.; Wu, G.; Desta, S.; Zuo, X.; Wang, Z.;
28 Jing, L.; Ding, X.; Daelemans, D.; De Clercq, E.; Pannecouque, C.; Zhan, P.; Liu, X.
29 Discovery of novel diarylpyrimidine derivatives as potent HIV-1 NNRTIs targeting the
30 "NNRTI adjacent" binding site. *ACS Med. Chem. Lett.* **2018**, *9*, 334–338.
31
32

33
34 135. Feng, D.; Zuo, X.; Jing, L.; Chen, C. H.; Olotu, F. A.; Lin, H.; Soliman, M.; De
35 Clercq, E.; Pannecouque, C.; Lee, K. H.; Kang, D.; Liu, X.; Zhan, P. Design, synthesis,
36 and evaluation of "dual-site"-binding diarylpyrimidines targeting both NNIBP and the
37 NNRTI adjacent site of the HIV-1 reverse transcriptase. *Eur. J. Med. Chem.* **2021**, *211*,
38
39 113063.
40
41

42
43 136. Bailey, C. M.; Sullivan, T. J.; Iyidogan, P.; Tirado-Rives, J.; Chung, R.; Ruiz-
44 Caro, J.; Mohamed, E.; Jorgensen, W. L.; Hunter, R.; Anderson, K. S. Bifunctional
45
46
47
48
49
50
51
52
53
54
55
56
57
58
59
60

1
2
3
4 inhibition of human immunodeficiency virus type 1 reverse transcriptase: mechanism
5
6 and proof-of-concept as a novel therapeutic design strategy. *J. Med. Chem.* **2013**, *56*,
7
8 3959–3968.
9

10
11 137. Iyidogan, P.; Sullivan, T. J.; Chordia, M. D.; Frey, K. M.; Anderson, K. S. Design,
12
13 synthesis, and antiviral evaluation of chimeric inhibitors of HIV reverse transcriptase.
14
15 *ACS Med. Chem. Lett.* **2013**, *4*, 1183–1188.
16
17

18
19 138. Raevsky, O. A.; Grigorev, V. Y.; Polianczyk, D. E.; Raevskaja, O. E.; Dearden, J.
20
21 C. Aqueous drug solubility: what do we measure, calculate and QSPR predict? *Mini*
22
23 *Rev. Med. Chem.* **2019**, *19*, 362–372.
24
25

26
27 139. Das, T.; Mehta, C. H.; Nayak, U. Y. Multiple approaches for achieving drug
28
29 solubility: an in silico perspective. *Drug Discov. Today* **2020**, *25*, 1206–1212.
30
31

32
33 140. Walther, R.; Rautio, J.; Zelikin, A. N. Prodrugs in medicinal chemistry and enzyme
34
35 prodrug therapies. *Adv. Drug Deliv. Rev.* **2017**, *118*, 65–77.
36
37

38
39 141. Rautio, J.; Meanwell, N. A.; Di, L.; Hageman, M. J. The expanding role of
40
41 prodrugs in contemporary drug design and development. *Nat. Rev. Drug Discov.* **2018**,
42
43 *17*, 559–587.
44

45
46 142. Nussmeier, N. A.; Whelton, A. A.; Brown, M. T.; Langford, R. M.; Hoeft, A.;
47
48 Parlow, J. L.; Boyce, S. W.; Verburg, K. M. Complications of the COX-2 inhibitors
49
50 parecoxib and valdecoxib after cardiac surgery. *N. Engl. J. Med.* **2005**, *352*, 1081–1091.
51
52

53
54 143. Cho, A. Recent advances in oral prodrug discovery. *Annu. Rep. Med. Chem.* **2006**,
55
56 *41*, 395–407.
57

58
59 144. de Serres, M.; Moss, L.; Sigafos, J.; Sefler, A.; Castellino, S.; Bowers, G.;
60

1
2
3
4 Serabjit-Singh, C. The disposition and metabolism of GW695634: a non-nucleoside
5
6 reverse transcriptase inhibitor (NNRTi) for treatment of HIV/AIDS. *Xenobiotica* **2010**,
7
8 *40*, 437–445.
9

10
11 145. Boone, L. R. Next-generation HIV-1 non-nucleoside reverse transcriptase
12
13 inhibitors. *Curr. Opin. Investig. Drugs* **2006**, *7*, 128–135.
14
15

16
17 146. Al-Salama, Z. T. Elulfavirine: first global approval. *Drugs* **2017**, *77*, 1811–1816.
18

19
20 147. Rai, M. A.; Pannek, S.; Fichtenbaum, C. J. Emerging reverse transcriptase
21
22 inhibitors for HIV-1 infection. *Expert Opin. Emerg. Drugs* **2018**, *23*, 149–157.
23
24

25
26 148. Wang, Y.; De Clercq, E.; Li, G. Current and emerging non-nucleoside reverse
27
28 transcriptase inhibitors (NNRTIs) for HIV-1 treatment. *Expert Opin. Drug Metab.*
29
30 *Toxicol.* **2019**, *15*, 813–829.
31

32
33 149. Supuran, C. T.; Nocentini, A.; Yakubova, E.; Savchuk, N.; Kalinin, S.; Krasavin,
34
35 M. Biochemical profiling of anti-HIV prodrug Elulfavirine (Elpida[®]) and its active
36
37 form VM1500A against a panel of twelve human carbonic anhydrase isoforms. *J.*
38
39 *Enzyme Inhib. Med. Chem.* **2021**, *36*, 1056–1060.
40
41

42
43 150. Wang, Z.; Yu, Z.; Kang, D.; Zhang, J.; Tian, Y.; Daelemans, D.; De Clercq, E.;
44
45 Pannecouque, C.; Zhan, P.; Liu, X. Design, synthesis and biological evaluation of novel
46
47 acetamide-substituted doravirine and its prodrugs as potent HIV-1 NNRTIs. *Bioorg.*
48
49 *Med. Chem.* **2019**, *27*, 447–456.
50
51

52
53 151. Jiang, X.; Yu, J.; Zhou, Z.; Kongsted, J.; Song, Y.; Pannecouque, C.; De Clercq,
54
55 E.; Kang, D.; Poongavanam, V.; Liu, X.; Zhan, P. Molecular design opportunities
56
57 presented by solvent-exposed regions of target proteins. *Med. Res. Rev.* **2019**, *39*,
58
59
60

1
2
3
4 2194–2238.
5

6 152. Huang, B.; Chen, W.; Zhao, T.; Li, Z.; Jiang, X.; Ginex, T.; Vilchez, D.; Luque,
7 F. J.; Kang, D.; Gao, P.; Zhang, J.; Tian, Y.; Daelemans, D.; De Clercq, E.;
8 Pannecouque, C.; Zhan, P.; Liu, X. Exploiting the tolerant region I of the non-
9 nucleoside reverse transcriptase inhibitor (NNRTI) binding pocket: discovery of potent
10 diarylpyrimidine-typed HIV-1 NNRTIs against wild-type and E138K mutant virus with
11 significantly improved water solubility and favorable safety profiles. *J. Med. Chem.*
12 **2019**, *62*, 2083–2098.
13
14

15 153. Sun, Y.; Kang, D.; Da, F.; Zhang, T.; Li, P.; Zhang, B.; De Clercq, E.;
16 Pannecouque, C.; Zhan, P.; Liu, X. Identification of novel potent HIV-1 inhibitors by
17 exploiting the tolerant regions of the NNRTIs binding pocket. *Eur. J. Med. Chem.* **2021**,
18 *214*, 113204.
19
20

21 154. Lovering, F.; Bikker, J.; Humblet, C. Escape from flatland: increasing saturation
22 as an approach to improving clinical success. *J. Med. Chem.* **2009**, *52*, 6752–6756.
23
24

25 155. Wei, W.; Cherukupalli, S.; Jing, L.; Liu, X.; Zhan, P. Fsp³: A new parameter for
26 drug-likeness. *Drug Discov. Today* **2020**, *25*, 1839–1845.
27
28

29 156. Jiang, X.; Huang, B.; Olotu, F. A.; Li, J.; Kang, D.; Wang, Z.; De Clercq, E.;
30 Soliman, M. E. S.; Pannecouque, C.; Liu, X.; Zhan, P. Exploiting the tolerant region I
31 of the non-nucleoside reverse transcriptase inhibitor (NNRTI) binding pocket. Part 2:
32 Discovery of diarylpyrimidine derivatives as potent HIV-1 NNRTIs with high Fsp³
33 values and favorable drug-like properties. *Eur. J. Med. Chem.* **2021**, *213*, 113051.
34
35

36 157. Zhou, J.; Jiang, X.; He, S.; Jiang, H.; Feng, F.; Liu, W.; Qu, W.; Sun, H. Rational
37
38
39
40
41
42
43
44
45
46
47
48
49
50
51
52
53
54
55
56
57
58
59
60

1
2
3
4 design of multitarget-directed ligands: strategies and emerging paradigms. *J. Med.*
5
6 *Chem.* **2019**, *62*, 8881–8914.

7
8
9 158. Albertini, C.; Salerno, A.; de Sena Murteira Pinheiro, P.; Bolognesi, M. L. From
10 combinations to multitarget-directed ligands: A continuum in Alzheimer's disease
11 polypharmacology. *Med. Res. Rev.* **2021**, *41*, 2606–2633.

12
13
14 159. Zhan, P.; Liu, X. Rationally designed multitarget anti-HIV agents. *Curr. Med.*
15
16 *Chem.* **2013**, *20*, 1743–1758.

17
18
19 160. Zhan, P.; Liu, X. Designed multiple ligands: an emerging anti-HIV drug discovery
20
21 paradigm. *Curr. Pharm. Des.* **2009**, *15*, 1893–1917.

22
23
24 161. Gill, M. S. A.; Hassan, S. S.; Ahemad, N. Evolution of HIV-1 reverse transcriptase
25
26 and integrase dual inhibitors: Recent advances and developments. *Eur. J. Med. Chem.*
27
28 **2019**, *179*, 423–448.

29
30
31 162. Gu, S. X.; Xue, P.; Ju, X. L.; Zhu, Y. Y. Advances in rationally designed dual
32
33 inhibitors of HIV-1 reverse transcriptase and integrase. *Bioorg. Med. Chem.* **2016**, *24*,
34
35 5007–5016.

36
37
38 163. Wang, Z.; Bennett, E. M.; Wilson, D. J.; Salomon, C.; Vince, R. Rationally
39
40 designed dual inhibitors of HIV reverse transcriptase and integrase. *J. Med. Chem.* **2007**,
41
42 *50*, 3416–3419.

43
44
45 164. Wang, Z.; Tang, J.; Salomon, C. E.; Dreis, C. D.; Vince, R. Pharmacophore and
46
47 structure-activity relationships of integrase inhibition within a dual inhibitor scaffold of
48
49 HIV reverse transcriptase and integrase. *Bioorg. Med. Chem.* **2010**, *18*, 4202–4211.

50
51
52 165. Wang, Z.; Vince, R. Design and synthesis of dual inhibitors of HIV reverse
53
54
55
56
57
58
59
60

1
2
3
4 transcriptase and integrase: introducing a diketoacid functionality into delavirdine.

5
6 *Bioorg. Med. Chem.* **2008**, *16*, 3587–3595.

7
8
9 166. Tang, J.; Maddali, K.; Dreis, C. D.; Sham, Y. Y.; Vince, R.; Pommier, Y.; Wang,
10 Z. N-3 hydroxylation of pyrimidine-2,4-diones yields dual inhibitors of HIV reverse
11 transcriptase and integrase. *ACS Med. Chem. Lett.* **2011**, *2*, 63–67.

12
13
14
15
16 167. Tang, J.; Maddali, K.; Metifiot, M.; Sham, Y. Y.; Vince, R.; Pommier, Y.; Wang,
17 Z. 3-Hydroxypyrimidine-2,4-diones as an inhibitor scaffold of HIV integrase. *J. Med.*
18
19
20
21
22 *Chem.* **2011**, *54*, 2282–2292.

23
24
25 168. Bai, L.; Zhou, H.; Xu, R.; Zhao, Y.; Chinnaswamy, K.; McEachern, D.; Chen, J.;
26 Yang, C. Y.; Liu, Z.; Wang, M.; Liu, L.; Jiang, H.; Wen, B.; Kumar, P.; Meagher, J. L.;
27 Sun, D.; Stuckey, J. A.; Wang, S. A potent and selective small-molecule degrader of
28 STAT3 achieves complete tumor regression in vivo. *Cancer Cell* **2019**, *36*, 498–511.

29
30
31
32
33 169. Wang, M.; Lu, J.; Wang, M.; Yang, C. Y.; Wang, S. Discovery of SHP2-D26 as a
34 first, potent, and effective PROTAC degrader of SHP2 protein. *J. Med. Chem.* **2020**,
35
36
37
38
39
40
41
42 *63*, 7510–7528.

43 170. de Wispelaere, M.; Du, G.; Donovan, K. A.; Zhang, T.; Eleuteri, N. A.; Yuan, J.
44 C.; Kalabathula, J.; Nowak, R. P.; Fischer, E. S.; Gray, N. S.; Yang, P. L. Small
45 molecule degraders of the hepatitis C virus protease reduce susceptibility to resistance
46 mutations. *Nat. Commun.* **2019**, *10*, 3468.

47
48
49
50
51
52 171. Campbell, E. M.; Hope, T. J. HIV-1 capsid: the multifaceted key player in HIV-1
53 infection. *Nat. Rev. Microbiol.* **2015**, *13*, 471–483.

54
55
56
57
58
59 172. Christensen, D. E.; Ganser-Pornillos, B. K.; Johnson, J. S.; Pornillos, O.;
60

1
2
3
4 Sundquist, W. I. Reconstitution and visualization of HIV-1 capsid-dependent
5
6 replication and integration in vitro. *Science* **2020**, *370*, eabc8420.
7

8
9 173. Lansdon, E. B.; Brendza, K. M.; Hung, M.; Wang, R.; Mukund, S.; Jin, D.; Birkus,
10
11 G.; Kutty, N.; Liu, X. Crystal structures of HIV-1 reverse transcriptase with etravirine
12
13 (TMC125) and rilpivirine (TMC278): implications for drug design. *J. Med. Chem.* **2010**,
14
15 *53*, 4295–4299.
16
17

18
19 174. Bull, S. D.; Davidson, M. G.; Van den Elsen, J. M. H.; Fossey, J. S.; Jenkins, A.
20
21 T. A.; Jiang, Y. B.; Kubo, Y.; Marken, F.; Sakurai, K.; Zhao, J. Z.; James, T. D.
22
23 Exploiting the reversible covalent bonding of boronic acids: recognition, sensing, and
24
25 assembly. *Acc. Chem. Res.* **2013**, *46*, 312–326.
26
27

28
29 175. Purser, S.; Moore, P. R.; Swallow, S.; Gouverneur, V. Fluorine in medicinal
30
31 chemistry. *Chem. Soc. Rev.* **2008**, *37*, 320–330.
32
33

34
35 176. Losada, N.; Ruiz, F. X.; Curreli, F.; Gruber, K.; Pilch, A.; Altieri, A.; Kurkin, A.
36
37 V.; Das, K.; Debnath, A. K.; Arnold, E. HIV-1 gp120 antagonists also inhibit HIV-1
38
39 reverse transcriptase by bridging the NNRTI and NRTI sites. *J. Med. Chem.* **2021**, *64*,
40
41 16530–16540.
42
43

44
45 177. Kaufmann, S. H. E.; Dorhoi, A.; Hotchkiss, R. S.; Bartenschlager, R. Host-directed
46
47 therapies for bacterial and viral infections. *Nat. Rev. Drug Discov.* **2018**, *17*, 35–56.
48
49

50
51 178. Ji, X.; Li, Z. Medicinal chemistry strategies toward host targeting antiviral agents.
52
53 *Med. Res. Rev.* **2020**, *40*, 1519–1557.
54
55

56
57 179. Jeang, K. T.; Yedavalli, V. Role of RNA helicases in HIV-1 replication. *Nucleic*
58
59 *Acids Res.* **2006**, *34*, 4198–4205.
60

- 1
2
3
4 180. Roy, B. B.; Hu, J.; Guo, X. F.; Russell, R. S.; Guo, F.; Kleiman, L.; Liang, C.
5
6 Association of RNA helicase a with human immunodeficiency virus type 1 particles. *J.*
7
8
9 *Biol. Chem.* **2006**, *281*, 12625–12635.
10
11
12 181. Brady, S.; Singh, G.; Bolinger, C.; Song, Z.; Boeras, I.; Weng, K.; Trent, B.;
13
14 Brown, W. C.; Singh, K.; Boris-Lawrie, K.; Heng, X. Virion-associated, host-derived
15
16 DHX9/RNA helicase A enhances the processivity of HIV-1 reverse transcriptase on
17
18 genomic RNA. *J. Biol. Chem.* **2019**, *294*, 11473–11485.
19
20
21
22 182. Westby, M.; Lewis, M.; Whitcomb, J.; Youle, M.; Pozniak, A. L.; James, I. T.;
23
24 Jenkins, T. M.; Perros, M.; van der Ryst, E. Emergence of CXCR4-using human
25
26 immunodeficiency virus type 1 (HIV-1) variants in a minority of HIV-1-infected
27
28 patients following treatment with the CCR5 antagonist maraviroc is from a
29
30 pretreatment CXCR4-using virus reservoir. *J. Virol.* **2006**, *80*, 4909–4920.
31
32
33
34
35 183. Roche, M.; Salimi, H.; Duncan, R.; Wilkinson, B. L.; Chikere, K.; Moore, M. S.;
36
37 Webb, N. E.; Zappi, H.; Sterjovski, J.; Flynn, J. K.; Ellett, A.; Gray, L. R.; Lee, B.;
38
39 Jubb, B.; Westby, M.; Ramsland, P. A.; Lewin, S. R.; Payne, R. J.; Churchill, M. J.;
40
41 Gorry, P. R. A common mechanism of clinical HIV-1 resistance to the CCR5 antagonist
42
43 maraviroc despite divergent resistance levels and lack of common gp120 resistance
44
45 mutations. *Retrovirology* **2013**, *10*.
46
47
48
49
50
51 184. Westby, M.; Smith-Burchnell, C.; Mori, J.; Lewis, M.; Mosley, M.; Stockdale, M.;
52
53 Dorr, P.; Ciaramella, G.; Perros, M. Reduced maximal inhibition in phenotypic
54
55 susceptibility assays indicates that viral strains resistant to the CCR5 antagonist
56
57 maraviroc utilize inhibitor-bound receptor for entry. *J. Virol.* **2007**, *81*, 2359–2371.
58
59
60

1
2
3
4 185. Overton, E. T.; Richmond, G.; Rizzardini, G.; Jaeger, H.; Orrell, C.; Nagimova,
5
6 F.; Bredeek, F.; Delatoro, M. G.; Swindells, S.; Andrade-Villanueva, J. F.; Wong, A.;
7
8 Khuong-Josses, M. A.; Van Solingen-Ristea, R.; van Eygen, V.; Crauwels, H.; Ford,
9
10 S.; Talarico, C.; Benn, P.; Wang, Y. Y.; Hudson, K. J.; Chounta, V.; Cutrell, A.; Patel,
11
12 P.; Shaefer, M.; Margolis, D. A.; Smith, K. Y.; Vanveggel, S.; Spreen, W. Long-acting
13
14 cabotegravir and rilpivirine dosed every 2 months in adults with HIV-1 infection
15
16 (ATLAS-2M), 48-week results: a randomised, multicentre, open-label, phase 3b, non-
17
18 inferiority study. *Lancet* **2021**, *396*, 1994–2005.

19
20
21
22
23
24 186. Swindells, S.; Andrade-Villanueva, J. F.; Richmond, G. J.; Rizzardini, G.;
25
26 Baumgarten, A.; Masia, M.; Latiff, G.; Pokrovsky, V.; Bredeek, F.; Smith, G.; Cahn,
27
28 P.; Kim, Y. S.; Ford, S. L.; Talarico, C. L.; Patel, P.; Chounta, V.; Crauwels, H.; Parys,
29
30 W.; Vanveggel, S.; Mrus, J.; Huang, J.; Harrington, C. M.; Hudson, K. J.; Margolis, D.
31
32 A.; Smith, K. Y.; Williams, P. E.; Spreen, W. R. Long-acting cabotegravir and
33
34 rilpivirine for maintenance of HIV-1 suppression. *N. Engl. J. Med.* **2020**, *382*,
35
36 1112–1123.

37
38
39
40
41
42 187. Markham, A. Cabotegravir plus rilpivirine: first approval. *Drugs* **2020**, *80*,
43
44 915–922.

45
46
47
48 188. Nel, A.; van Niekerk, N.; Kapiga, S.; Bekker, L. G.; Gama, C.; Gill, K.; Kamali,
49
50 A.; Kotze, P.; Louw, C.; Mabude, Z.; Miti, N.; Kusemererwa, S.; Tempelman, H.;
51
52 Carstens, H.; Devlin, B.; Isaacs, M.; Malherbe, M.; Mans, W.; Nuttall, J.; Russell, M.;
53
54 Ntshela, S.; Smit, M.; Solai, L.; Spence, P.; Steytler, J.; Windle, K.; Borremans, M.;
55
56 Ressler, S.; Van Roey, J.; Parys, W.; Vangeneugden, T.; Van Baelen, B.; Rosenberg,
57
58
59
60

1
2
3
4 Z.; Ring Study Team. Safety and efficacy of a dapivirine vaginal ring for HIV
5 prevention in women. *N. Engl. J. Med.* **2016**, *375*, 2133–2143.

6
7
8
9 189. Wincelous, S. J. Dapivirine vaginal ring for HIV-1 prevention. *N. Engl. J. Med.*
10 **2017**, *376*, 994–995.

11
12
13
14 190. Bhavaraju, N.; Shears, K.; Schwartz, K.; Mullick, S.; Jeckonia, P.; Murungu, J.;
15 Persaud, U.; Vij, A.; Torjesen, K. Introducing the dapivirine vaginal ring in sub-saharan
16 africa: what can we learn from oral PrEP? *Curr. HIV/AIDS Rep.* **2021**, *18*, 508–517.

17
18
19
20 191. Dousson, C.; Alexandre, F. R.; Amador, A.; Bonaric, S.; Bot, S.; Caillet, C.;
21 Convard, T.; da Costa, D.; Lioure, M. P.; Roland, A.; Rosinovsky, E.; Maldonado, S.;
22 Parsy, C.; Trochet, C.; Storer, R.; Stewart, A.; Wang, J.; Mayes, B. A.; Musiu, C.;
23 Poddesu, B.; Vargiu, L.; Liuzzi, M.; Moussa, A.; Jakubik, J.; Hubbard, L.; Seifer, M.;
24 Standing, D. Discovery of the aryl-phospho-indole IDX899, a highly potent anti-HIV
25 non-nucleoside reverse transcriptase inhibitor. *J. Med. Chem.* **2016**, *59*, 1891–1898.

26
27
28
29 192. Margolis, D. A.; Eron, J. J.; DeJesus, E.; White, S.; Wannamaker, P.; Stancil, B.;
30 Johnson, M. Unexpected finding of delayed-onset seizures in HIV-positive, treatment-
31 experienced subjects in the Phase IIb evaluation of fosdevirine (GSK2248761). *Antivir.*
32 *Ther.* **2014**, *19*, 69–78.

33
34
35
36 193. Gewurz, B. E.; Jacobs, M.; Proper, J. A.; Dahl, T. A.; Fujiwara, T.; Dezube, B. J.
37 Capravirine, a nonnucleoside reverse-transcriptase inhibitor in patients infected with
38 HIV-1: a phase 1 study. *J. Infect. Dis.* **2004**, *190*, 1957–1961.

39
40
41
42 194. Li, X.; Zhan, P.; De Clercq, E.; Liu, X. The HIV-1 non-nucleoside reverse
43 transcriptase inhibitors (part V): capravirine and its analogues. *Curr. Med. Chem.* **2012**,
44
45
46
47
48
49
50
51
52
53
54
55
56
57
58
59
60

1
2
3
4 19, 6138–6149.
5

6
7 195. Yang, H. B.; Lou, C. F.; Sun, L. X.; Li, J.; Cai, Y. C.; Wang, Z.; Li, W. H.; Liu,
8
9 G. X.; Tang, Y. admetSAR 2.0: web-service for prediction and optimization of
10
11 chemical ADMET properties. *Bioinformatics* **2019**, *35*, 1067–1069.
12

13
14 196. Xiong, G. L.; Wu, Z. X.; Yi, J. C.; Fu, L.; Yang, Z. J.; Hsieh, C. Y.; Yin, M. Z.;
15
16 Zeng, X. X.; Wu, C. K.; Lu, A. P.; Chen, X.; Hou, T. J.; Cao, D. S. ADMETlab 2.0: an
17
18 integrated online platform for accurate and comprehensive predictions of ADMET
19
20 properties. *Nucleic Acids Res.* **2021**, *49*, W5–W14.
21
22

23
24 197. Jeon, S.; Ko, M.; Lee, J.; Choi, I.; Byun, S. Y.; Park, S.; Shum, D.; Kim, S.
25
26 Identification of antiviral drug candidates against SARS-CoV-2 from FDA-approved
27
28 drugs. *Antimicrob. Agents Chemother.* **2020**, *64*, e00819-20.
29
30

31
32 198. Lima, W. G.; Brito, J. C. M.; Overhage, J.; Nizer, W. S. D. C. The potential of
33
34 drug repositioning as a short-term strategy for the control and treatment of COVID-19
35
36 (SARS-CoV-2): a systematic review. *Arch. Virol.* **2020**, *165*, 1729–1737.
37
38
39
40
41

42
43 **Table of Contents graphic**
44
45
46
47
48
49
50
51
52
53
54
55
56
57
58
59
60

